2013 激光技术创新应用高峰论坛

超短脉冲激光微纳加工新进展

Progress on ultrashort pulsed laser micro/nanoprocessing

赵 全 忠

中国科学院上海光学精密机械研究所

zqz@siom.ac.cn

2013年11月1日·武汉

背景及意义

新能源

高端装备制造　　信息技术

战略性新兴产业

新材料　　新能源汽车

节能环保　　生物

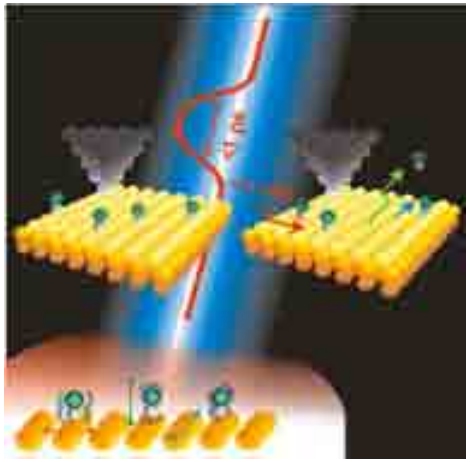

微观改性 → 表面 / 内部 → 精密微细加工

超短脉冲激光
（超快光子）

微纳结构
功能器件

超短脉冲激光

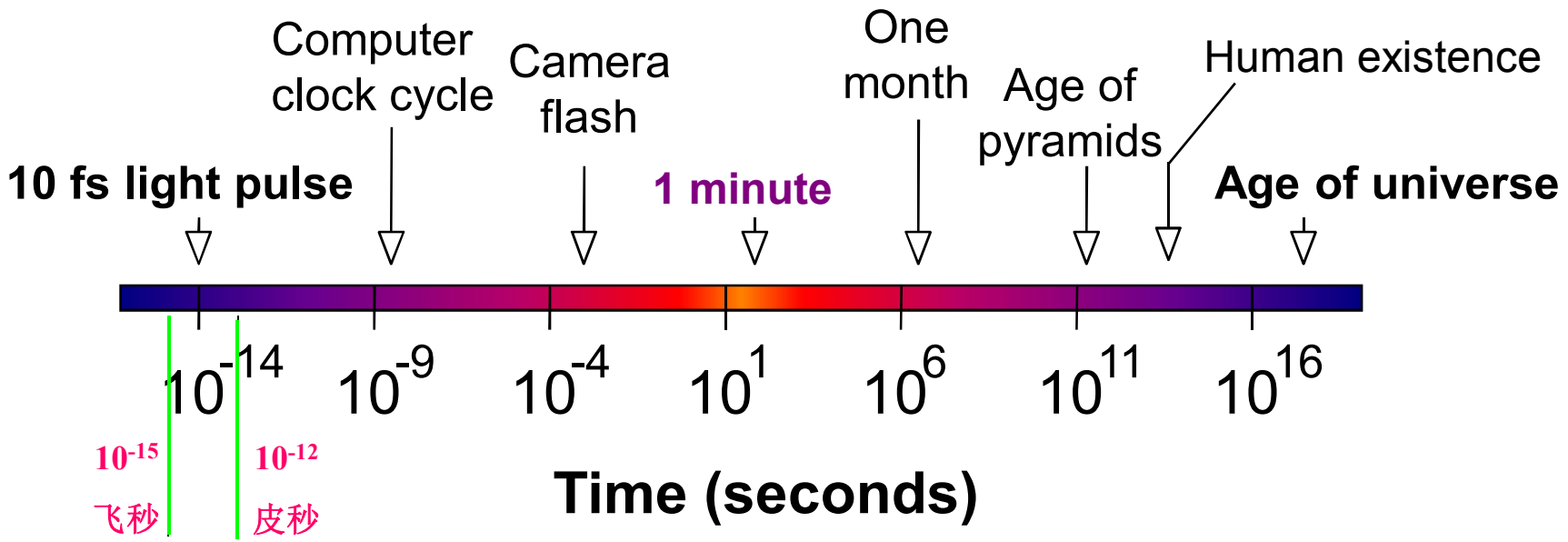

皮秒激光(picosecond laser)

飞秒激光(femtosecond laser)

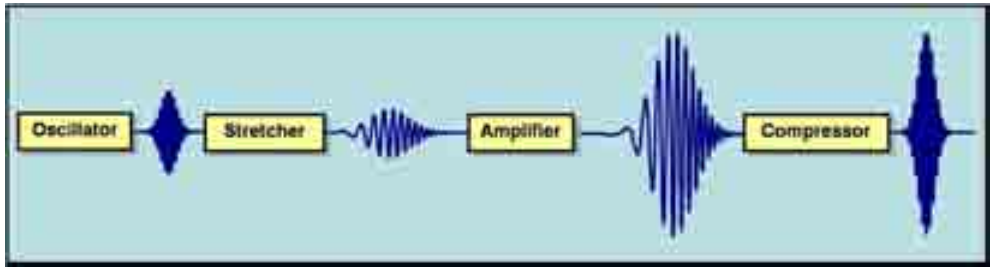

Question?

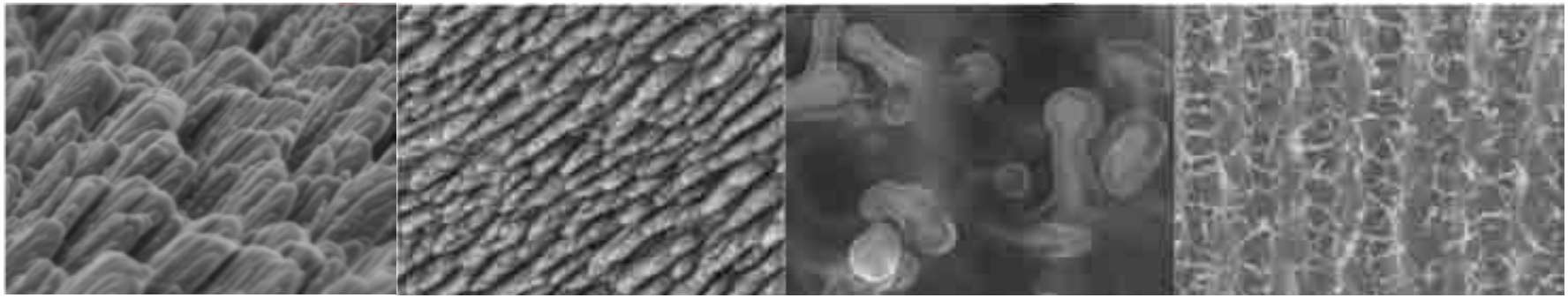

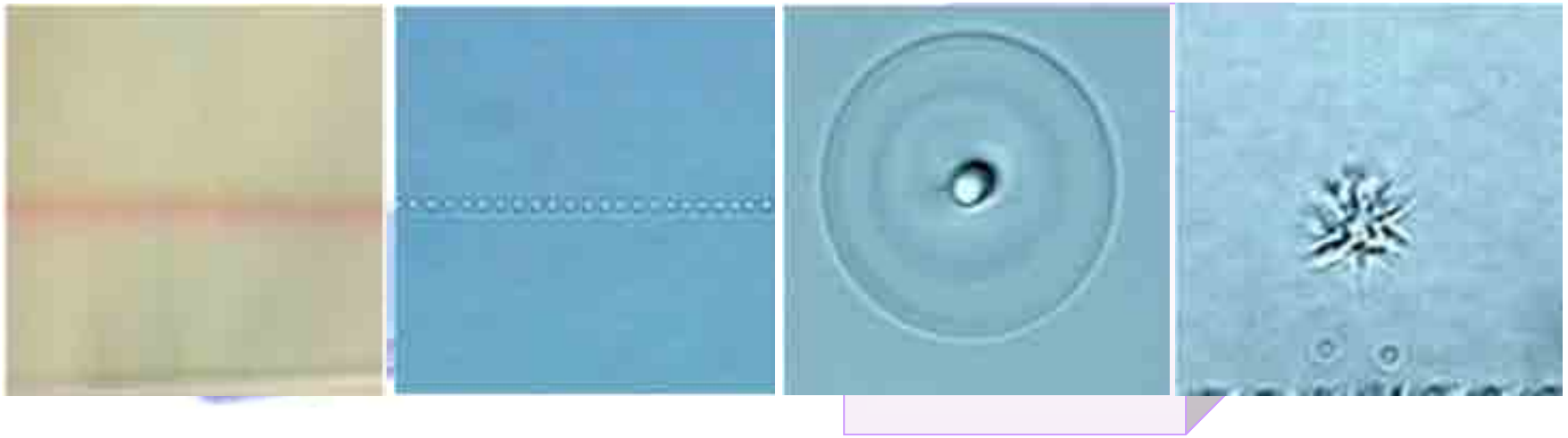

超短脉冲激光微纳改性分类

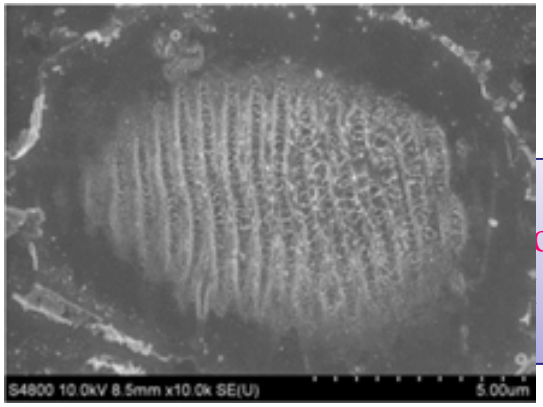

Morphology modification

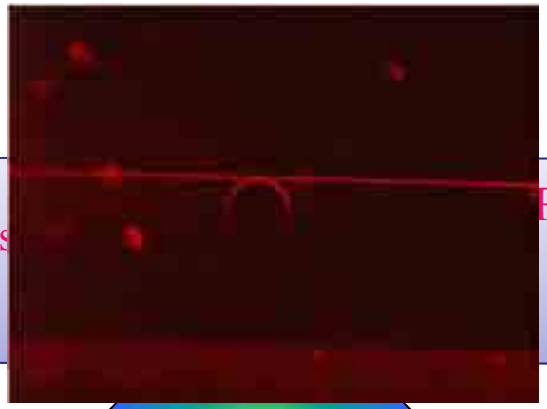

Refractive index modification

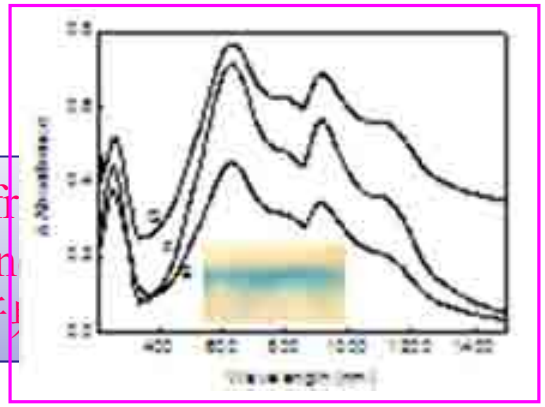

Defect modification

Crystal transition

Valence state

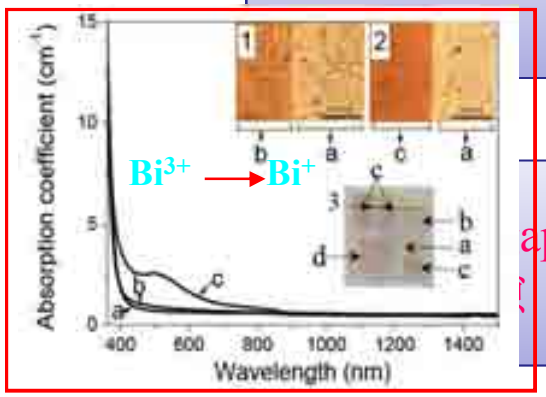

Valence state modification

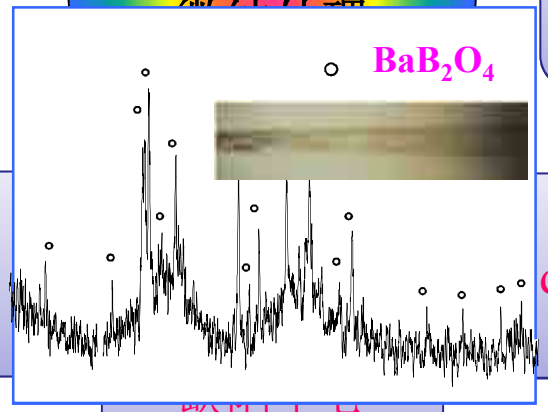

Crystal transition modification

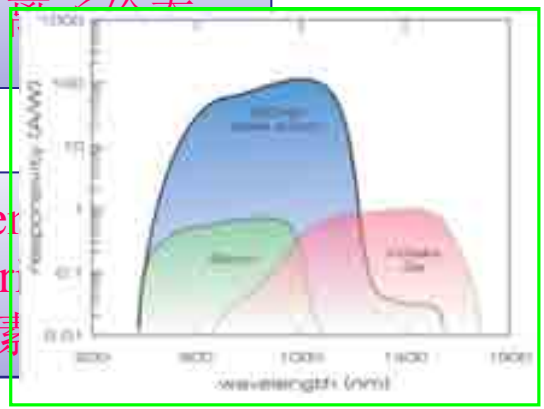

Bandgap modification

超短脉冲激光诱导材料表面功能结构

Fs laser induced ripple structures on metal surfaces

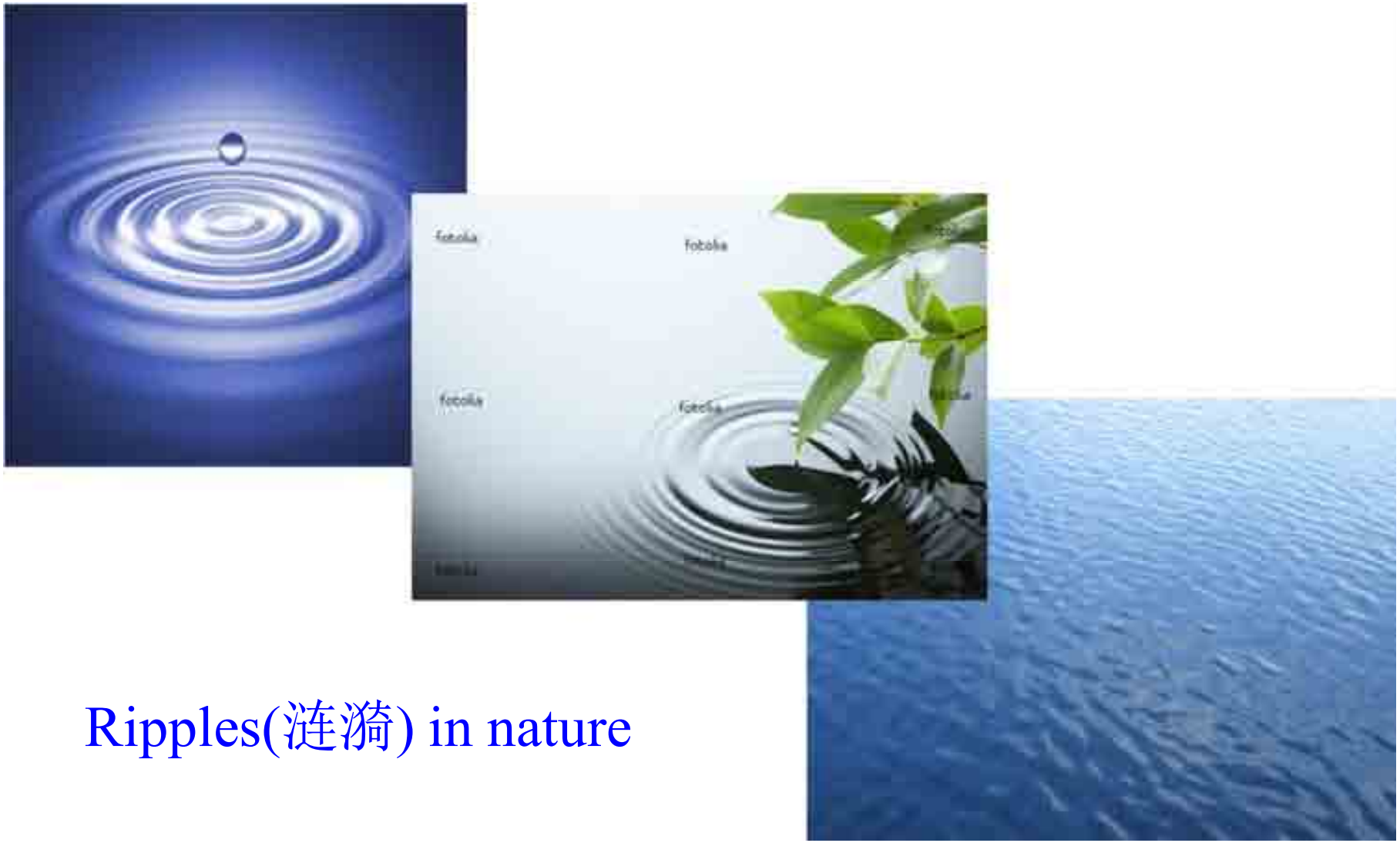

Ripples(涟漪) in nature

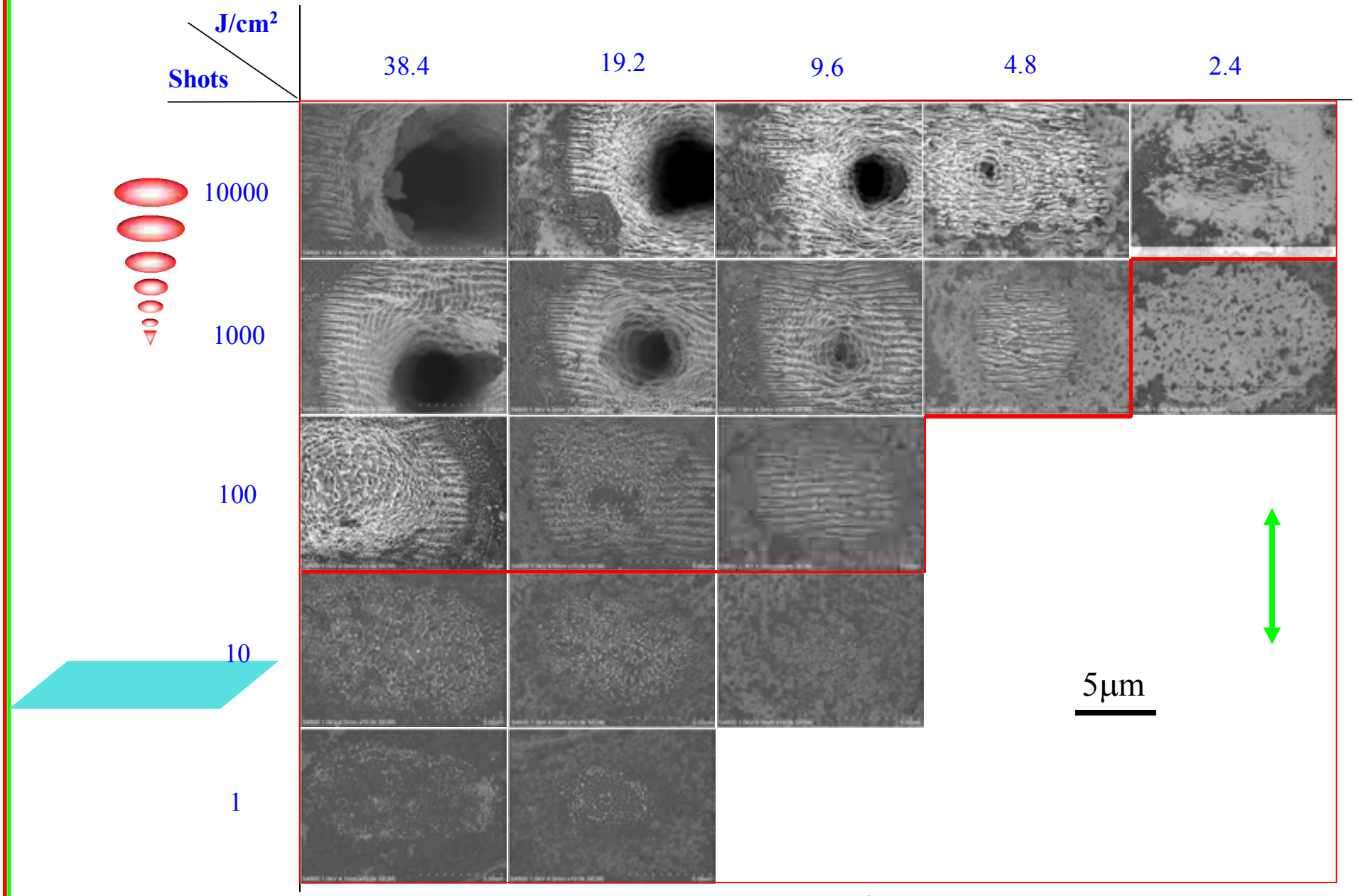

Opt. Lett. 32, 1932-1934 (2007)

Effects of incident angle on ripple period

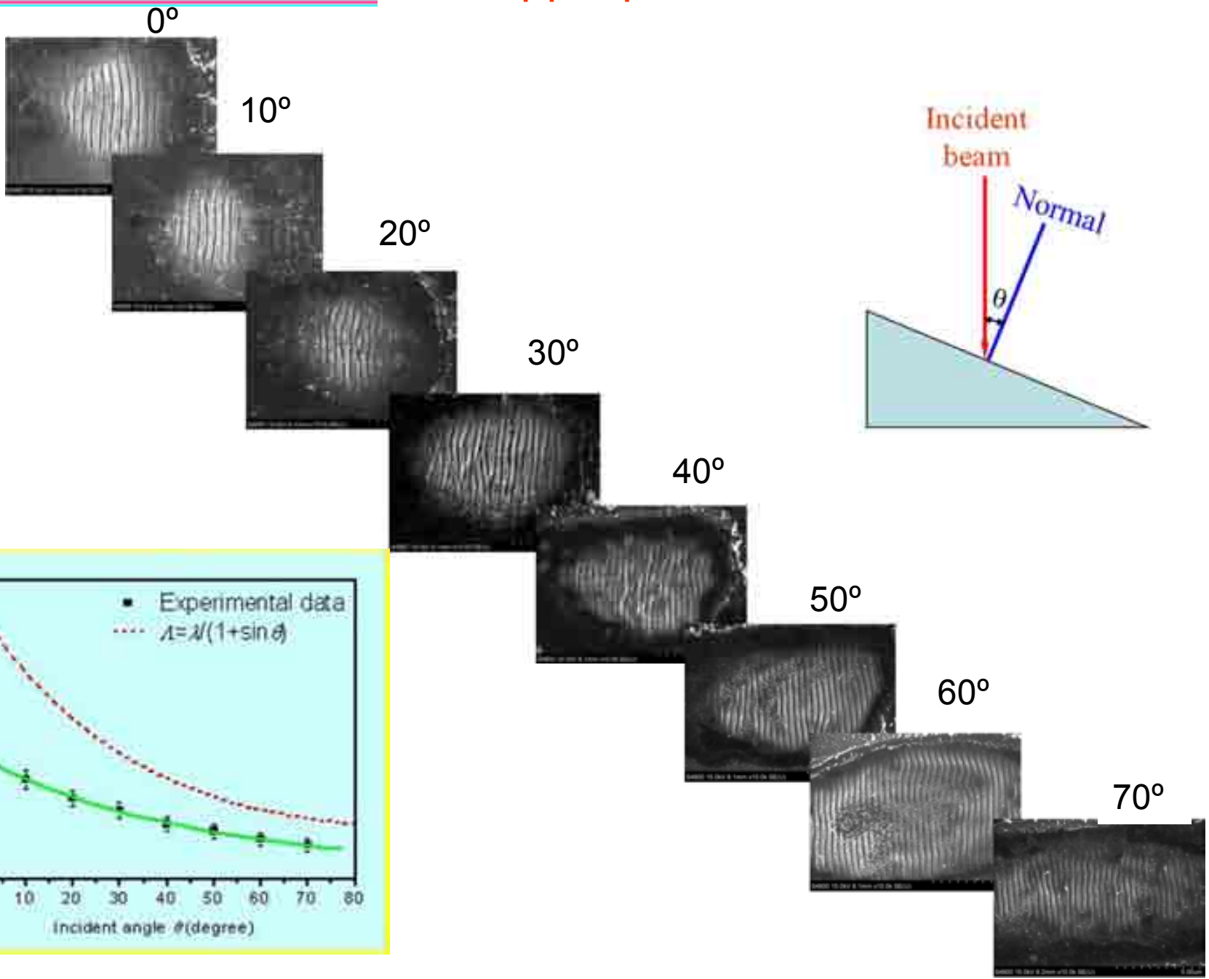

Polarization-dependent ripples

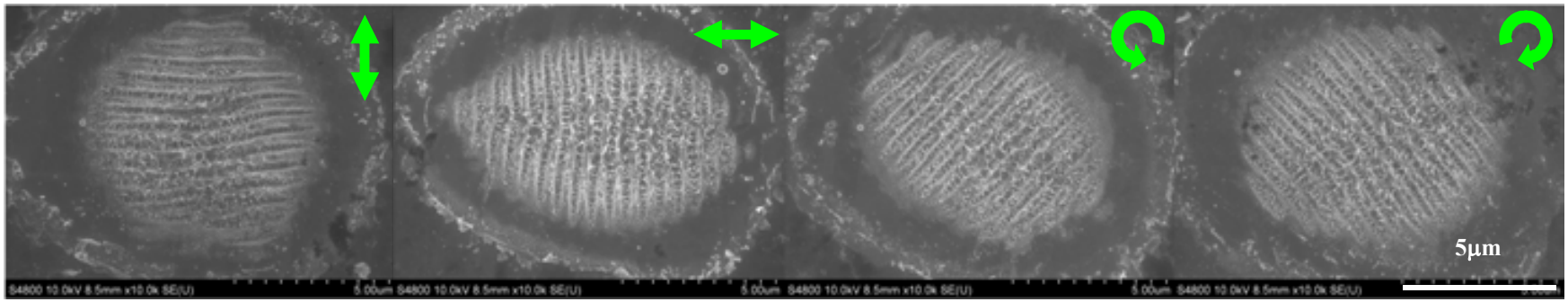

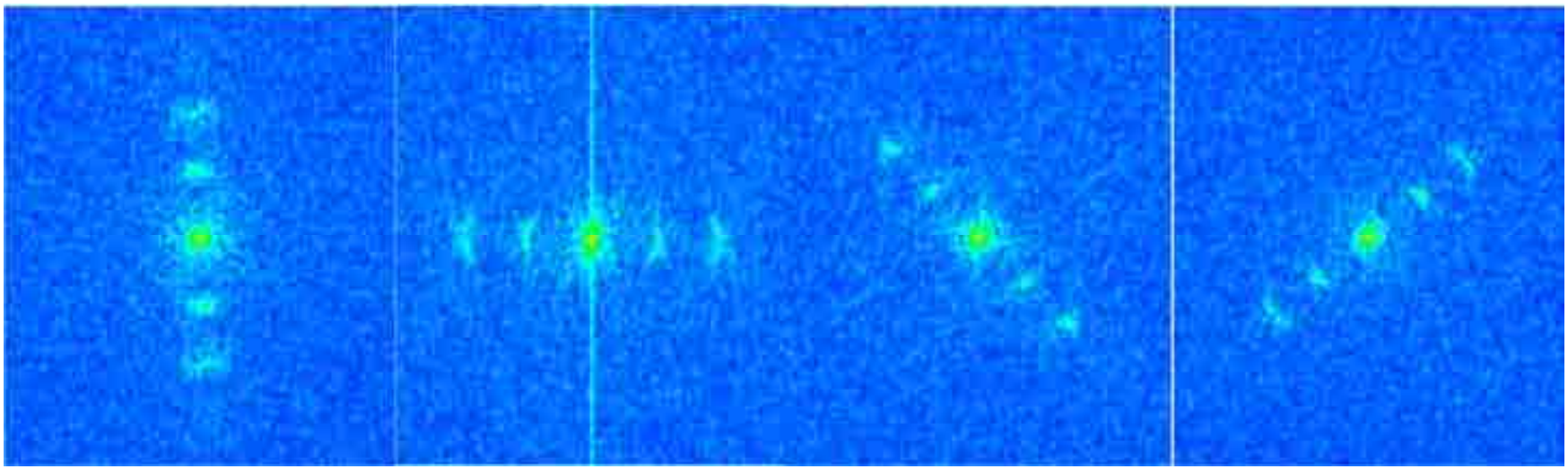

Nanospikes grown on ripples

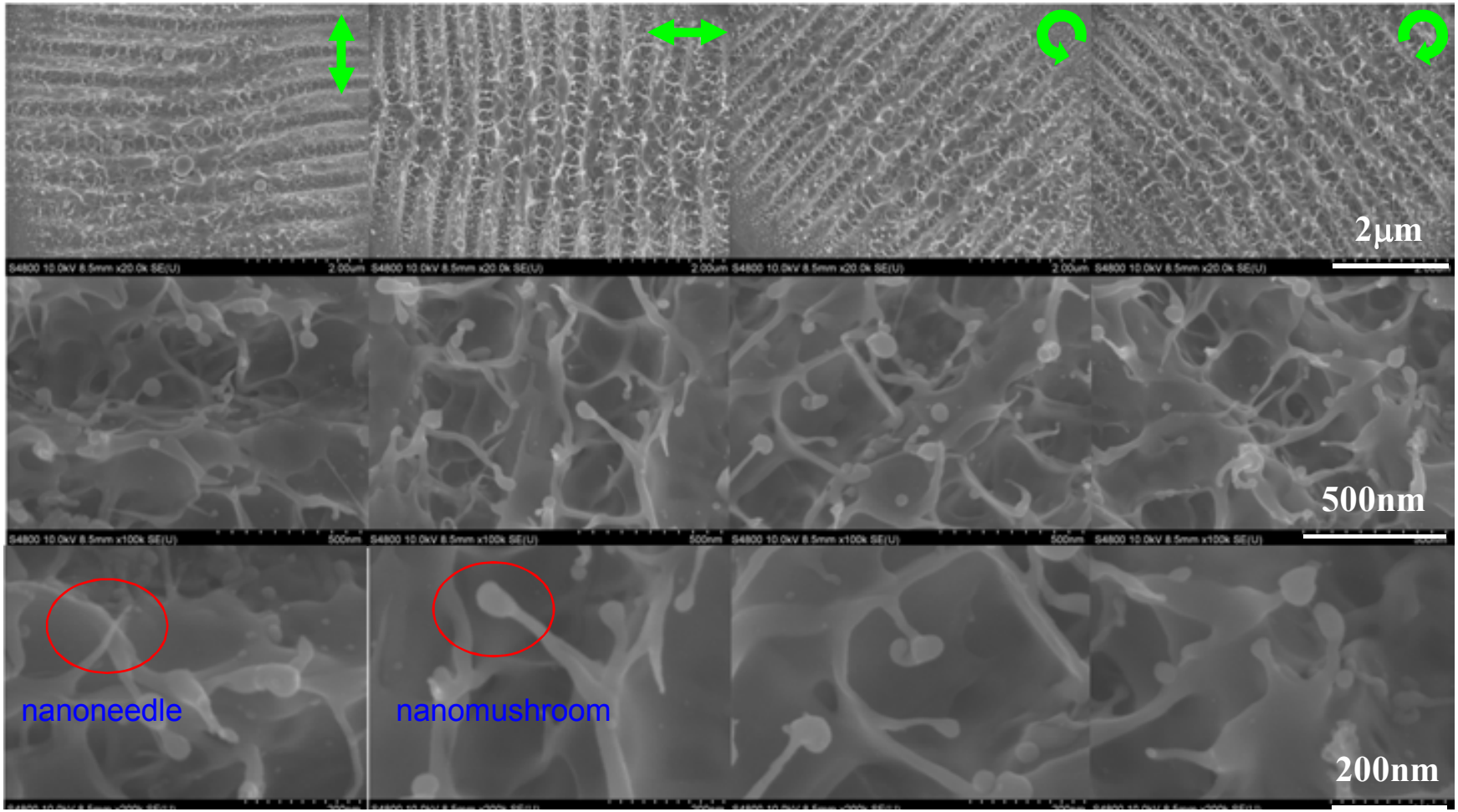

The nanospikes have a diameter ranging from 10 to 100 nm (at the neck of the mushroom-like spike) and up to 250 nm in length.

Opt. Express 15, 15741-15746 (2007)

Comparison between water ice spikes and metal spikes

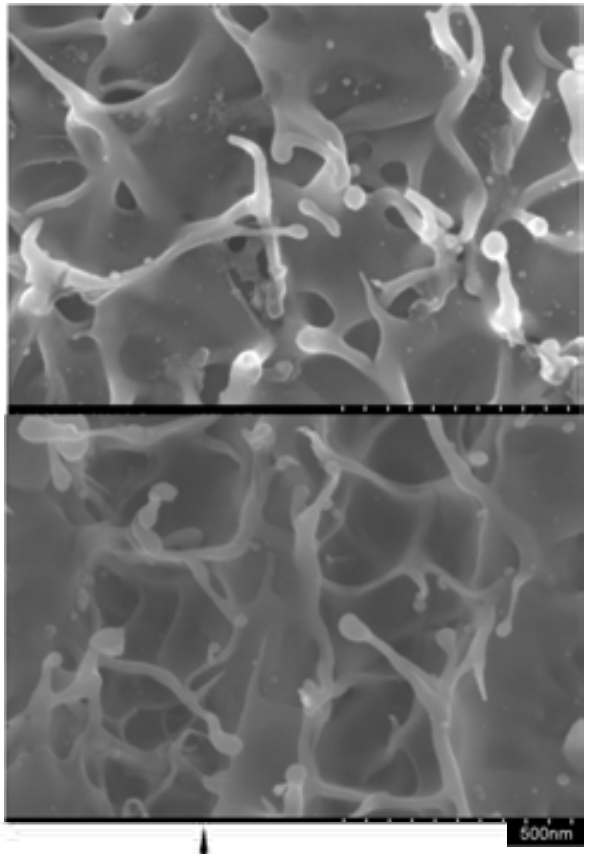

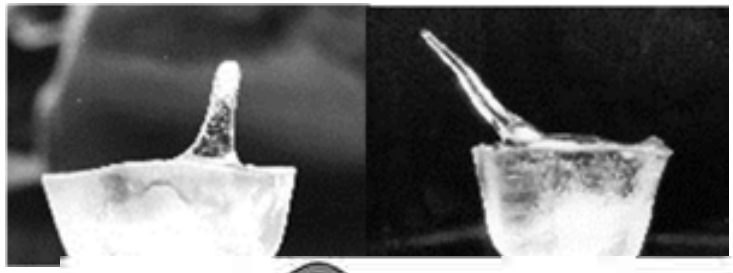

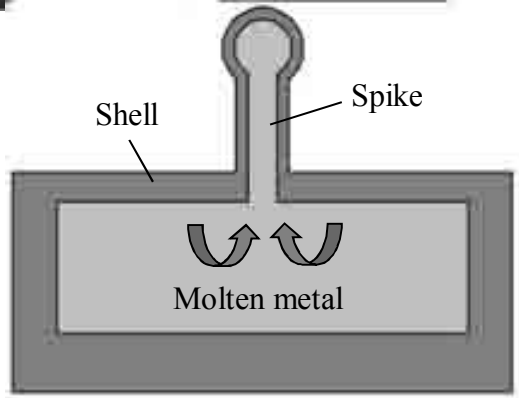

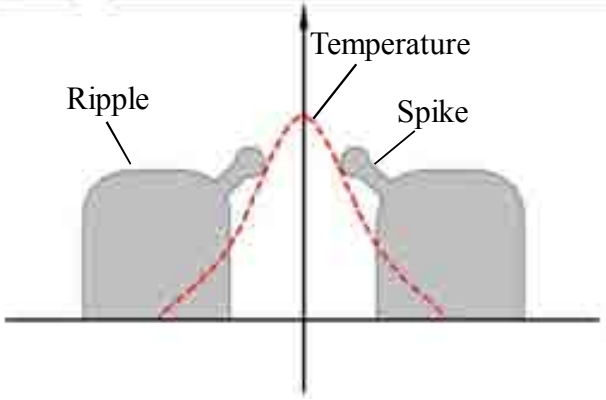

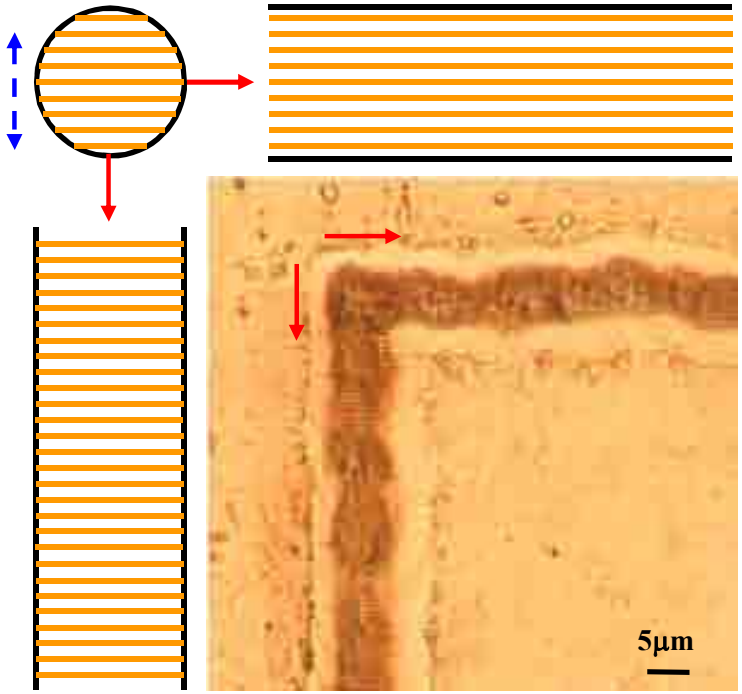
5μm

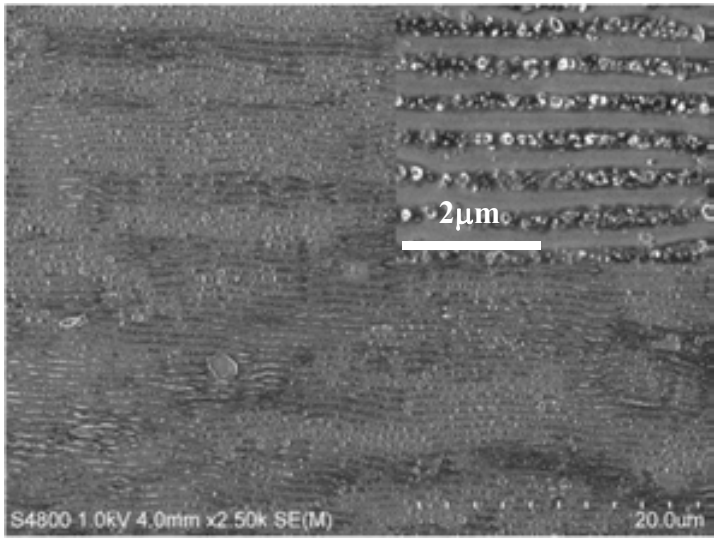
2μm
S4800 1.0kV 4.0mm x2.50k SE(M)
20.0um

Colored metal

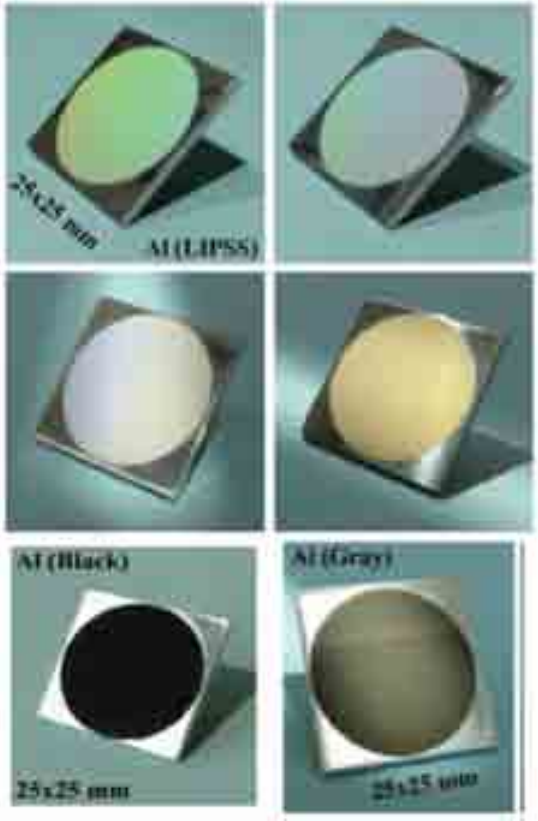

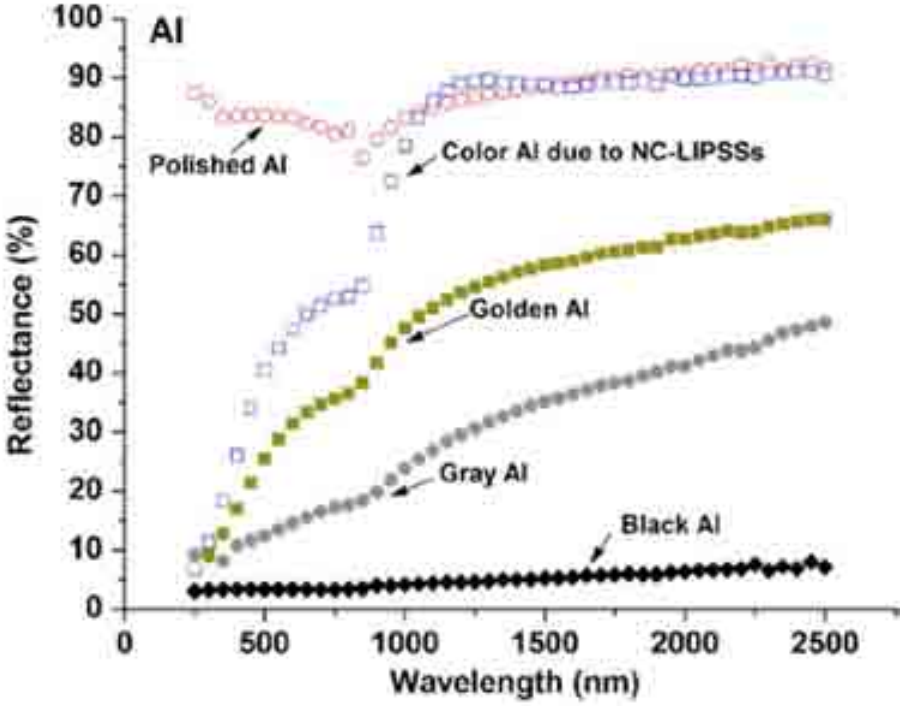

Appl. Phys. Lett. **92**, 041914 (2008).

Colored stainless steel

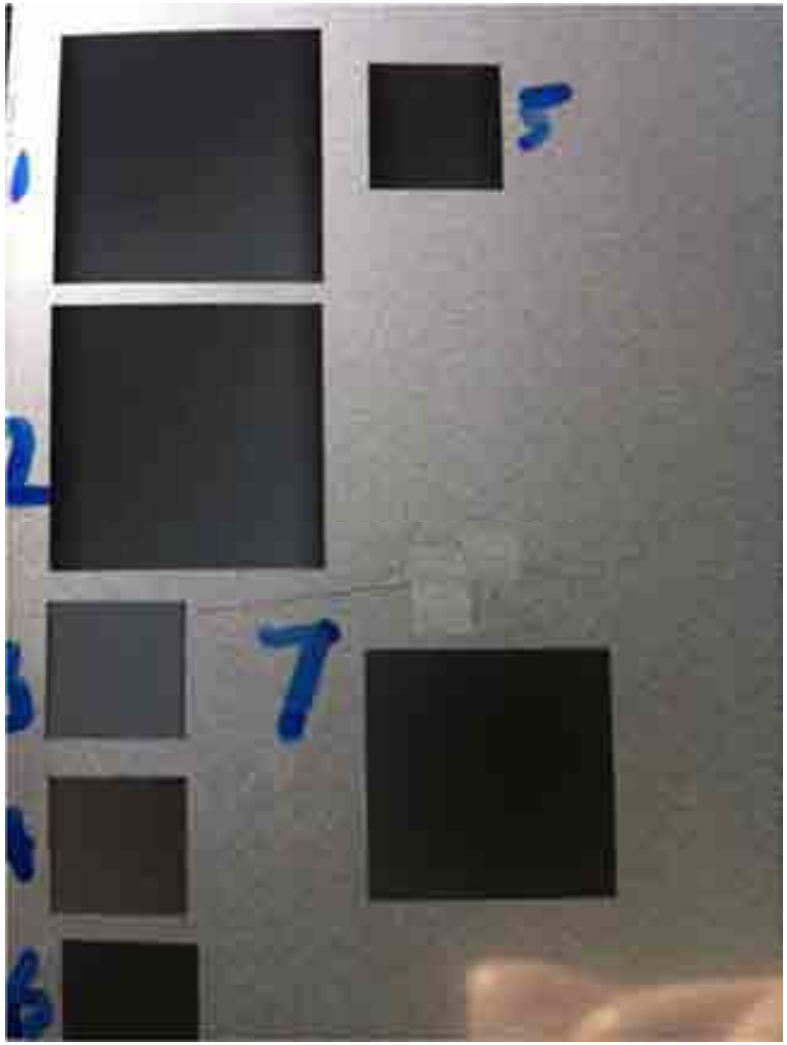

減小刀具摩擦阻力

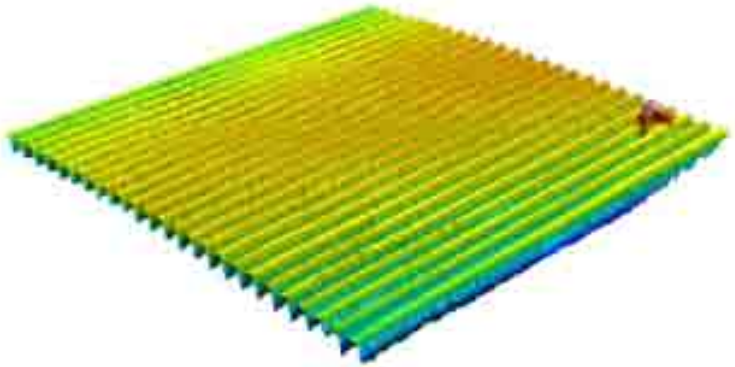

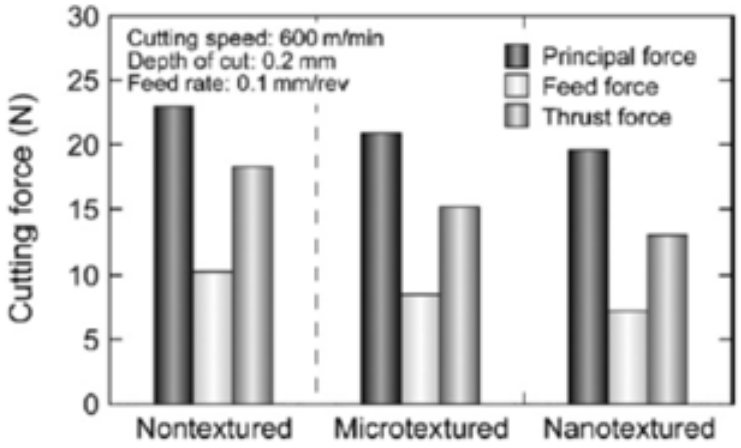

Precision Engineering 33, 248–254 (2009)

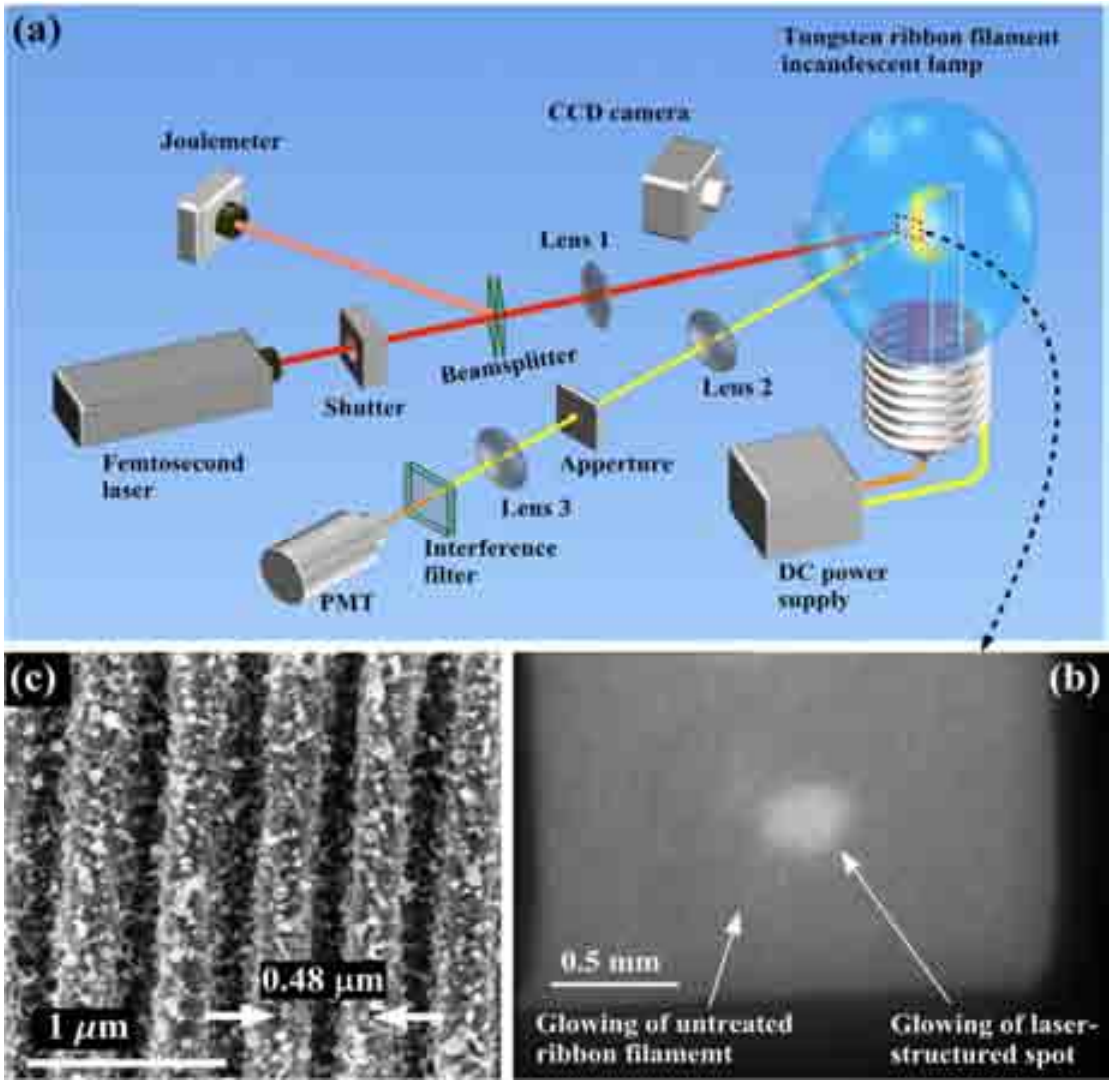

Phys. Rev. Lett. 102, 234301 (2009).

Superhydrophobic surfaces of metals

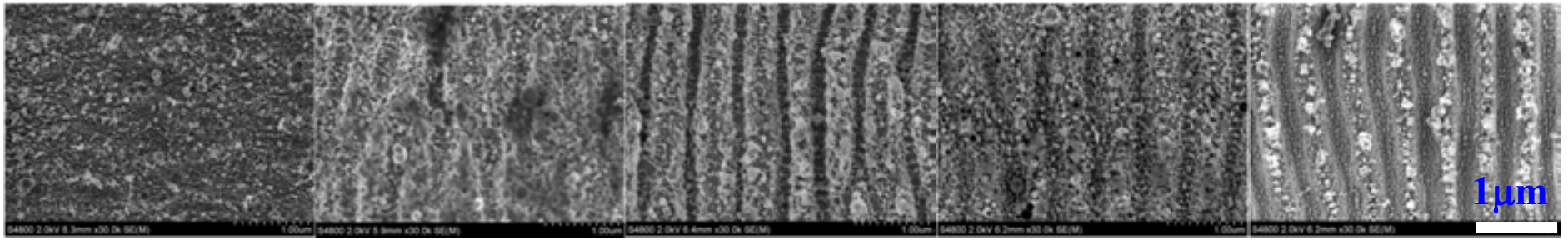

Copper Nickel Stainless steel Tantalum Tungsten

Contact angle>150º, superhydrophobic is achieved

Tuning of contact angles by the period of structures

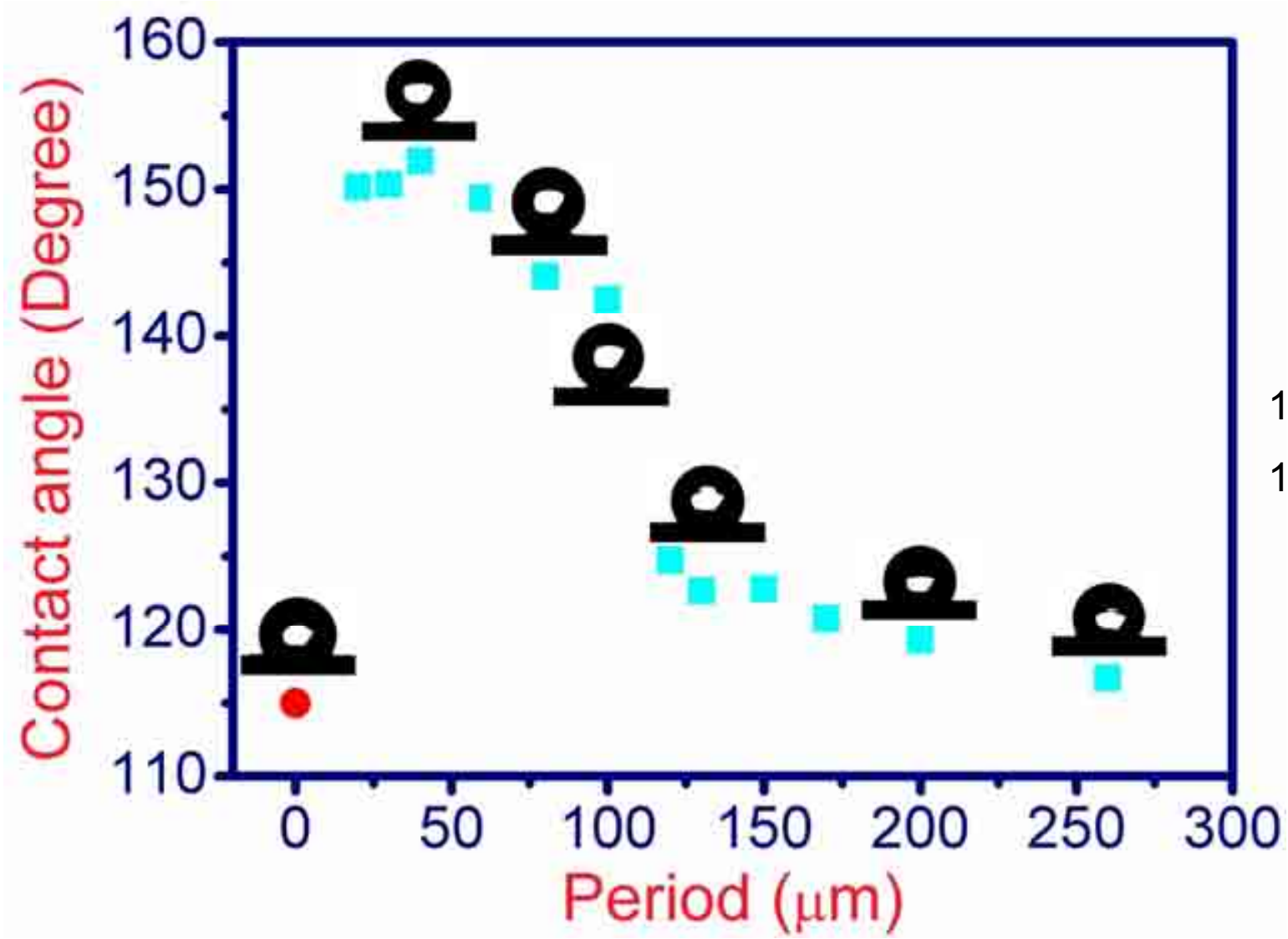

Transition from hydrophilic to hydrophobic

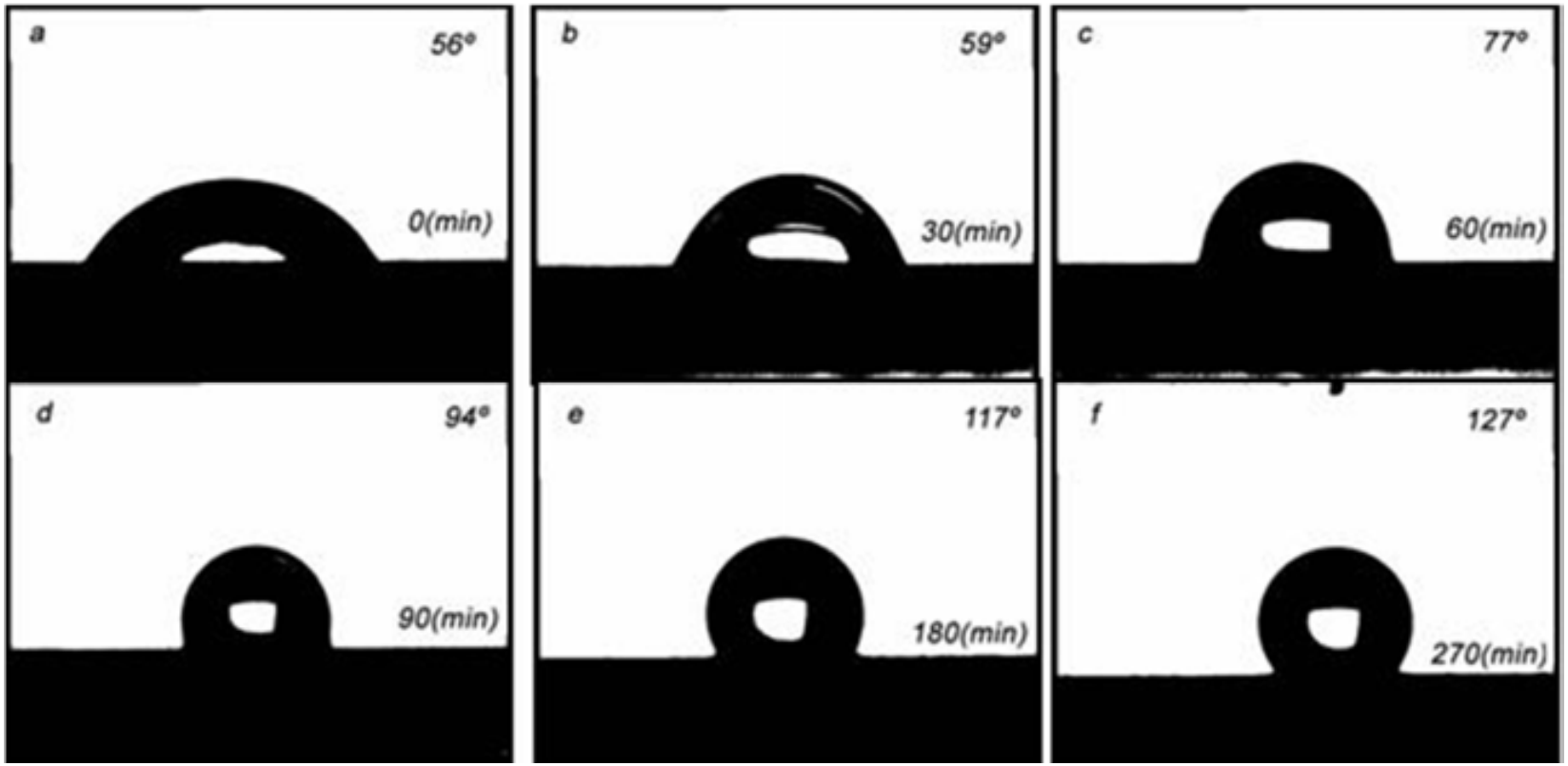

Fabrication of superhydrophobic surface on Si

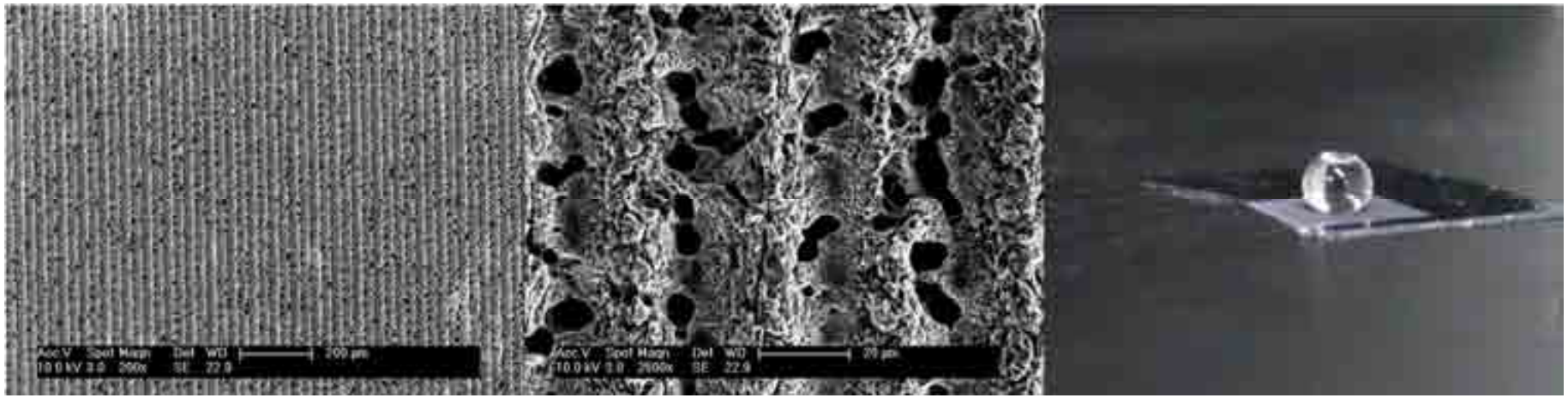

Synthesis of ZnO nanoflowers and their wettabilities

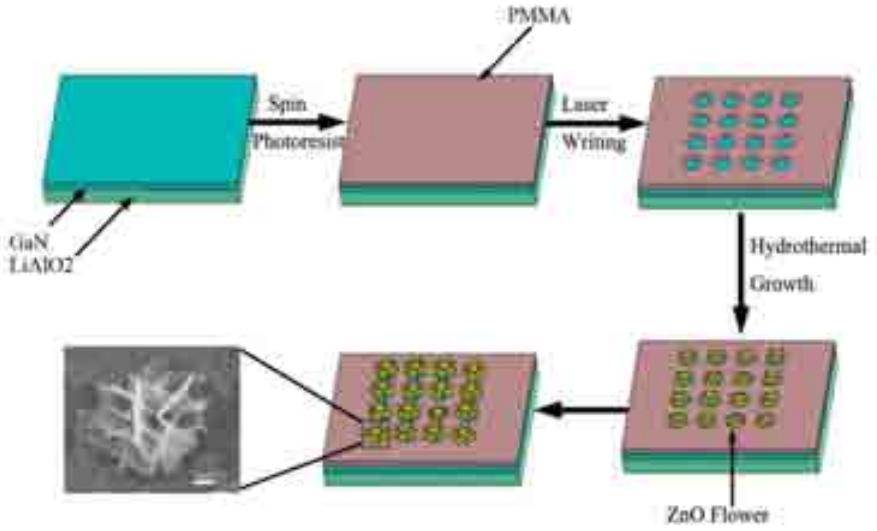

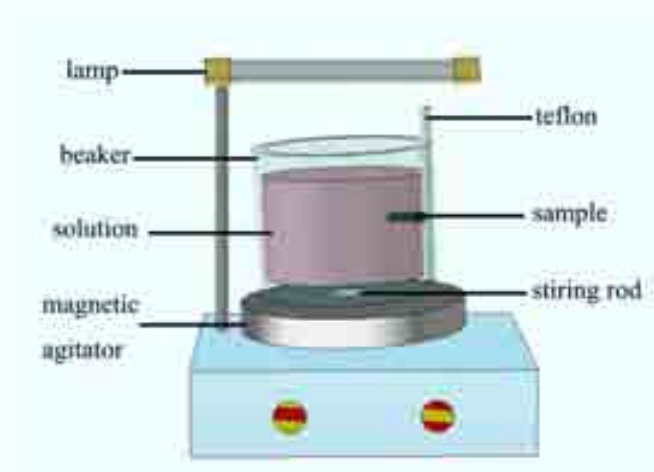

Synthesis of ZnO nanoflowers

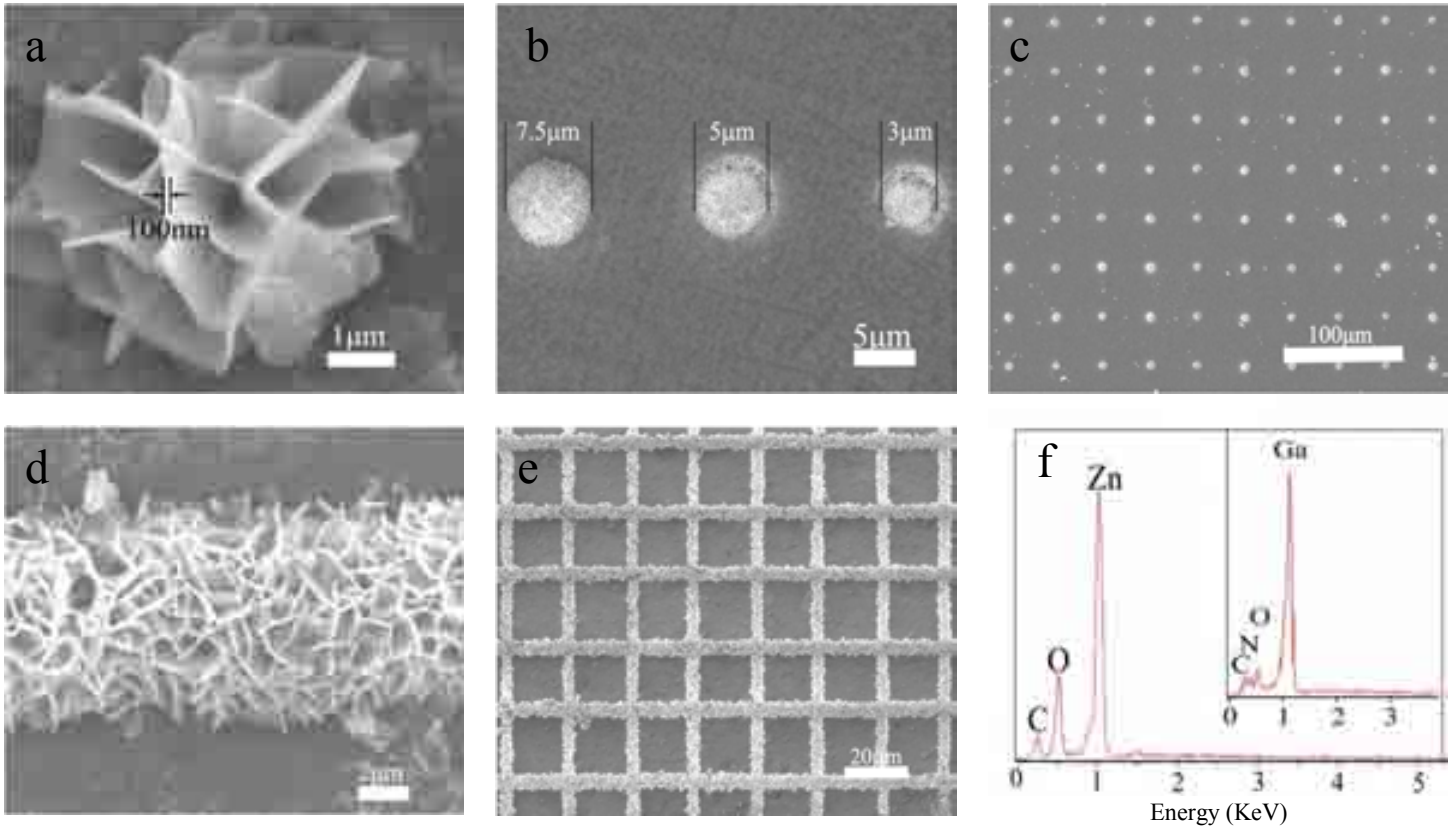

Time-dependent contact angles measurement

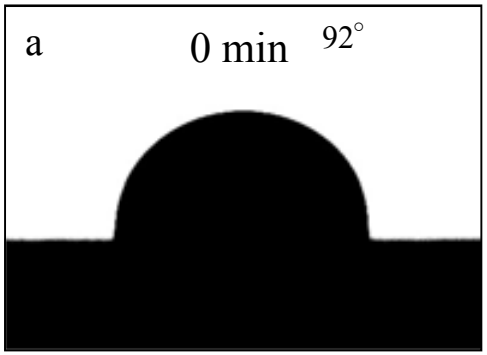

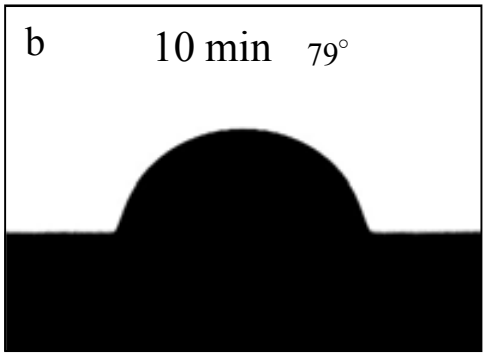

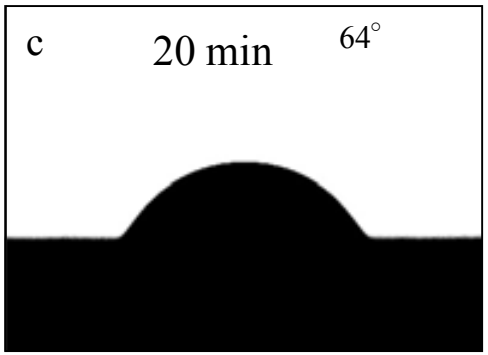

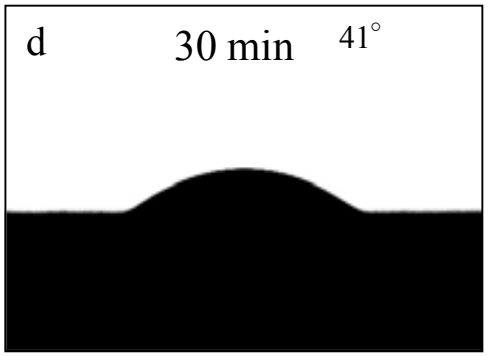

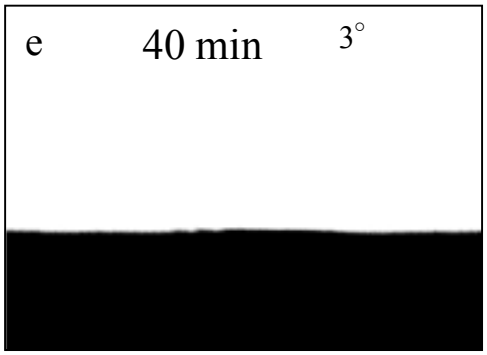

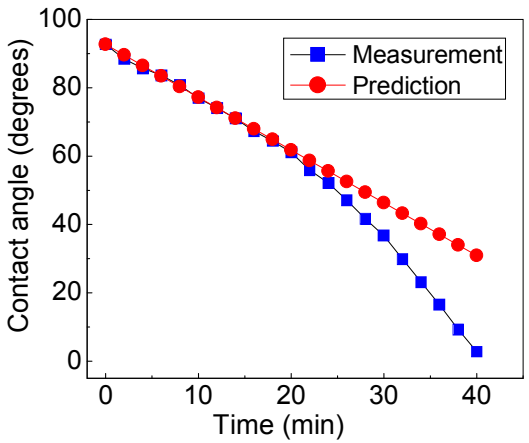

Photocatalytic Properties of ZnO Nanoflowers

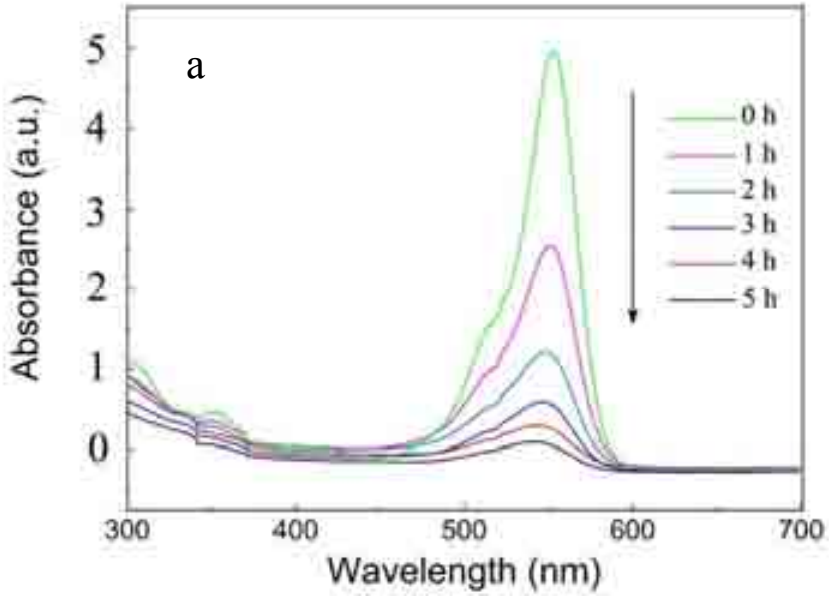

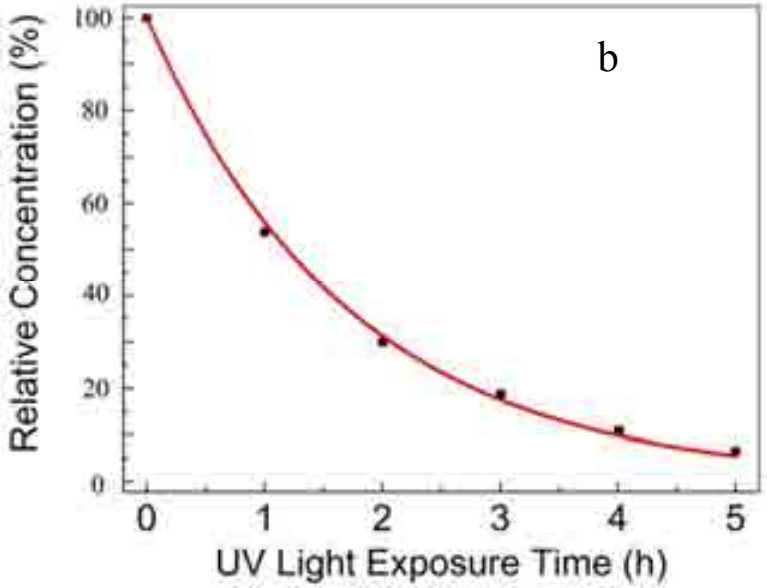

Absorption spectra of RB solution catalyzed by the ZnO nanostructure under UV irradiation.

Degradation of the RB under UV irradiation as a function of time.

Antireflection nanostructures fabricated by ultrashort laser pulses

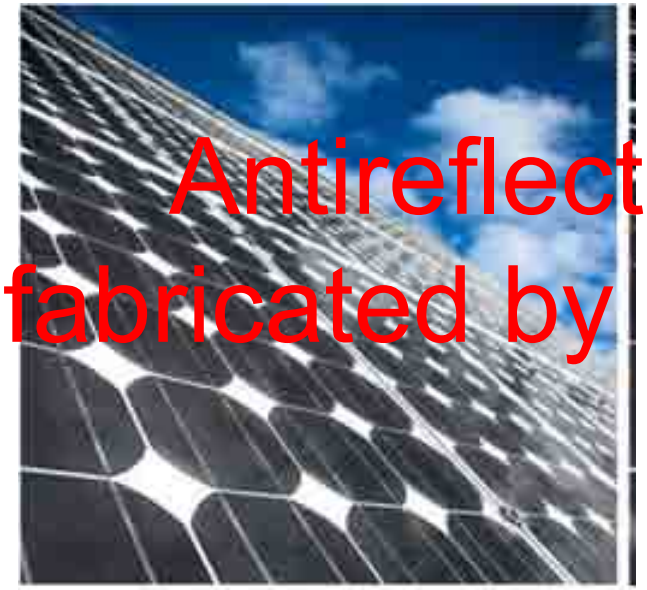

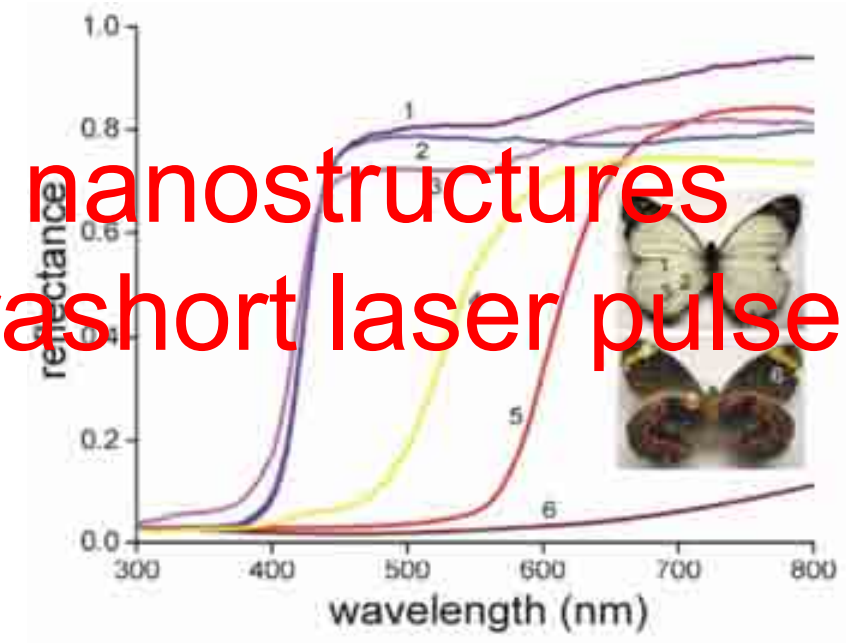

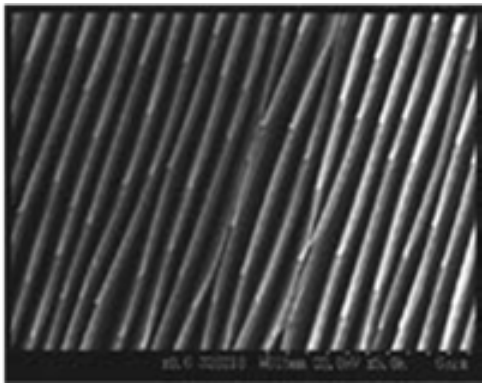

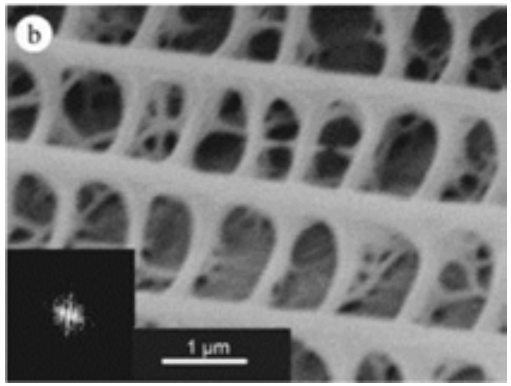

Opt. Express 14, 4880 (2006)

Fabrication of antireflection surface by fs laser nanostructuring of SiC

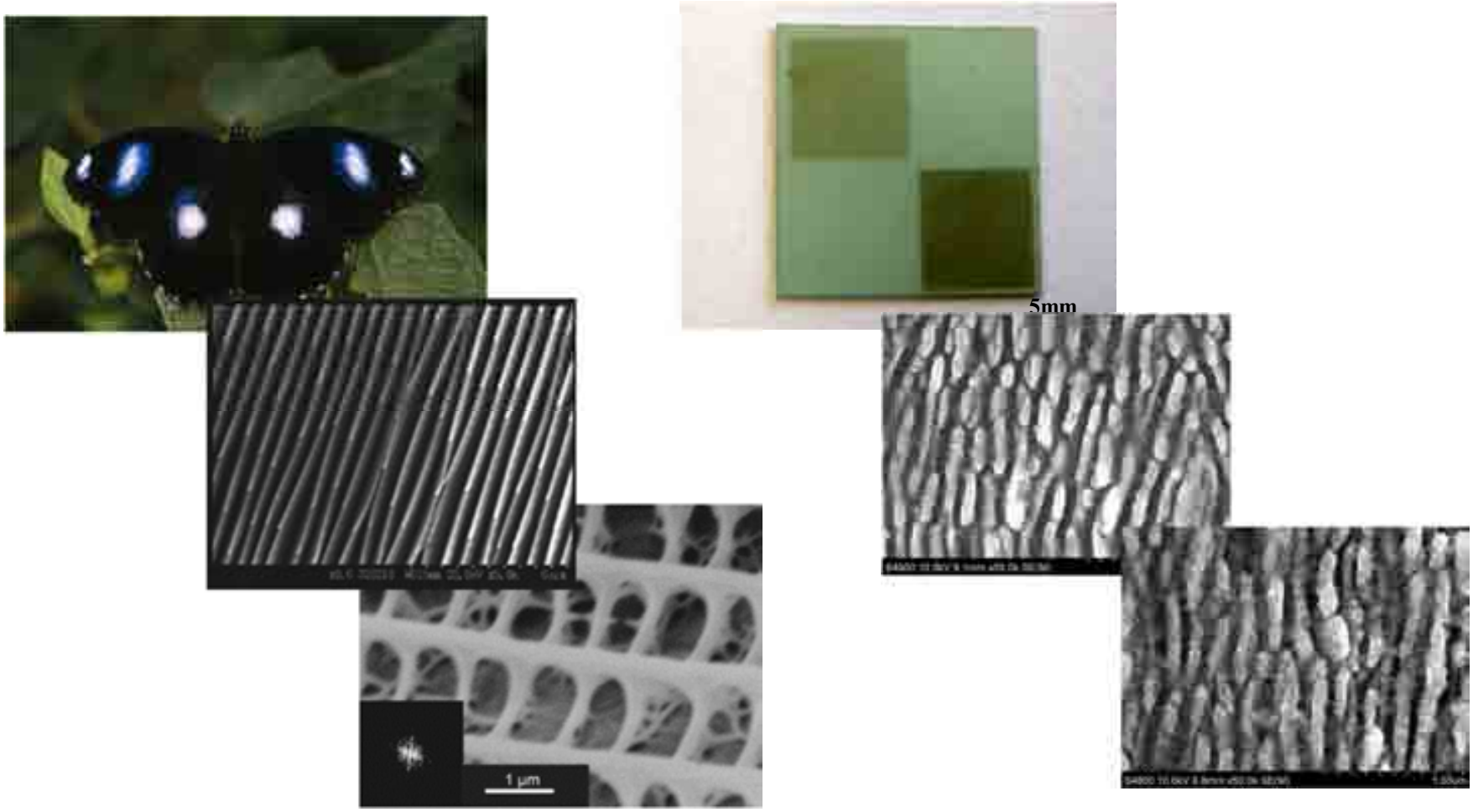

Enhancement of absorption and decreasing of reflection

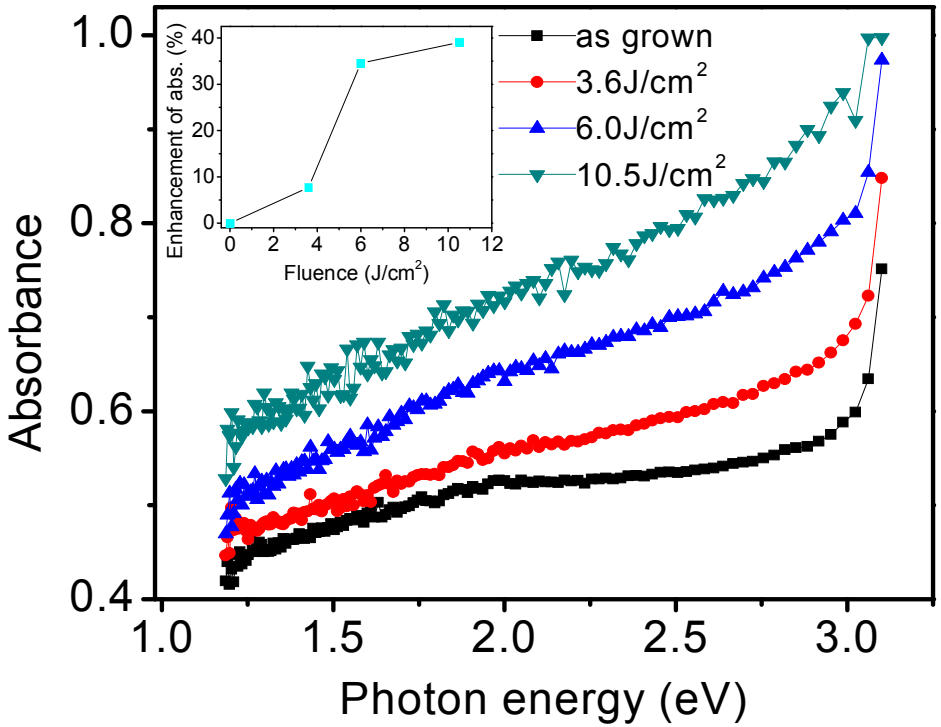

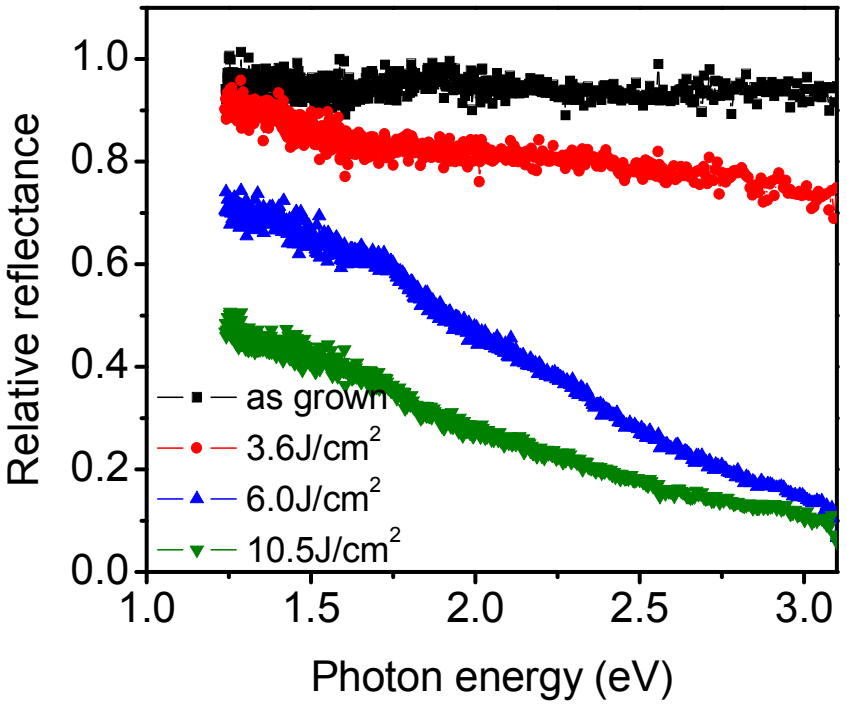

Enhancement of photocurrent

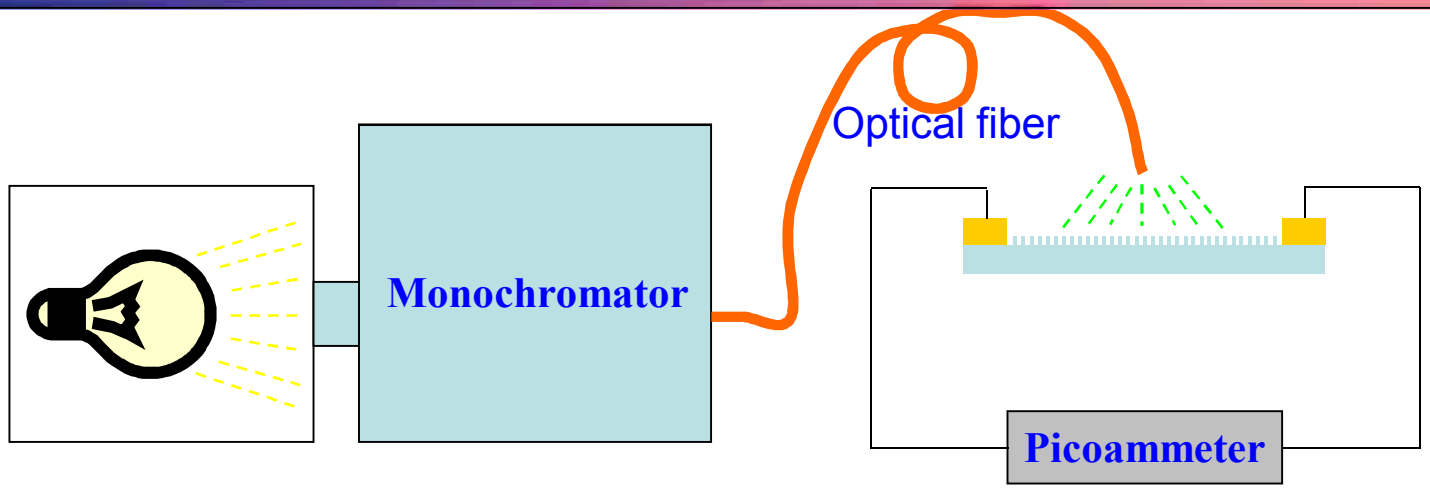

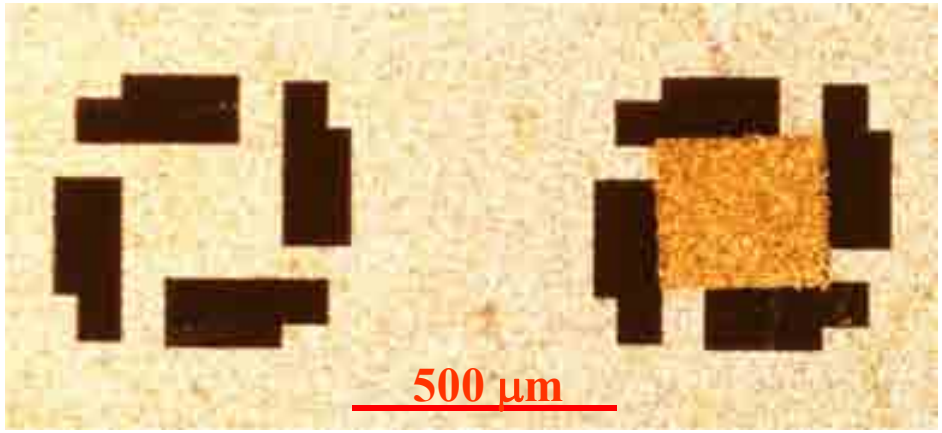

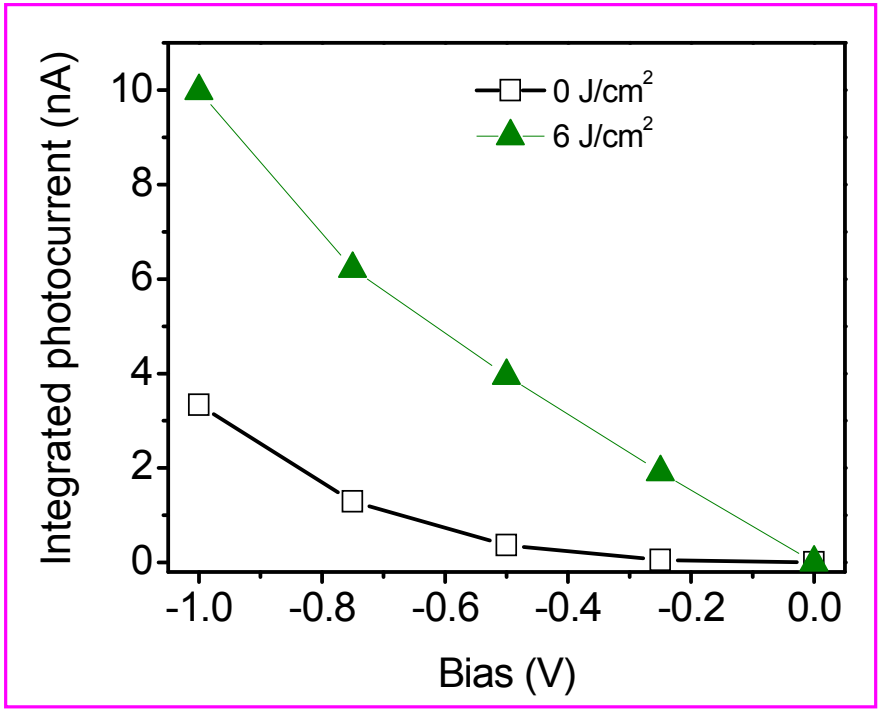

飞秒激光制备场发射的周期碳纳米结构

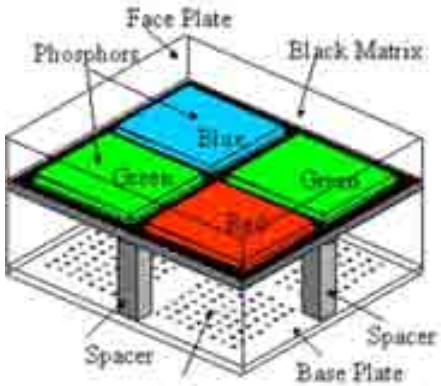

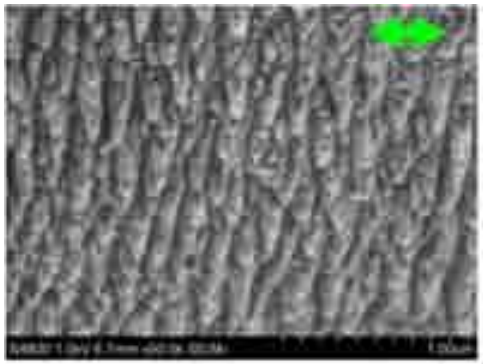

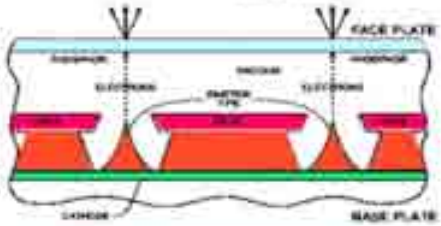

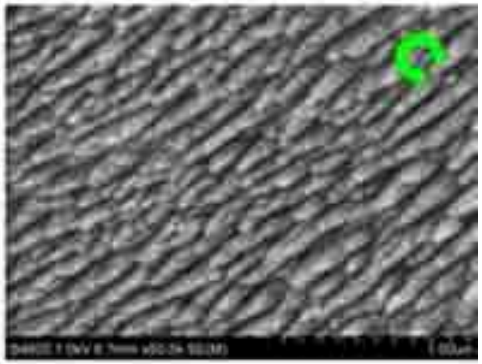

J. Appl. Phys. 105, 083103 (2009).

Polarization-dependent of nanochain orientation

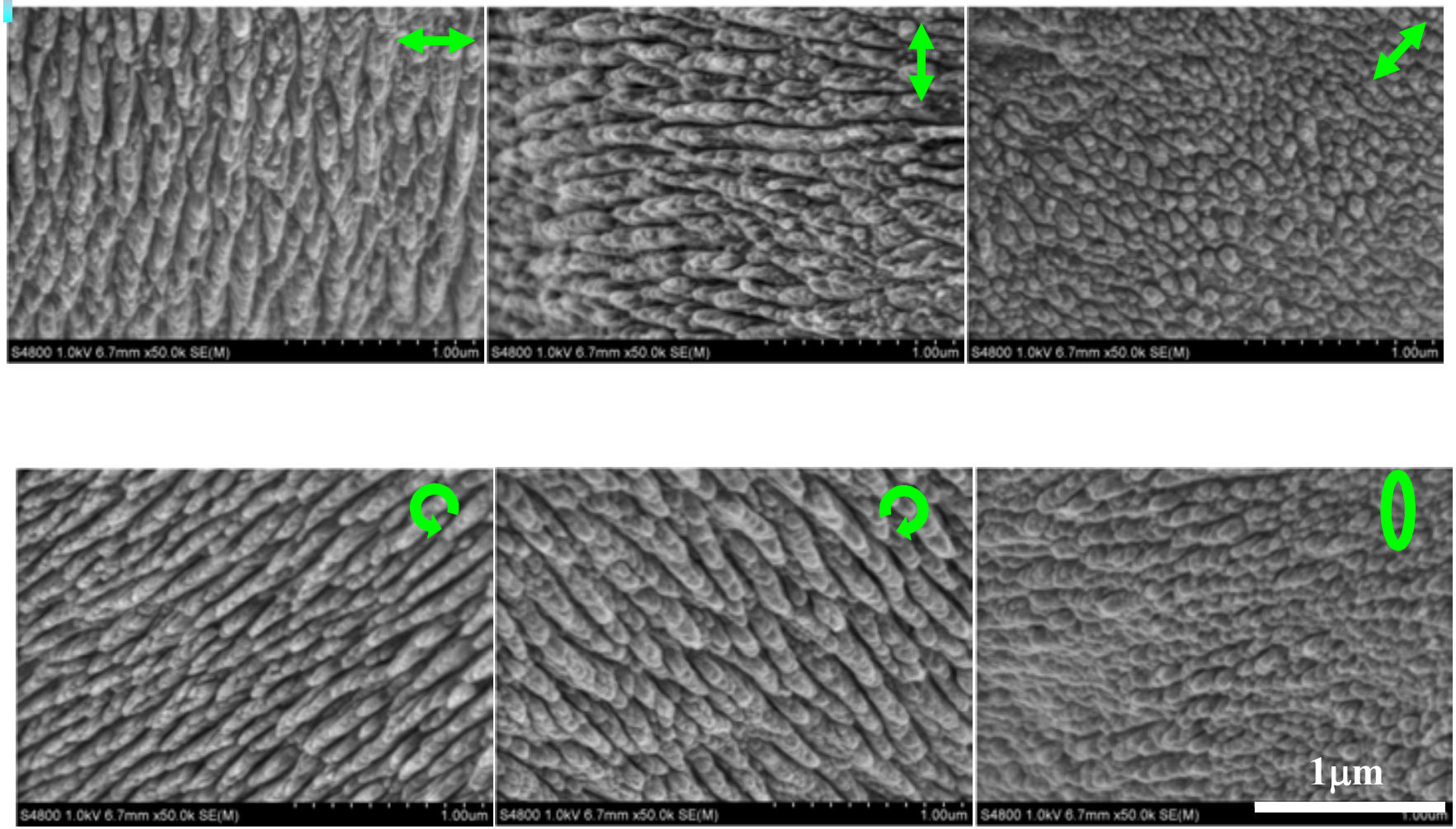

场发射性能

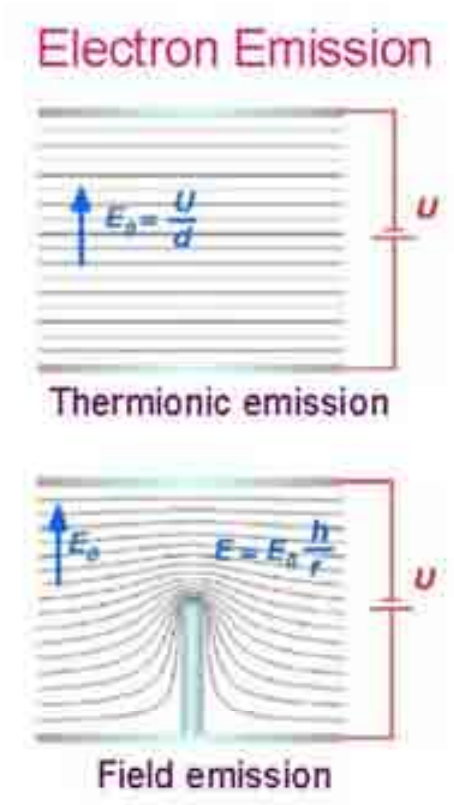

$$J = A\left(\beta^2 E^2/\phi\right)\exp\left(-B\phi^{3/2}/\beta E\right)$$

Fowler-Nordheim Equation

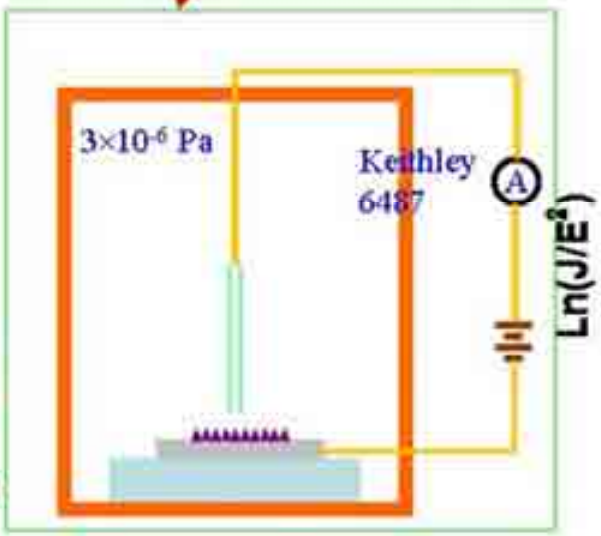

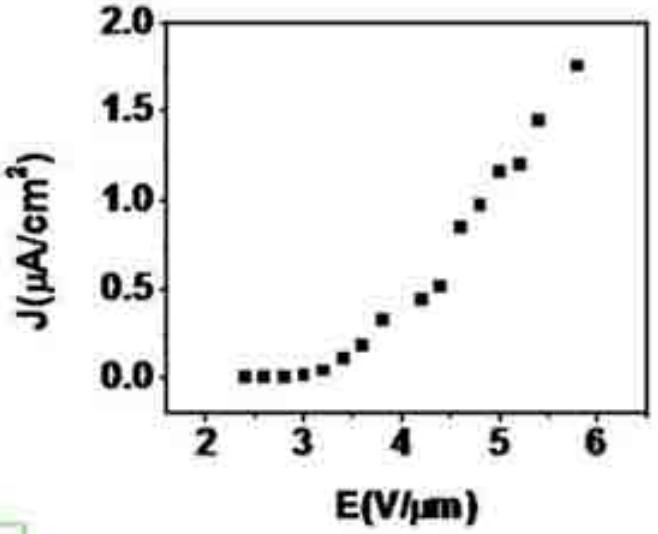

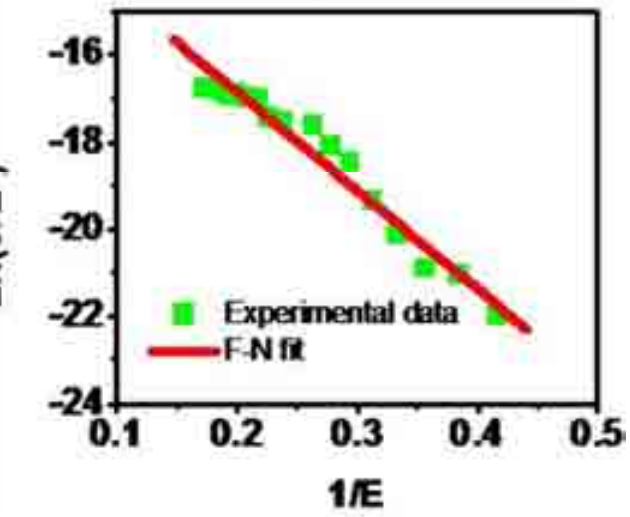

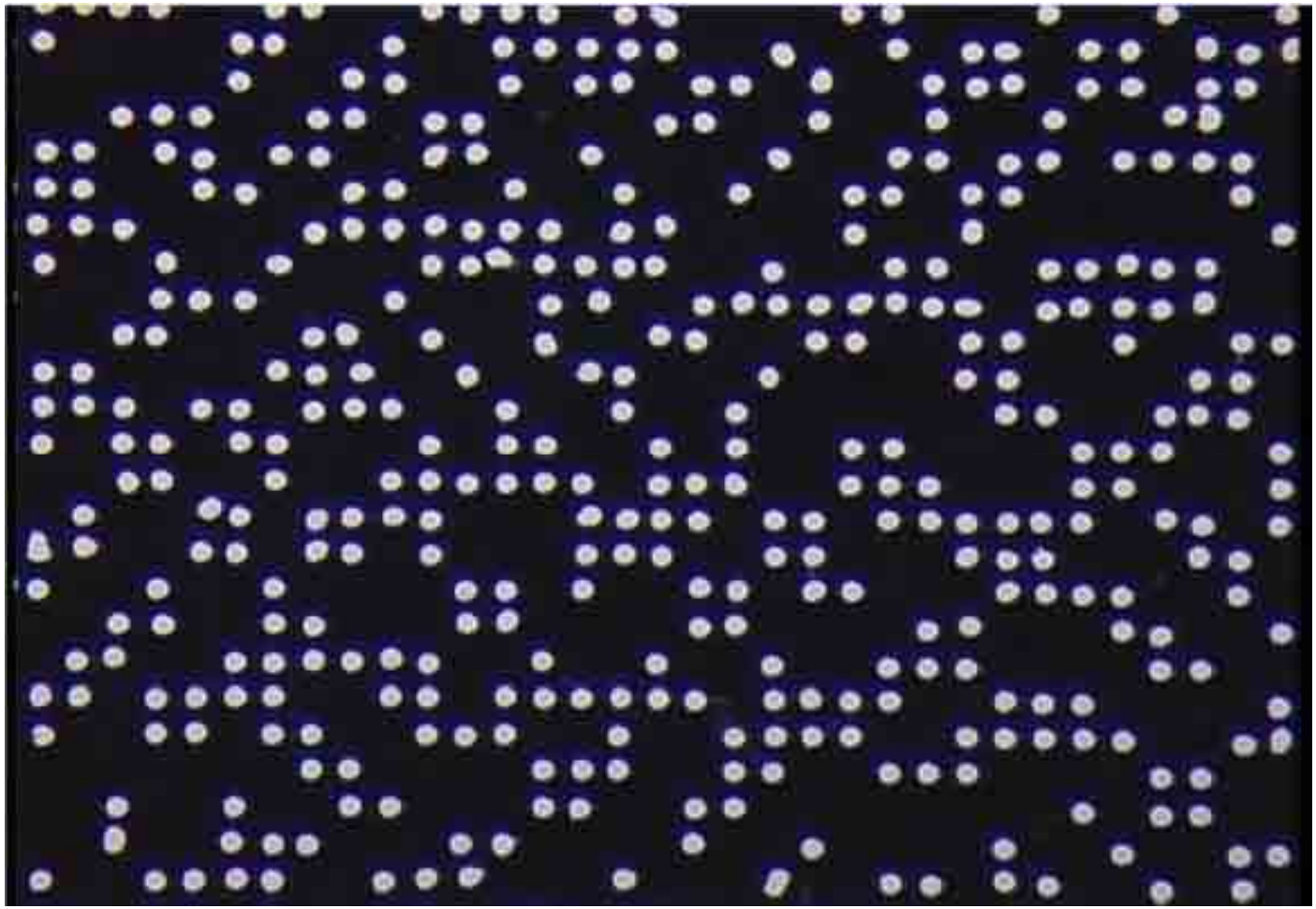

Recording

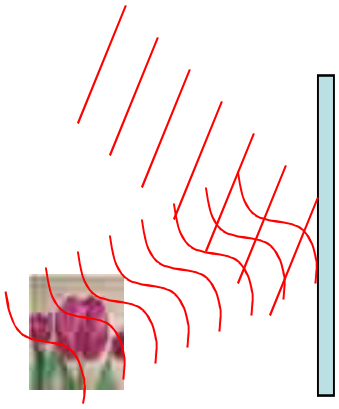

Reconstruction

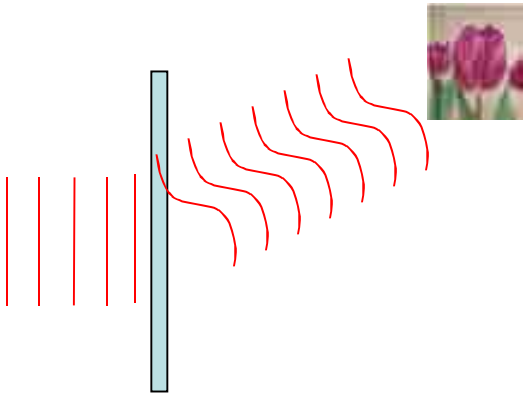

SIOM simulated algorithm → Data of binary phase → Input → Computer → Drive 3D stage → Laser writing

Fabrication of computer-generated holograms

SIOM

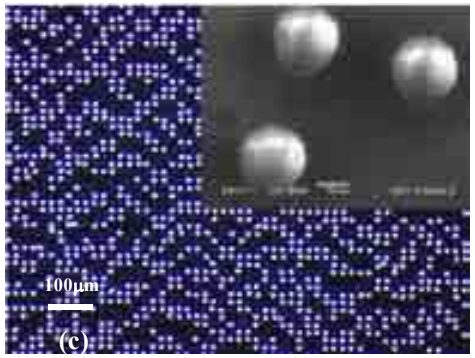

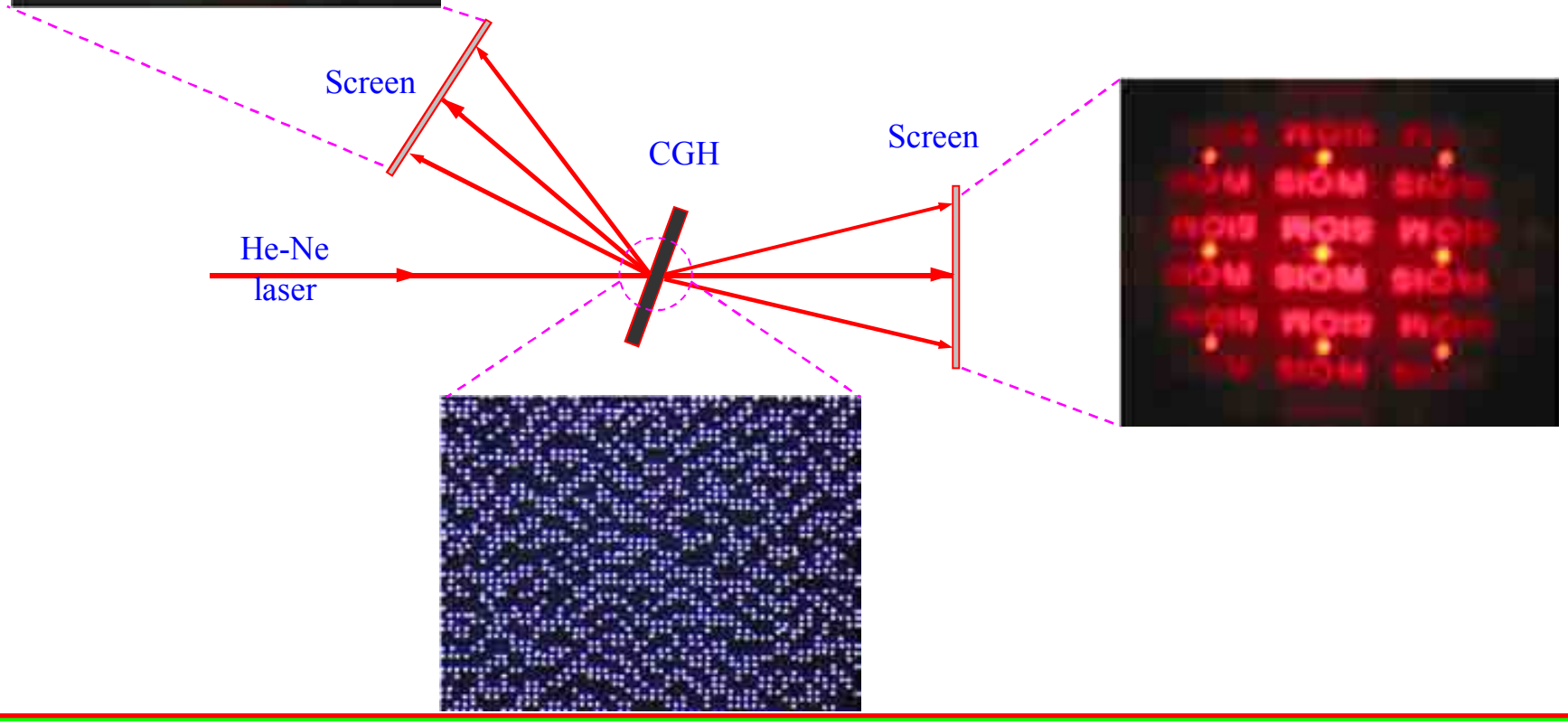

Fabrication of periodic microstructures by multibeam interfered fs laser pulses

1D

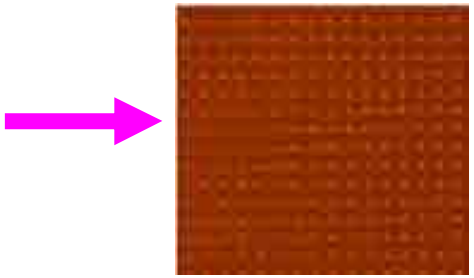

2D

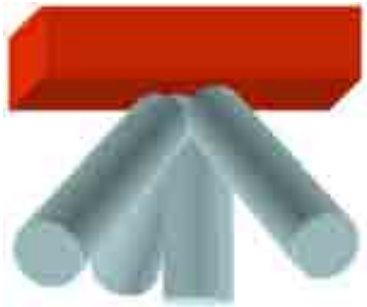

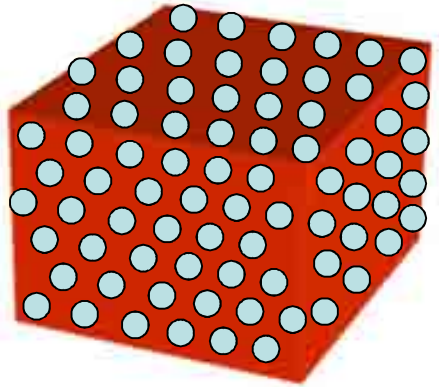

3D

Two kinds of beam delivery approaches

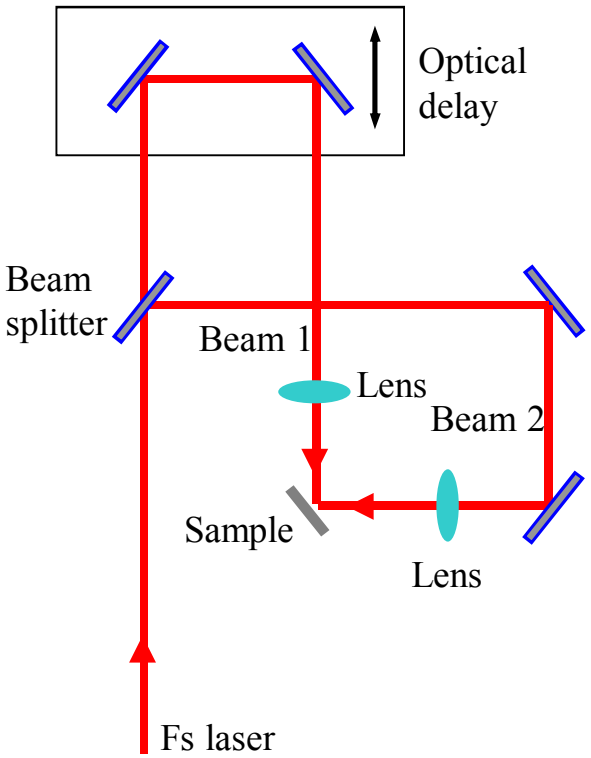

Precise adjustments of optical delay by observing the SHG or THG to obtain the temporal overlap of femtosecond pulses.

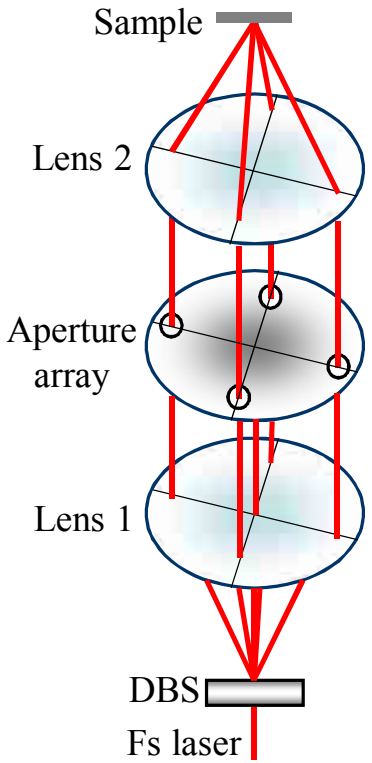

The optical setup is quite simple and temporal overlap is achieved without any adjustments.

Writing of micrograting in glass by two-beam fs laser interference

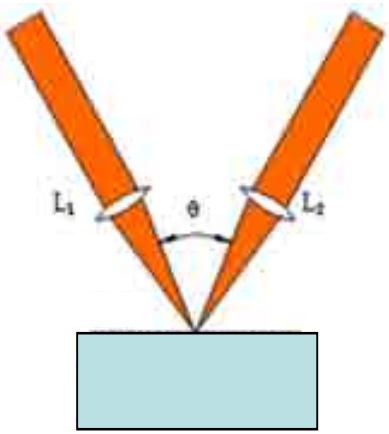

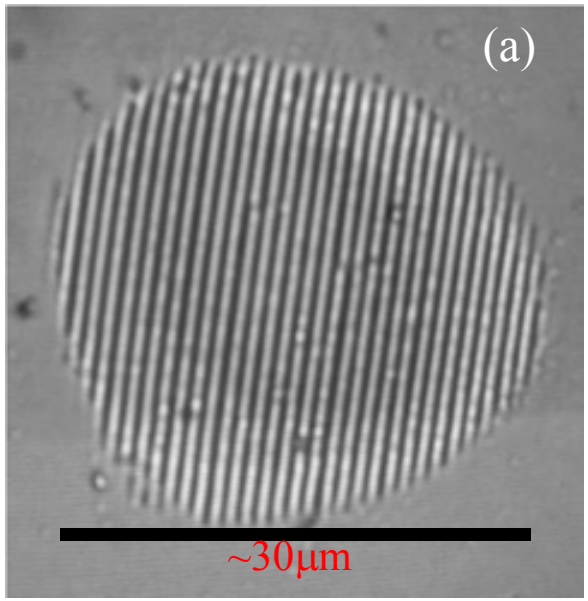

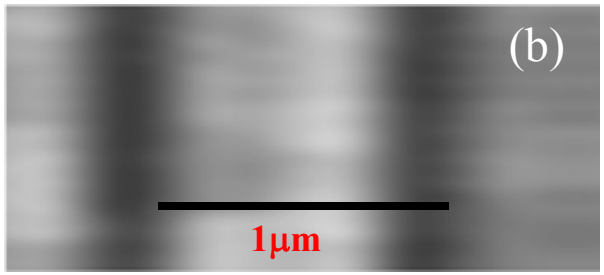

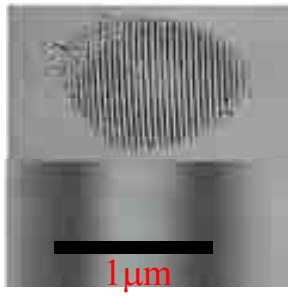

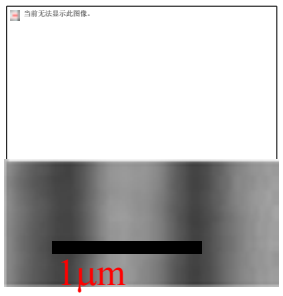

(a) $E_{1,2}$ ~70μJ, θ~40°

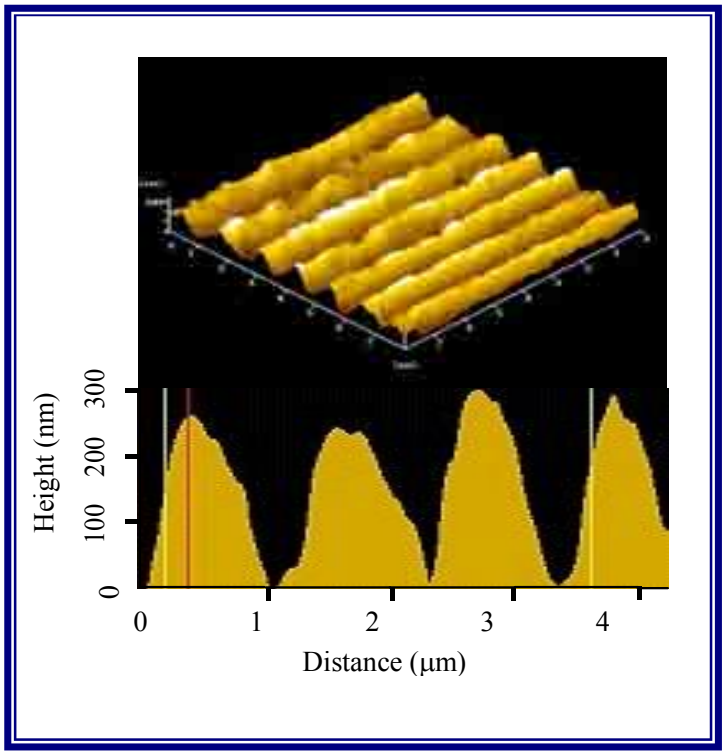

(b) $E_{1,2}$ ~100μJ, θ~85°

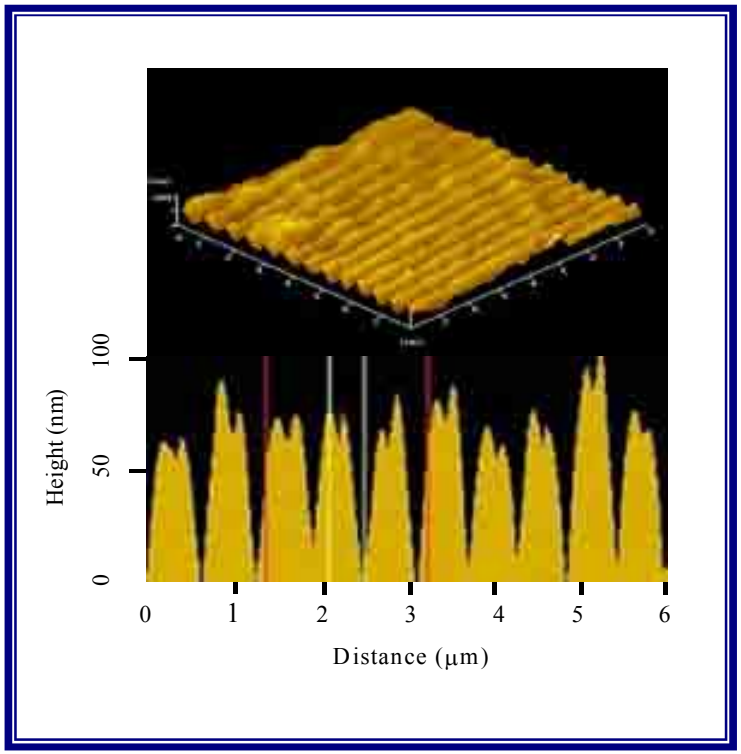

Formation of array microstructures on silicon

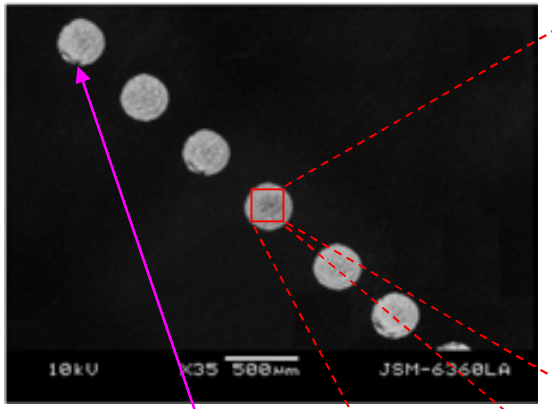

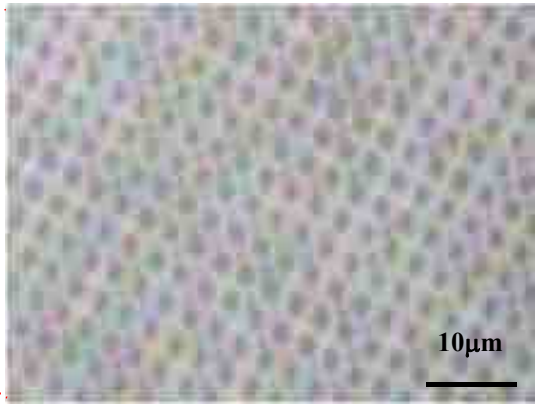

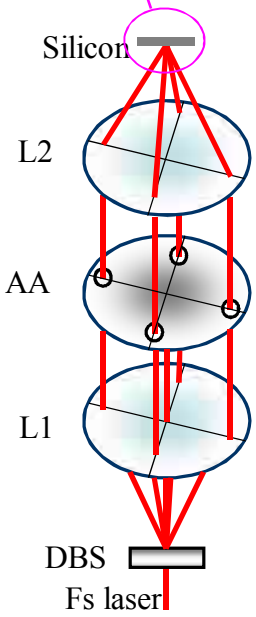

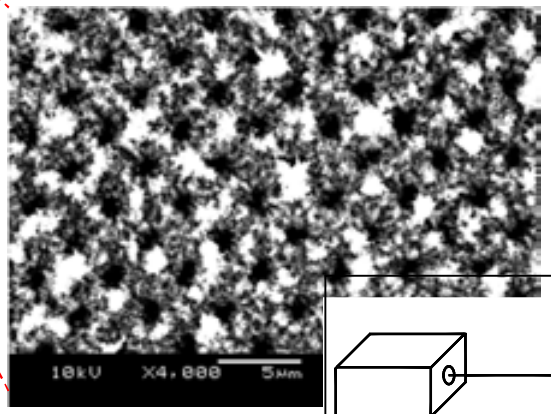

Spots with a diameter of about 300μm, exposure process (~5s).

A four-fold symmetric structure was induced on the silicon surface.

The period of array structures was about 2.5 μm.

As the exposure time is up to 5s, the ablated surface deposited much oxidized debris.

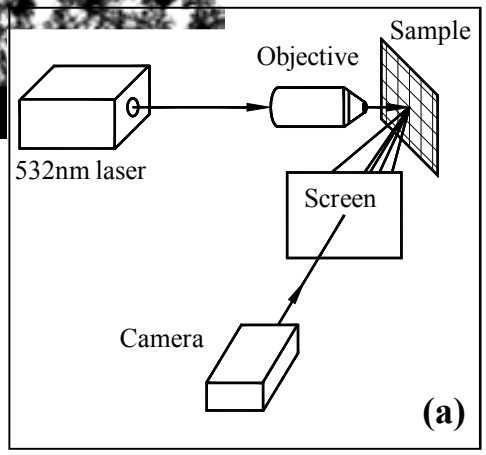

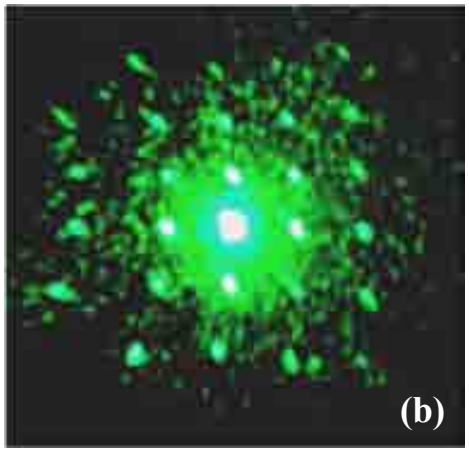

Formation of array microstructures on Al film

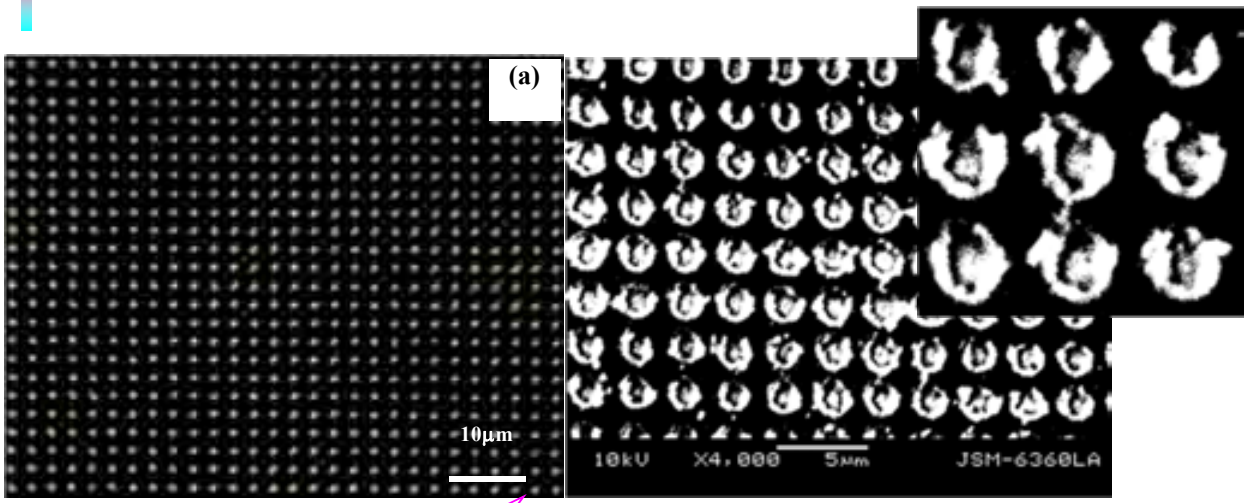

"bead in the hole"

Diffraction characteristics

Arrayed microstructures on Al film

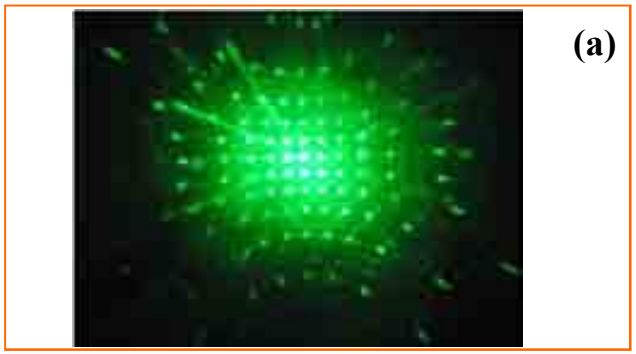

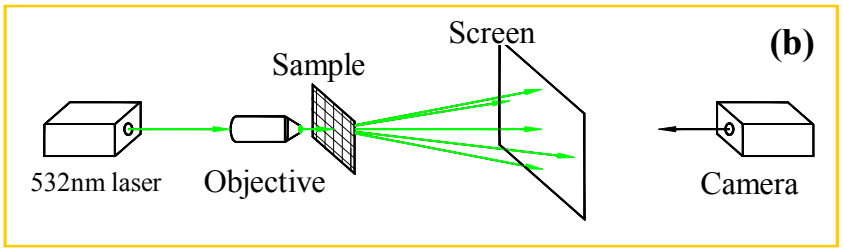

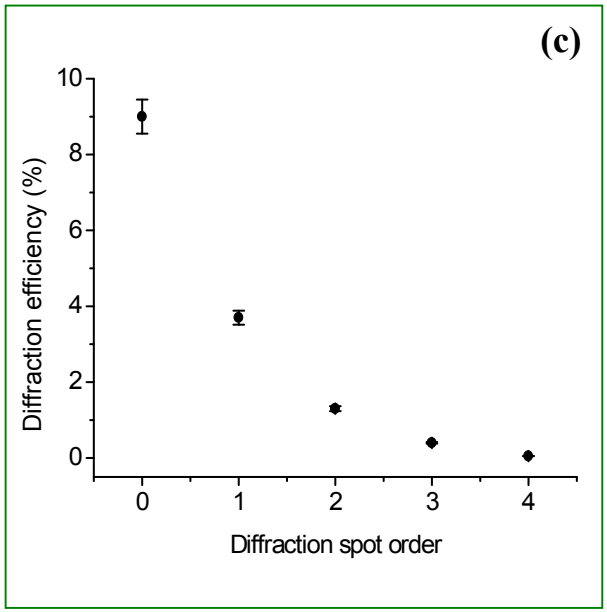

转写周期微结构

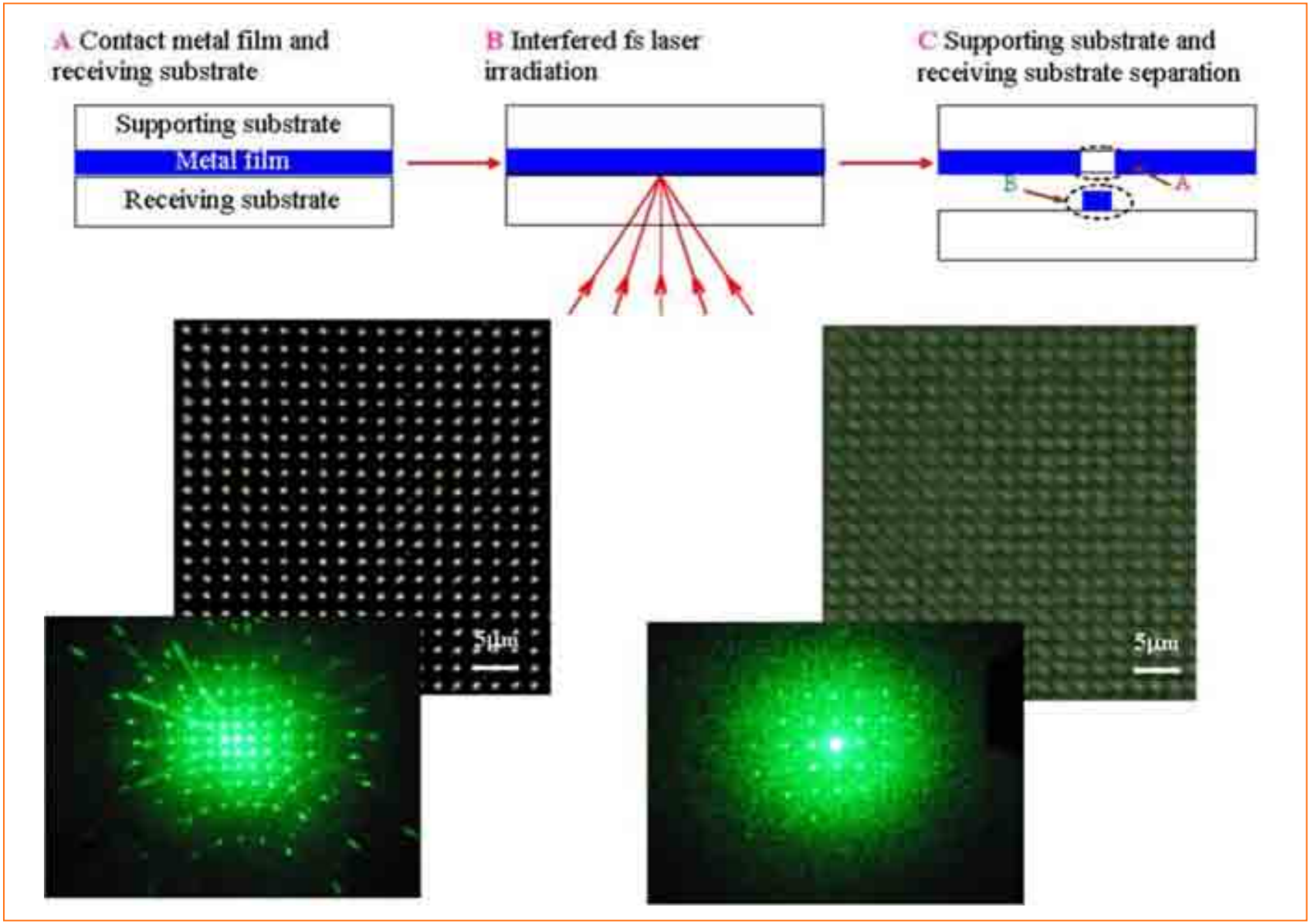
A Contact metal film and receiving substrate
B Interfered fs laser irradiation
C Supporting substrate and receiving substrate separation
Supporting substrate
Metal film
Receiving substrate
B
A
5μm
5μm

超短脉冲激光诱导材料内部功能结构

Fs laser induced refractive index change (Δn)

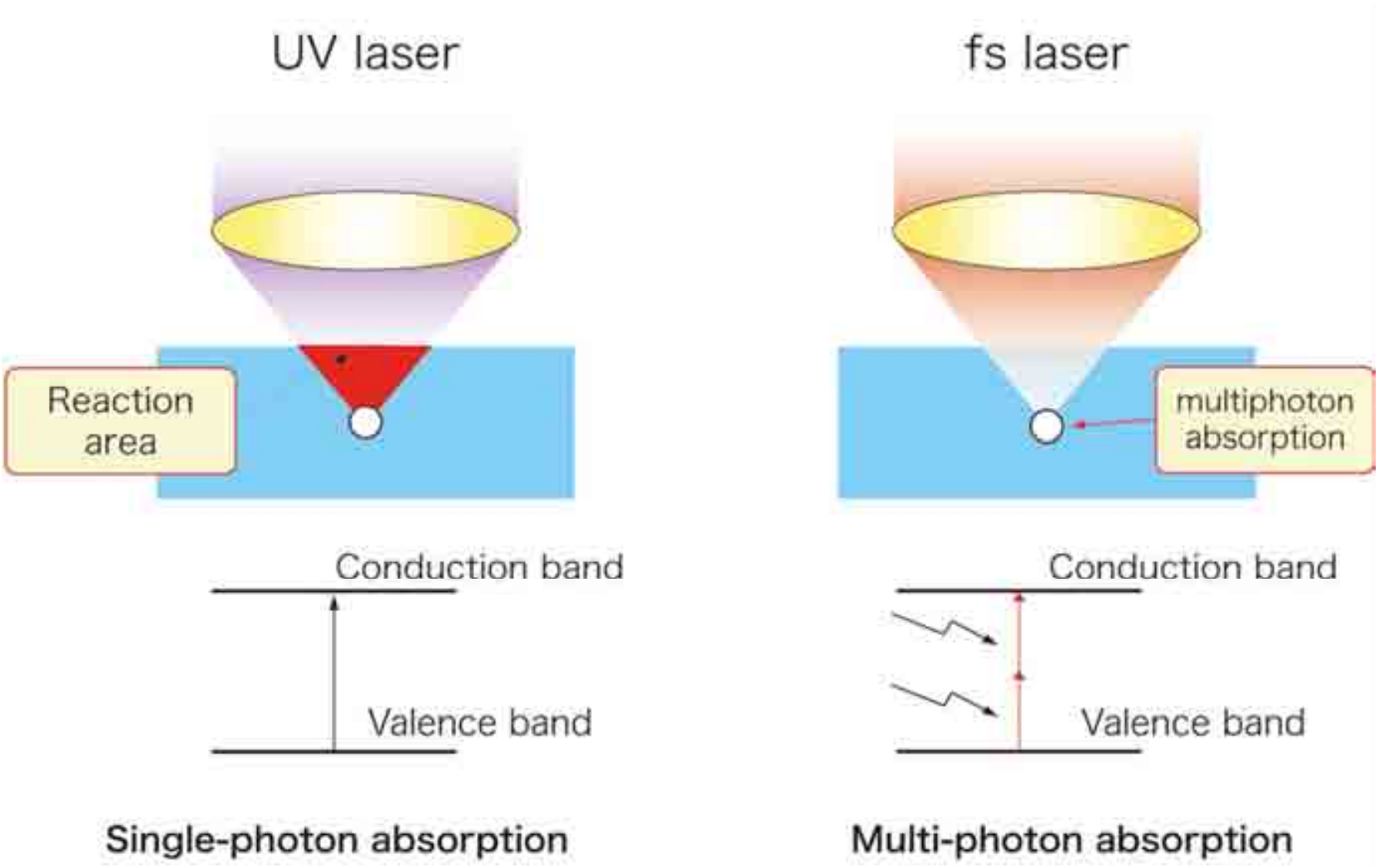

Femtosecond laser induced microstructures

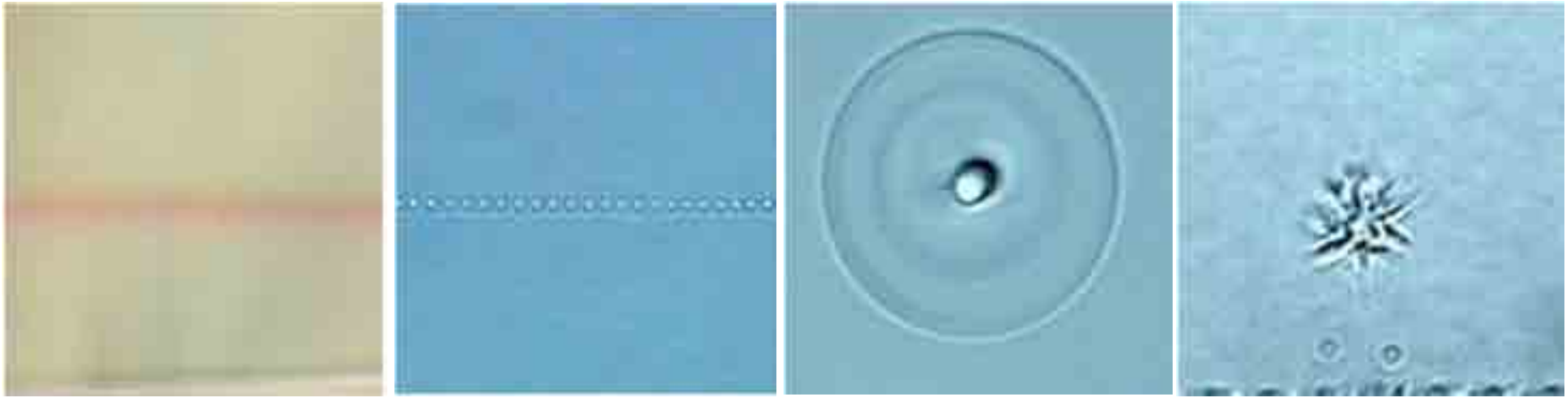

The Chem. Rec. 109, 25(2005).

Color centers formation in LiF

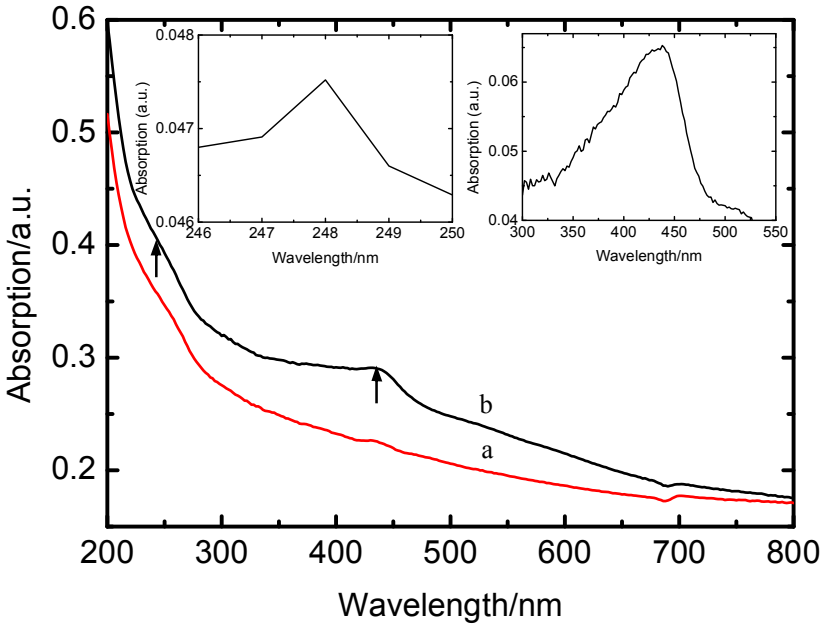

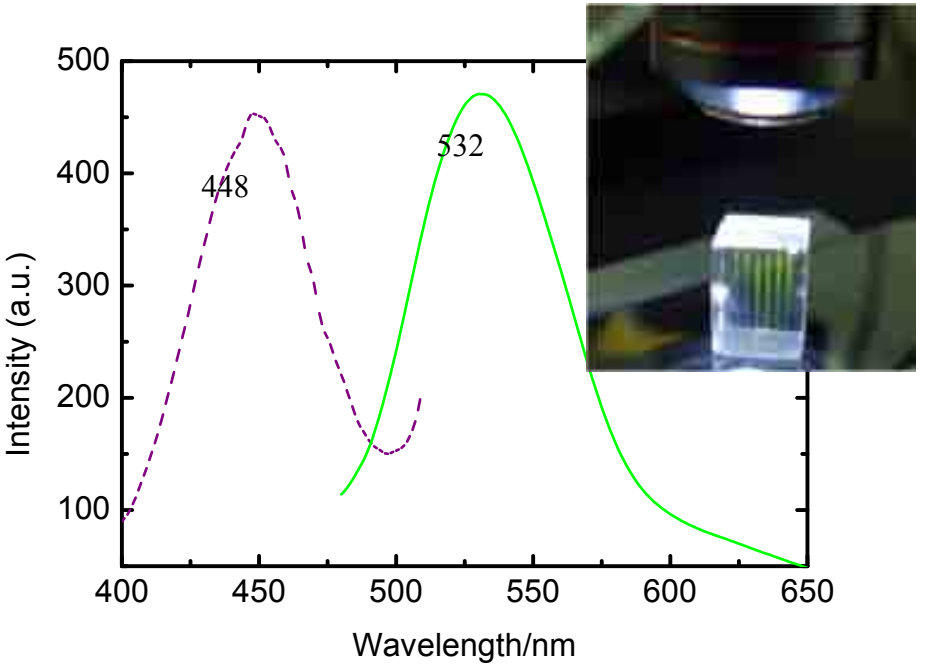

- A peak at 248nm – F center (an anion vacancy occupied by an electron)
- A peak at 448 nm – M absorption→ the overlap of two bands of F_2 centers (445 nm) and F_3^+ centers (448 nm).

Emission and excitation spectra for the fs laser-induced color centers in LiF

Color centers – LiF : DFB laser

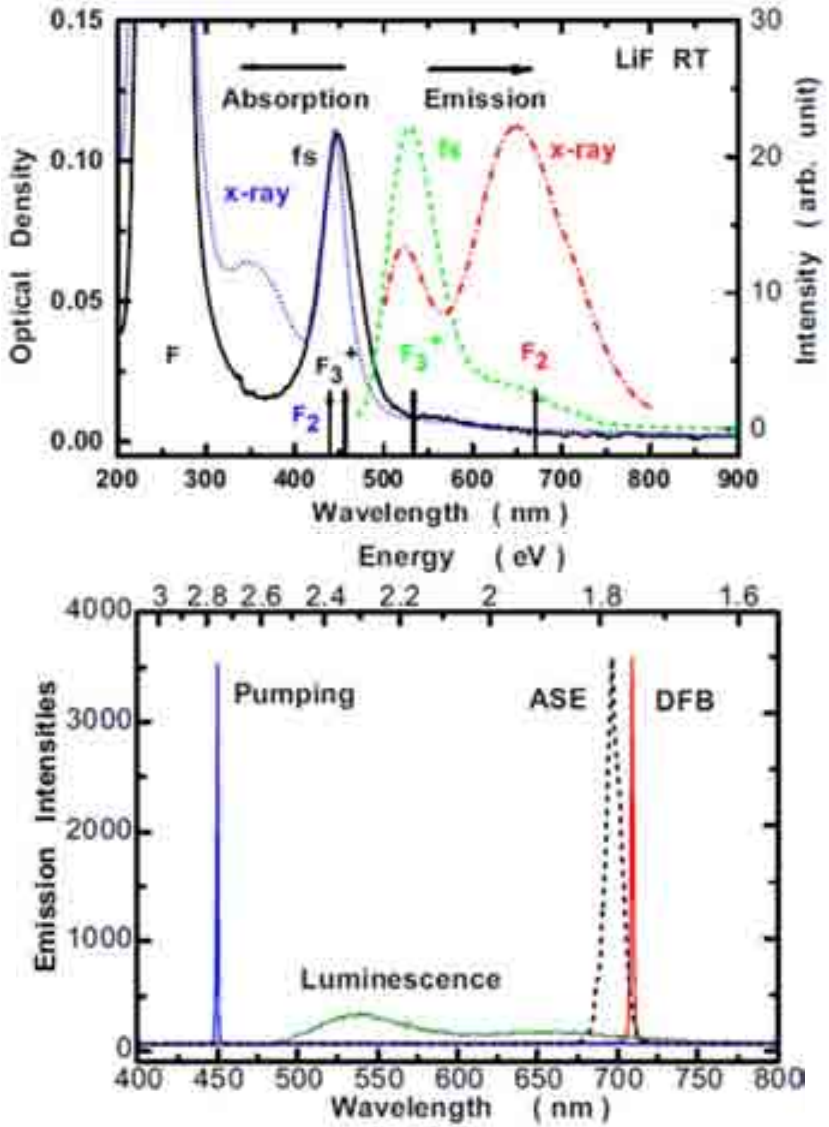

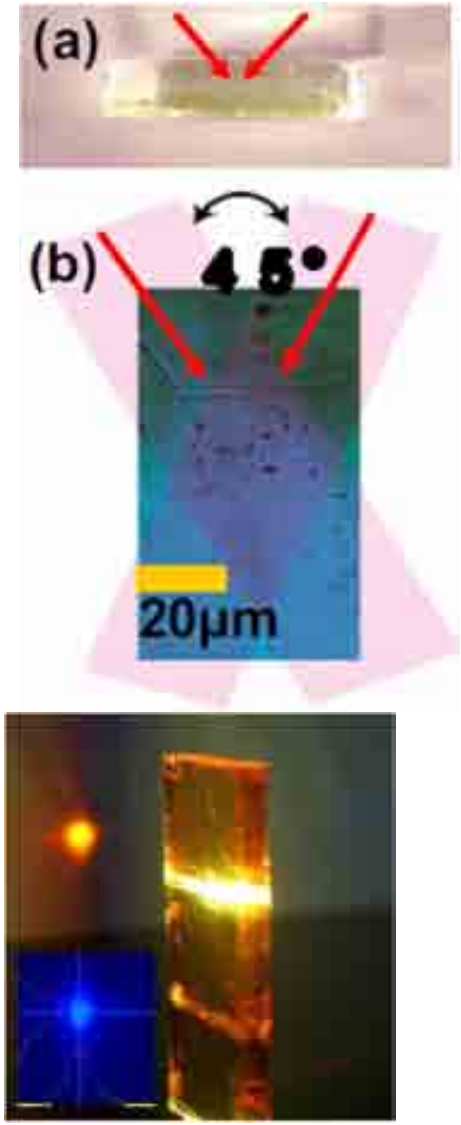

Applications of Δn

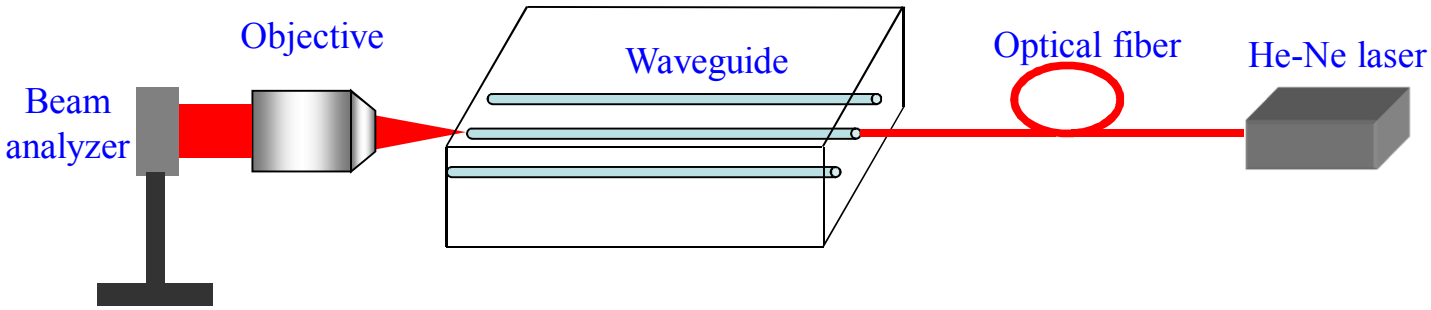

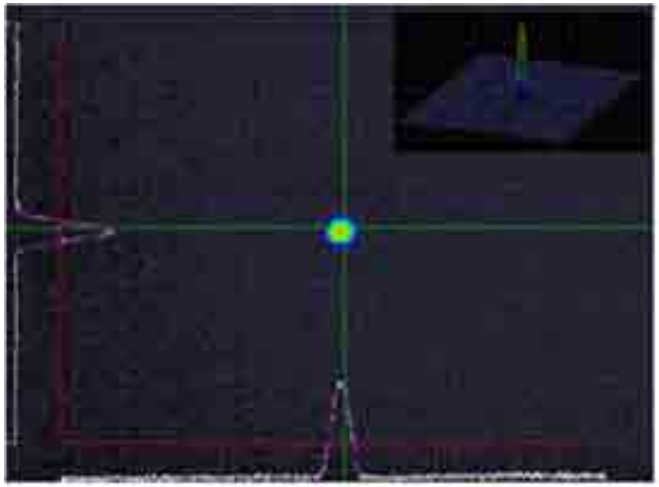

Near field distribution

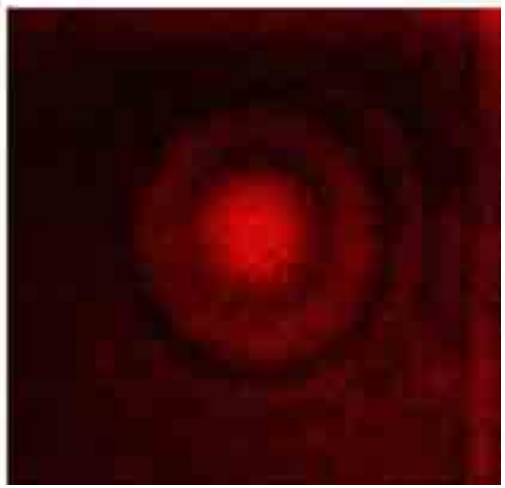

Far field distribution

2D and 3D preparation of optical waveguide

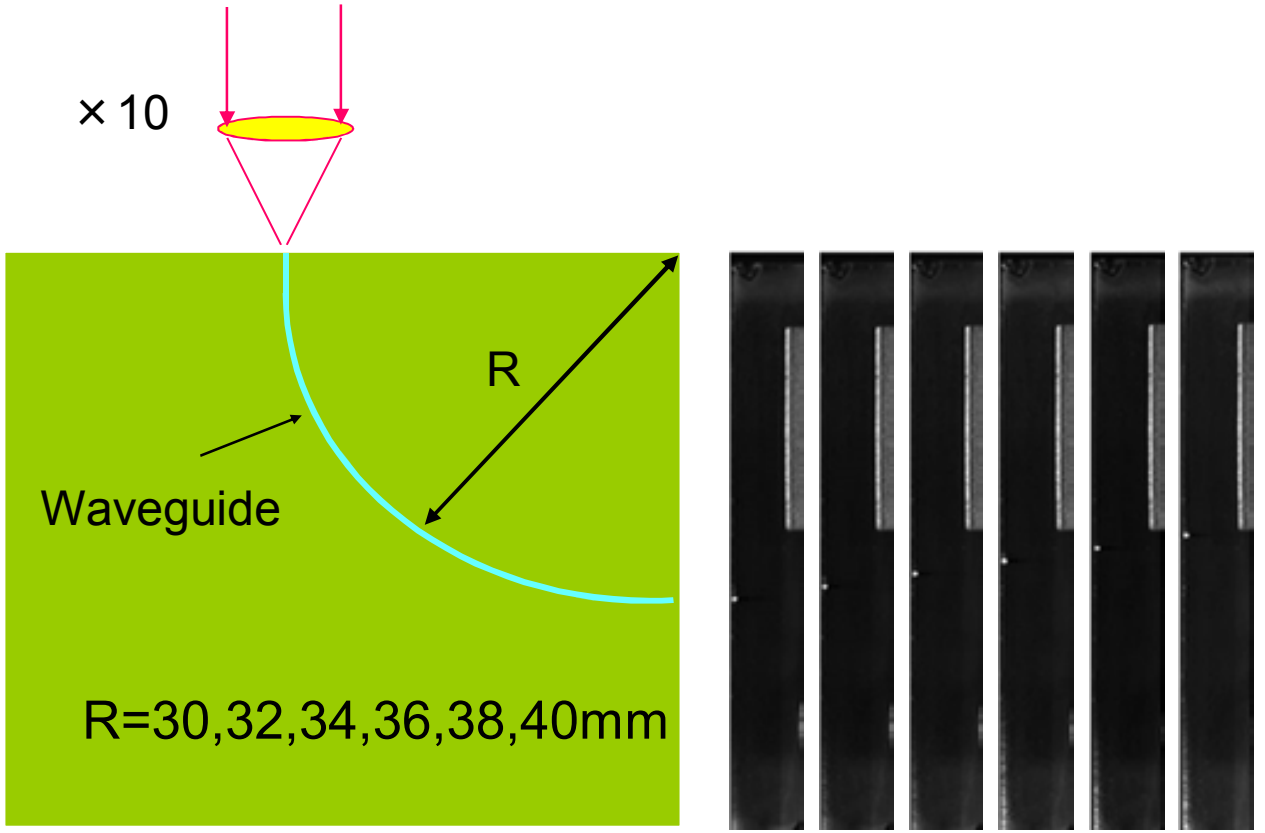

Transmission light of the end face of bending waveguides

Fresnel lens

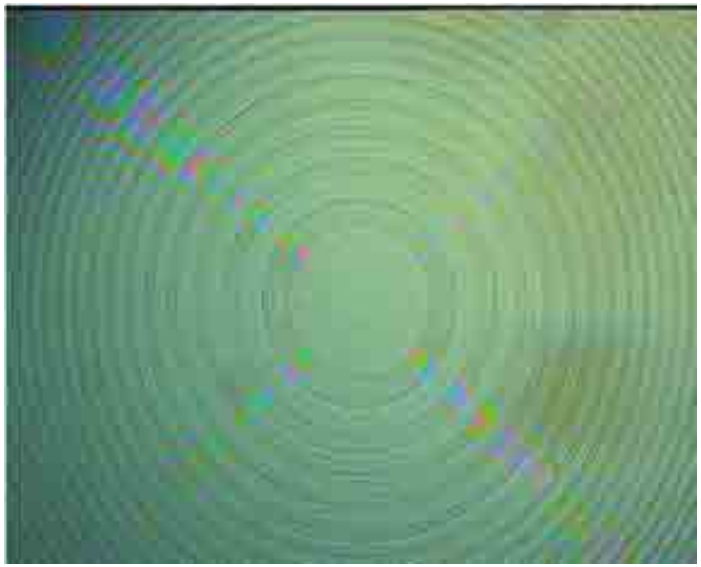

Fiber attenuator

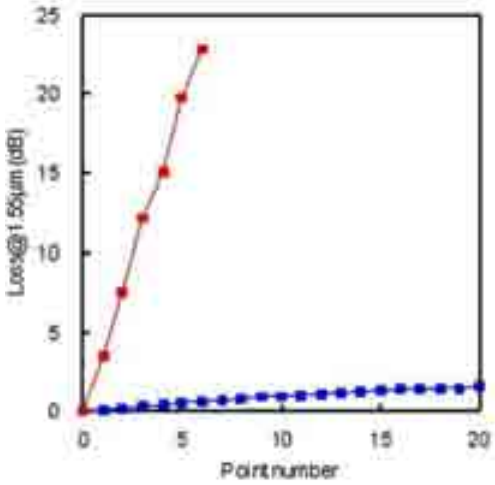

波导设计和制作

激光能量影响

波导截面调控

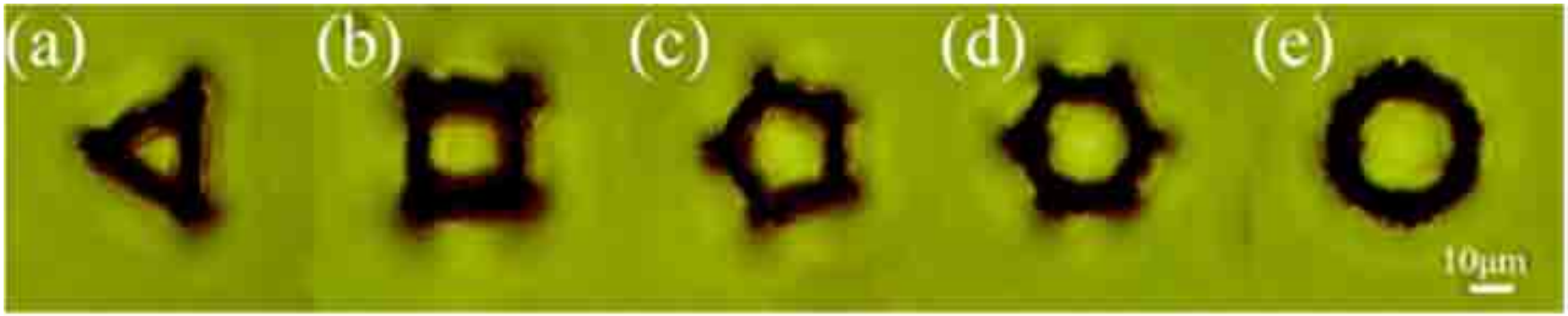

1-to-N分束器设计和制作

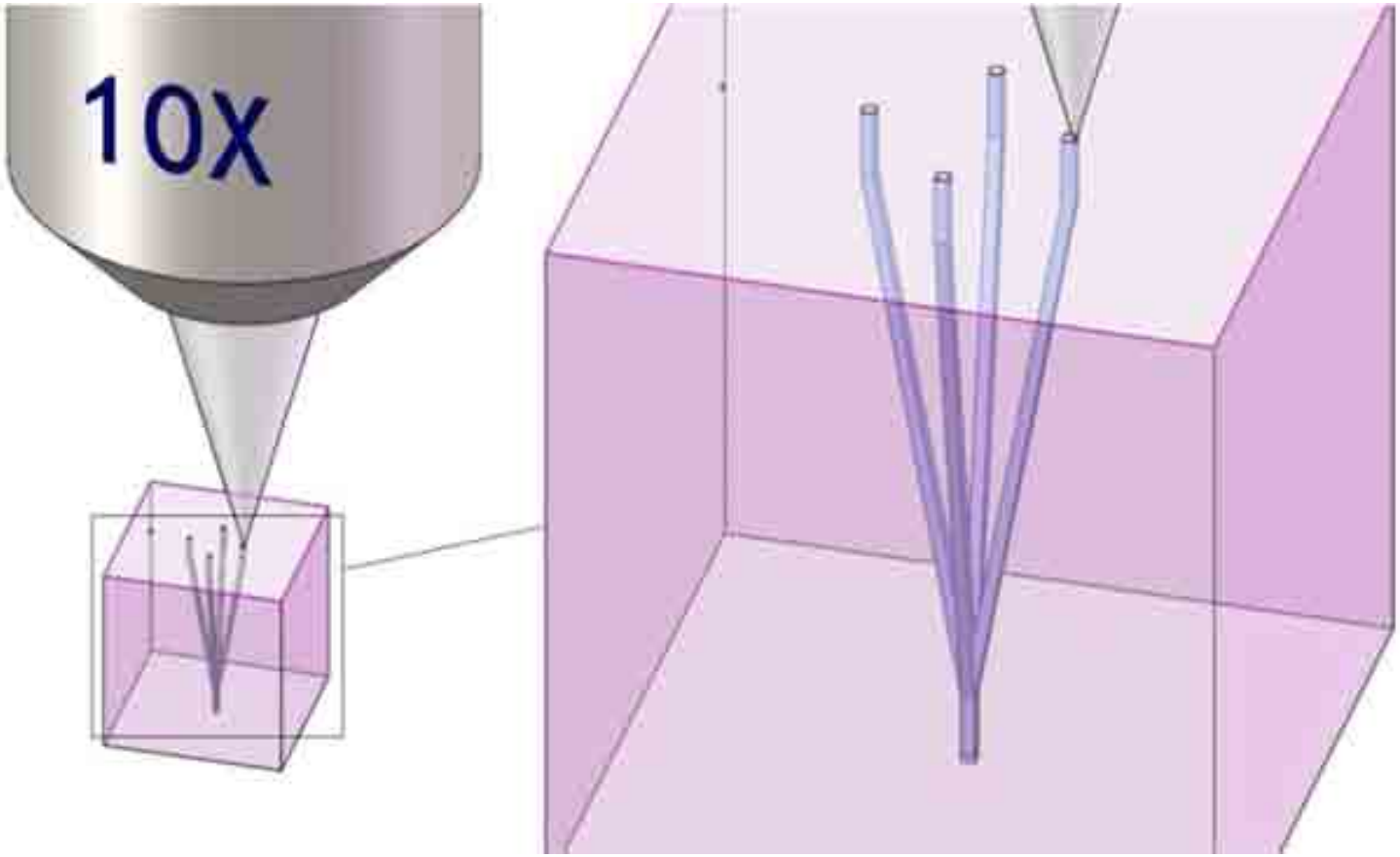

Applications of $\Delta n \rightarrow$ Coupler/splitter

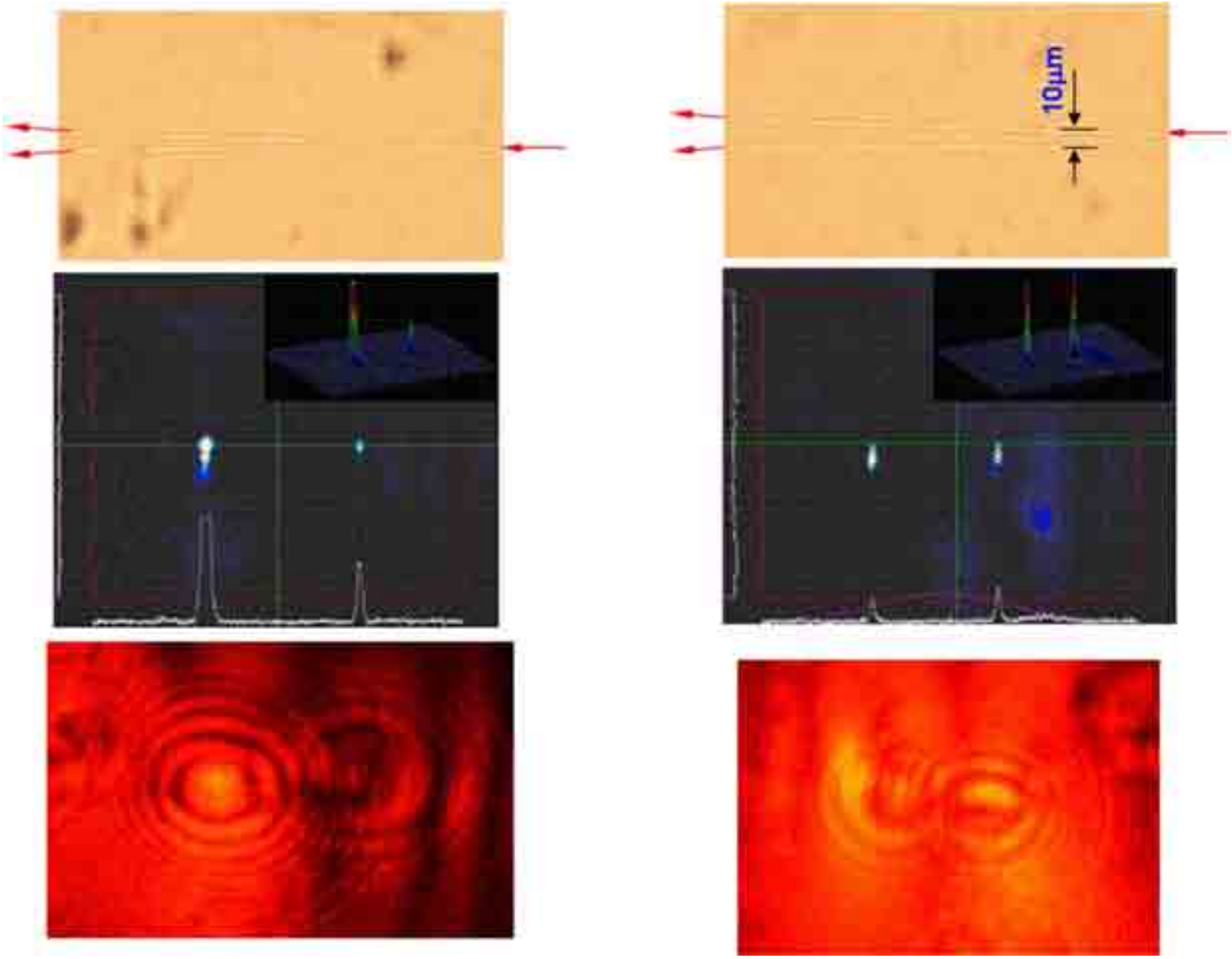

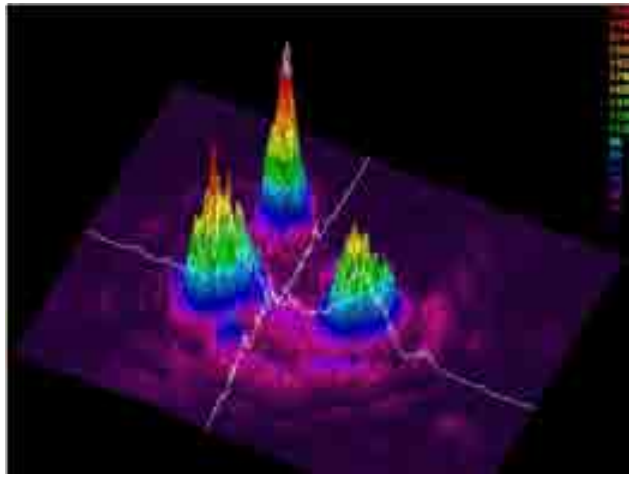

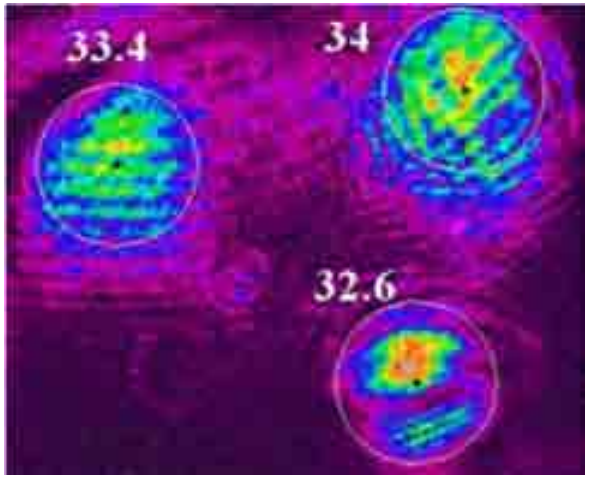
33.4
34
32.6

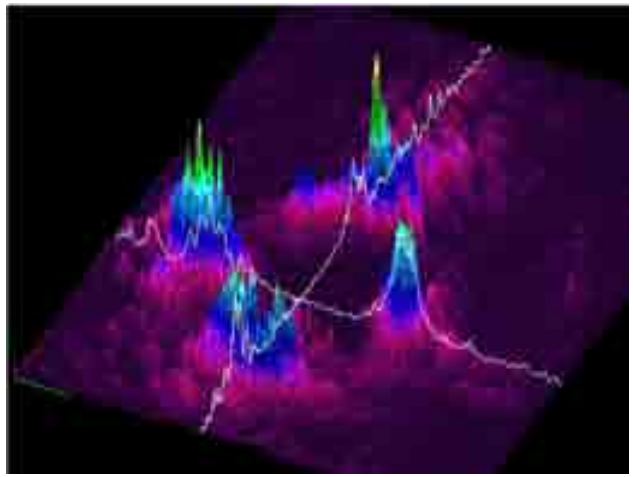

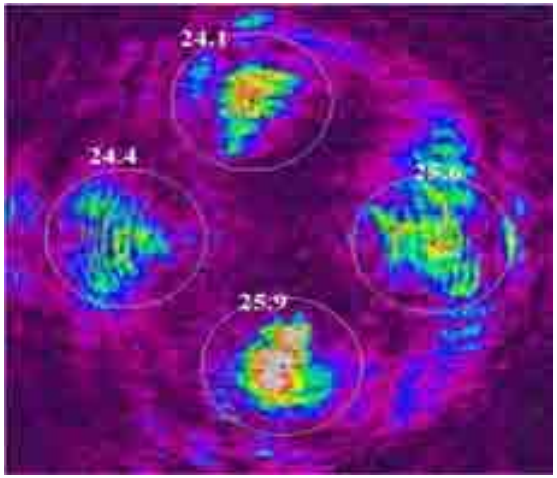
24.1
24.4
25.6
25.9

Applications of $\Delta n \rightarrow$ Ring-resonator

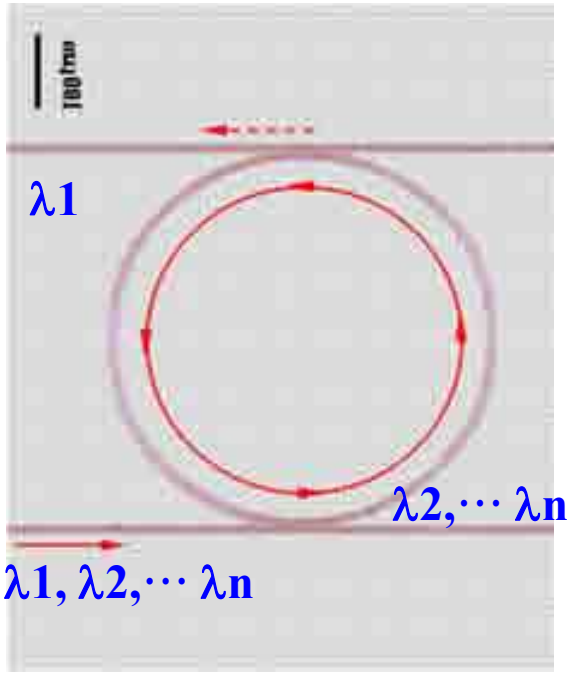

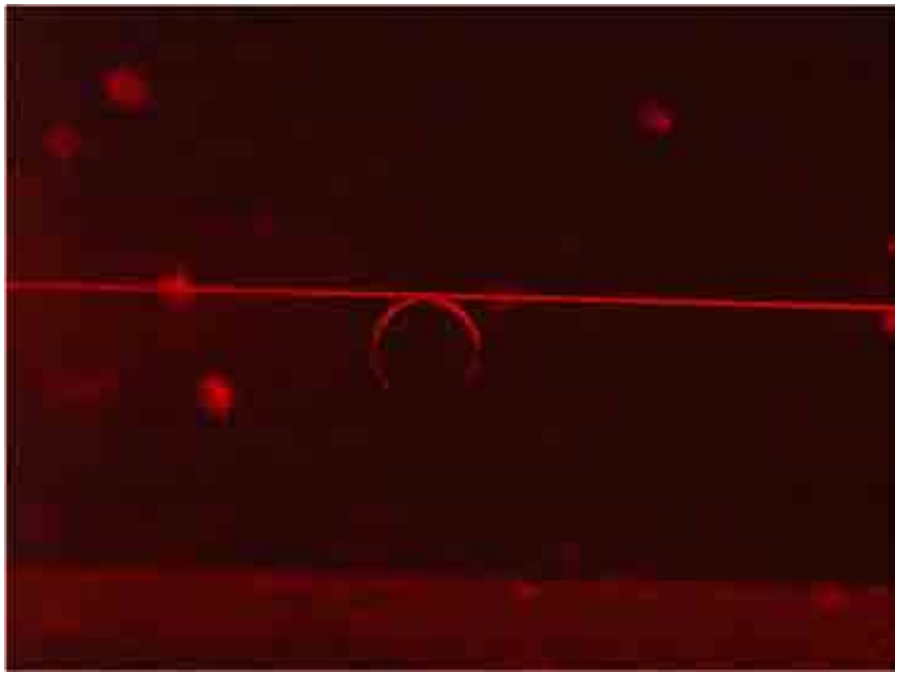

Applications of $\Delta n \rightarrow$ Interferometer

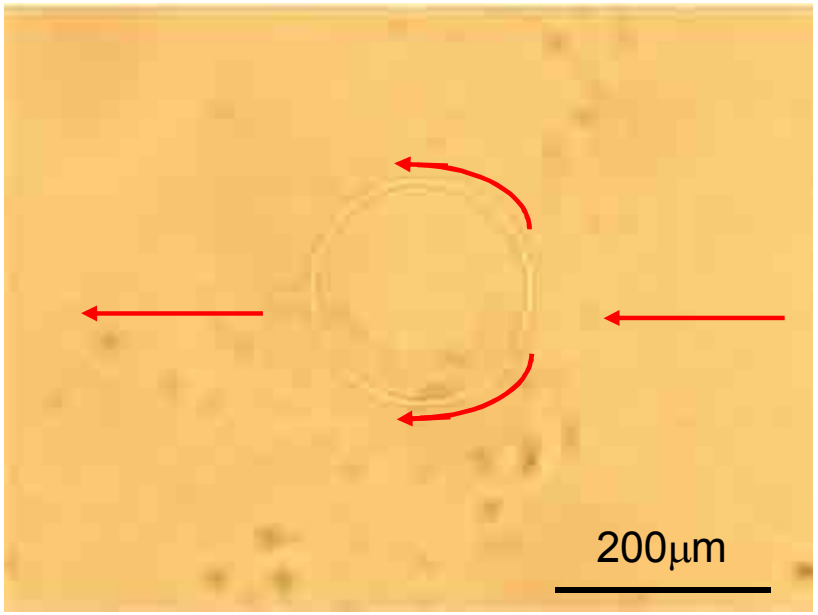

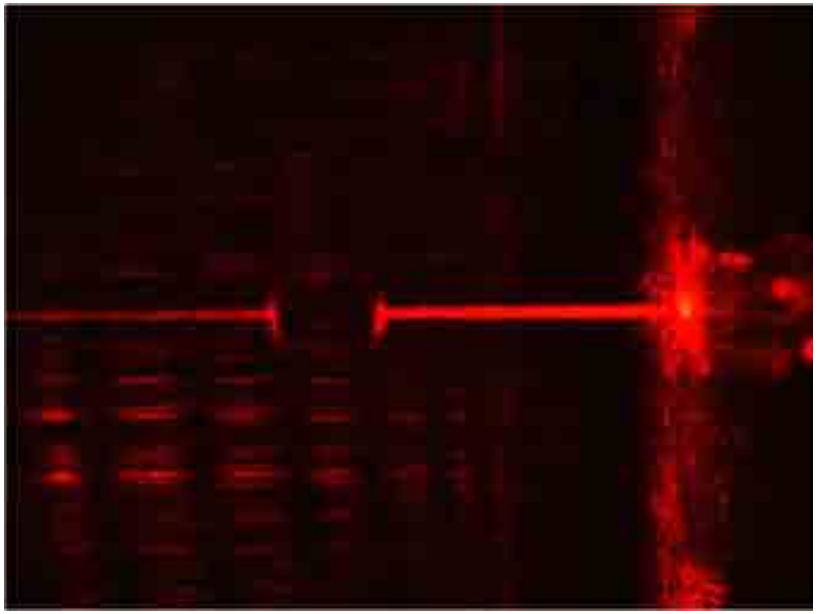

Applications of $\Delta n \rightarrow$ Talbot and Damman gratings

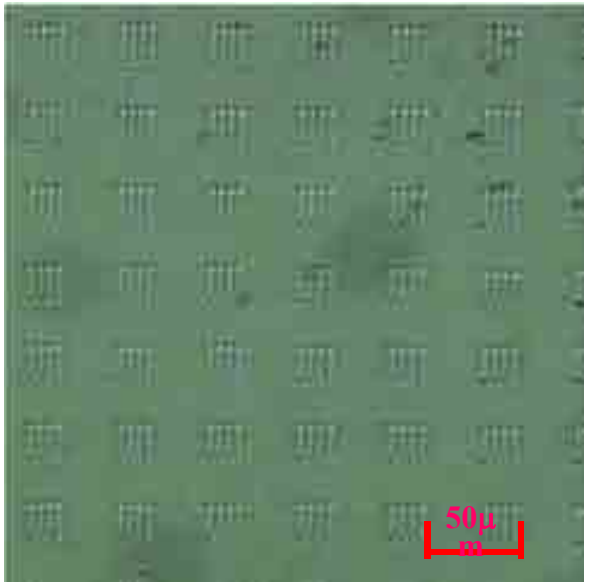

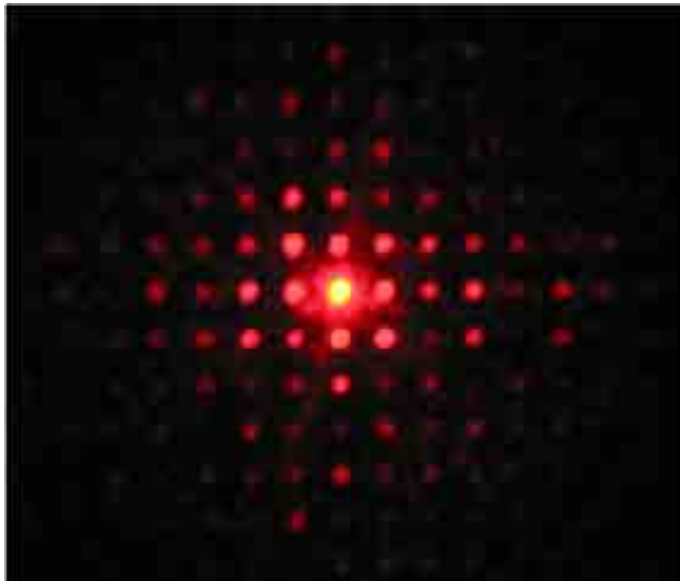

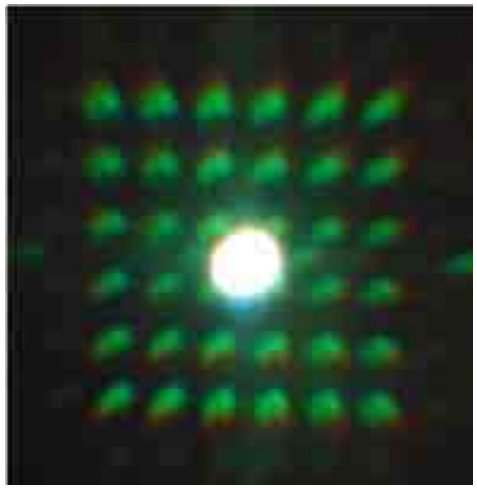

Single femtosecond laser beam-induced nanograting

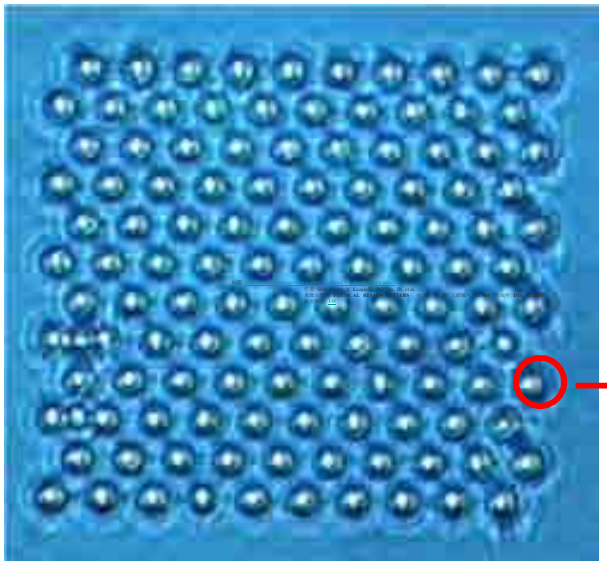

100× (0.95)
120fs
200kHz
200mW
1s

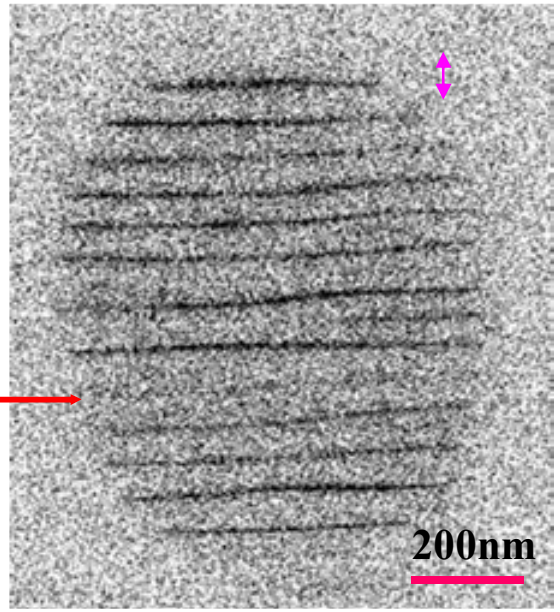

Optical microphotograph

BEI image of SEM

Phys. Rev. Lett., 91(2003)247405.

5D optical memory

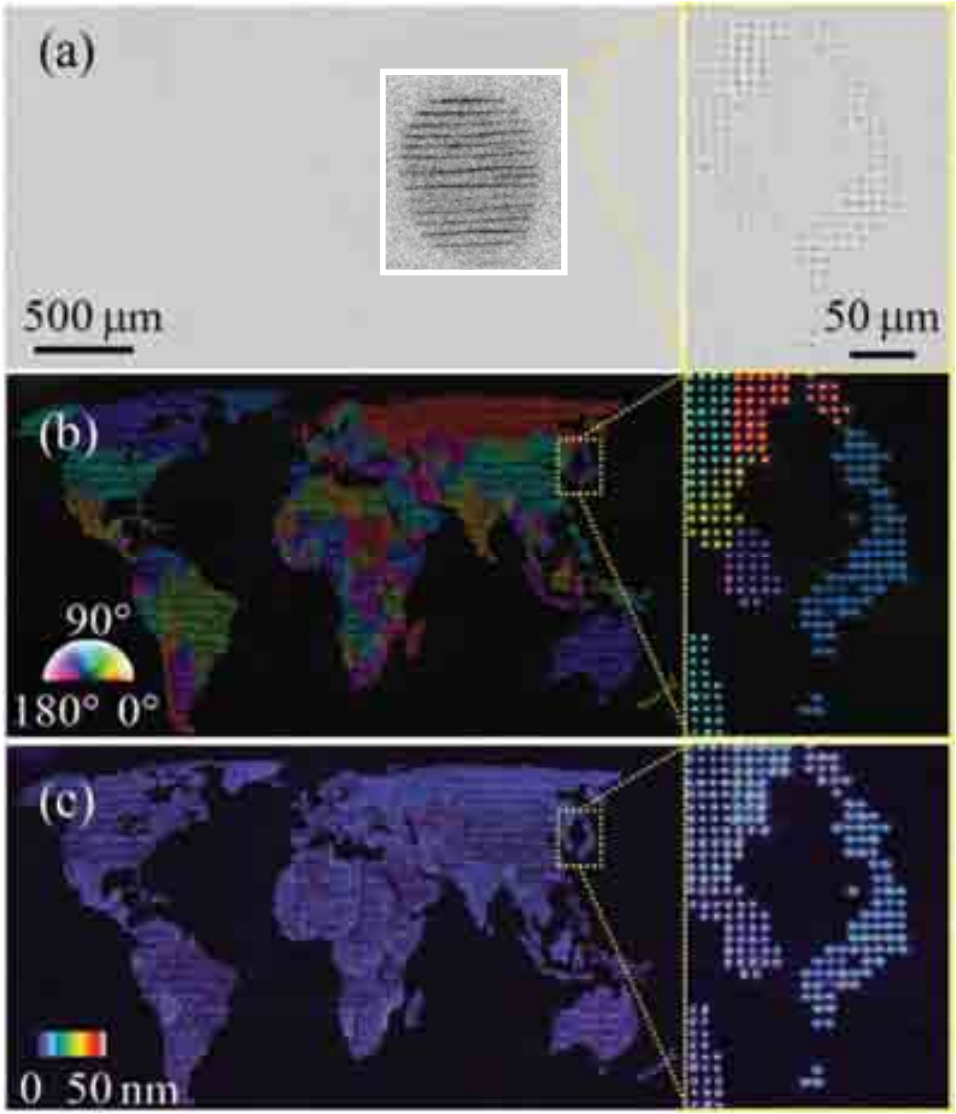

Adv. Mater., 24(2010)1-5.

Hole drilling of glass by femtosecond laser

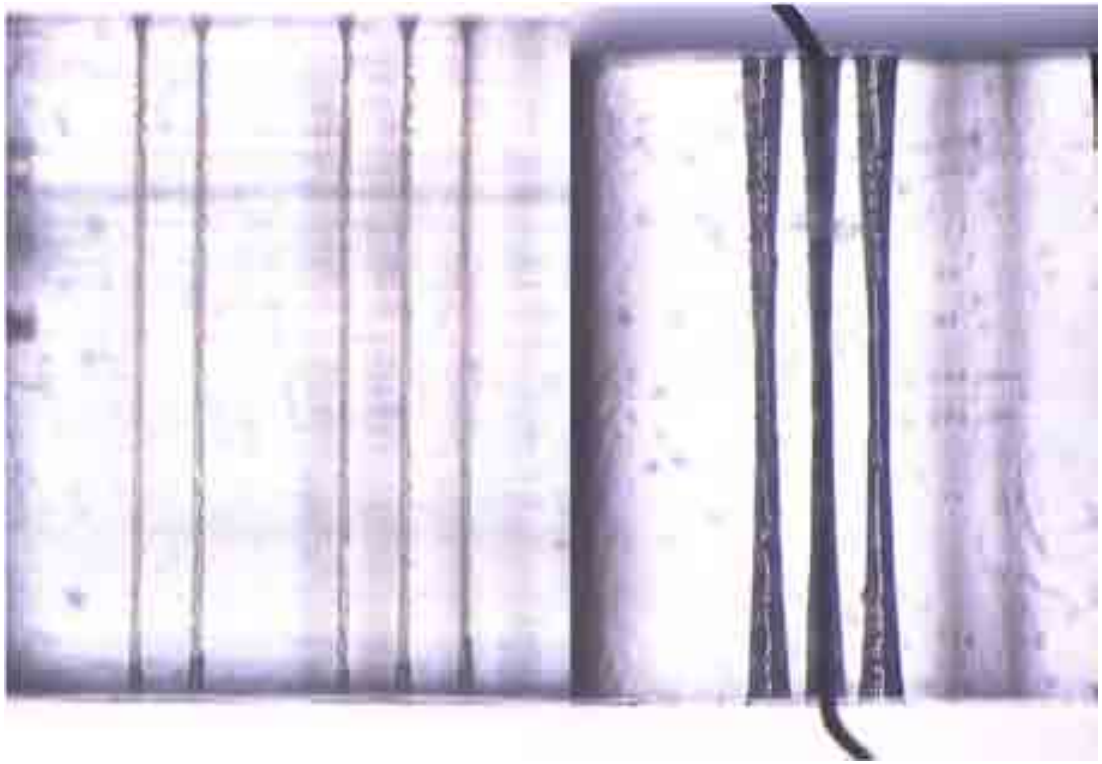

After drilling

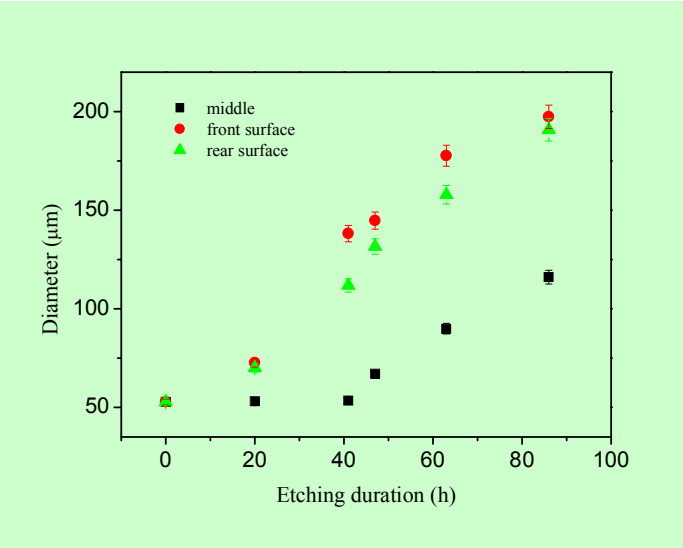

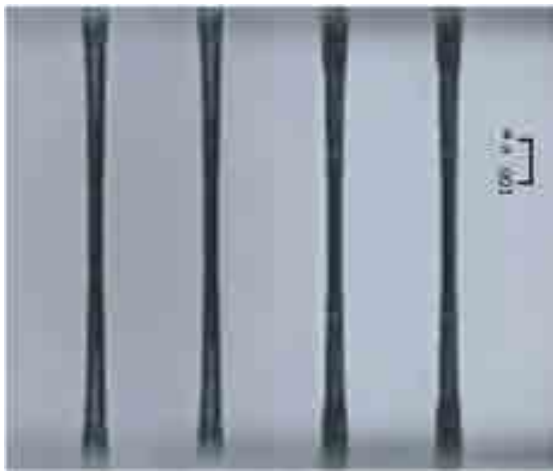

Etching for 90 h

Thickness 3 mm

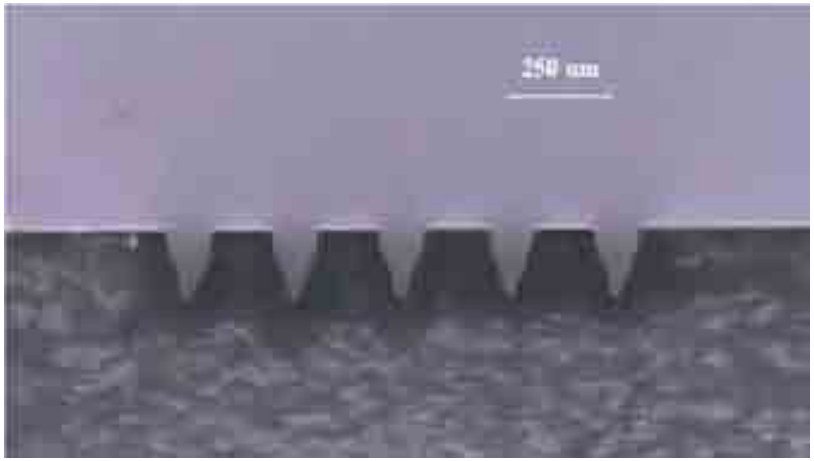
250 nm

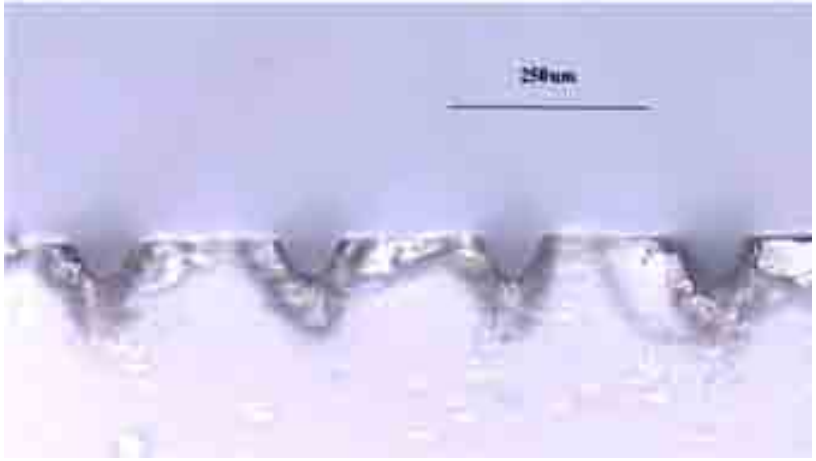
250nm

Photoreduction

- Photochromic Lenses

$$2AgX \xrightleftharpoons{\text{sunlight}} 2Ag + X_2$$

X —— halide ion

- Femtosecond laser photoreduction of ions
  - Nobel metal ions
  - Transition metal ions
  - Heavy metal ions
  - Rare earth ions

Formation of metal nanoparticles in glasses

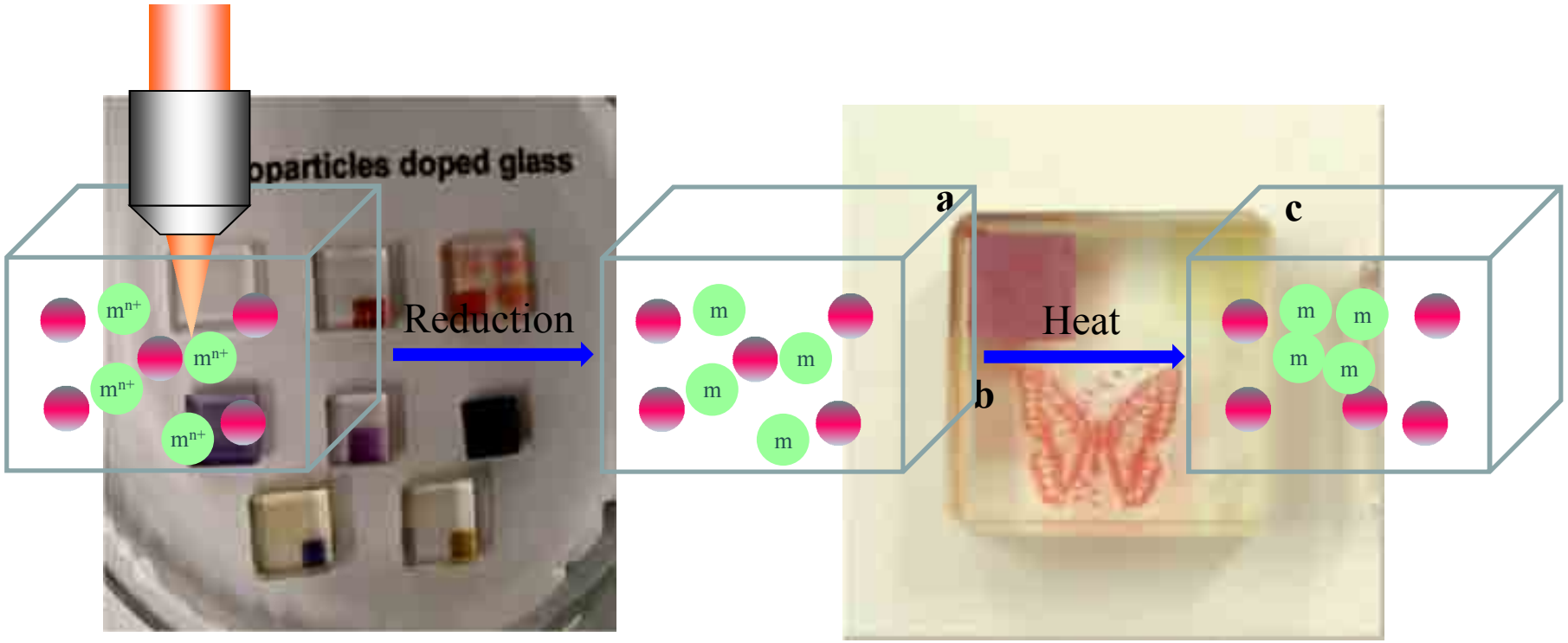

Refractive index change in femtosecond laser irradiated Au^{3+}-doped silicate glasses

J. Qiu *et al.* Angew. Chem. Int. Ed. 43, 2230 (2004).

Three-dimensional engrave in glass

Formation of semiconductor nanocrystals-glass composites

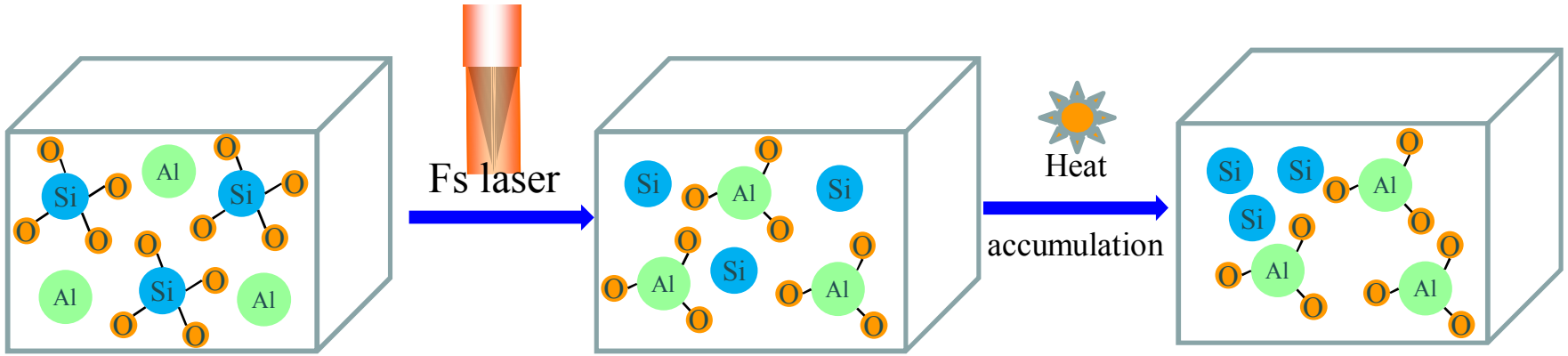

Appl. Phys. A 93, 183 (2008).

Opt. Lett. 36, 262 (2011).

Formation of Si nanocrystals-glass composites

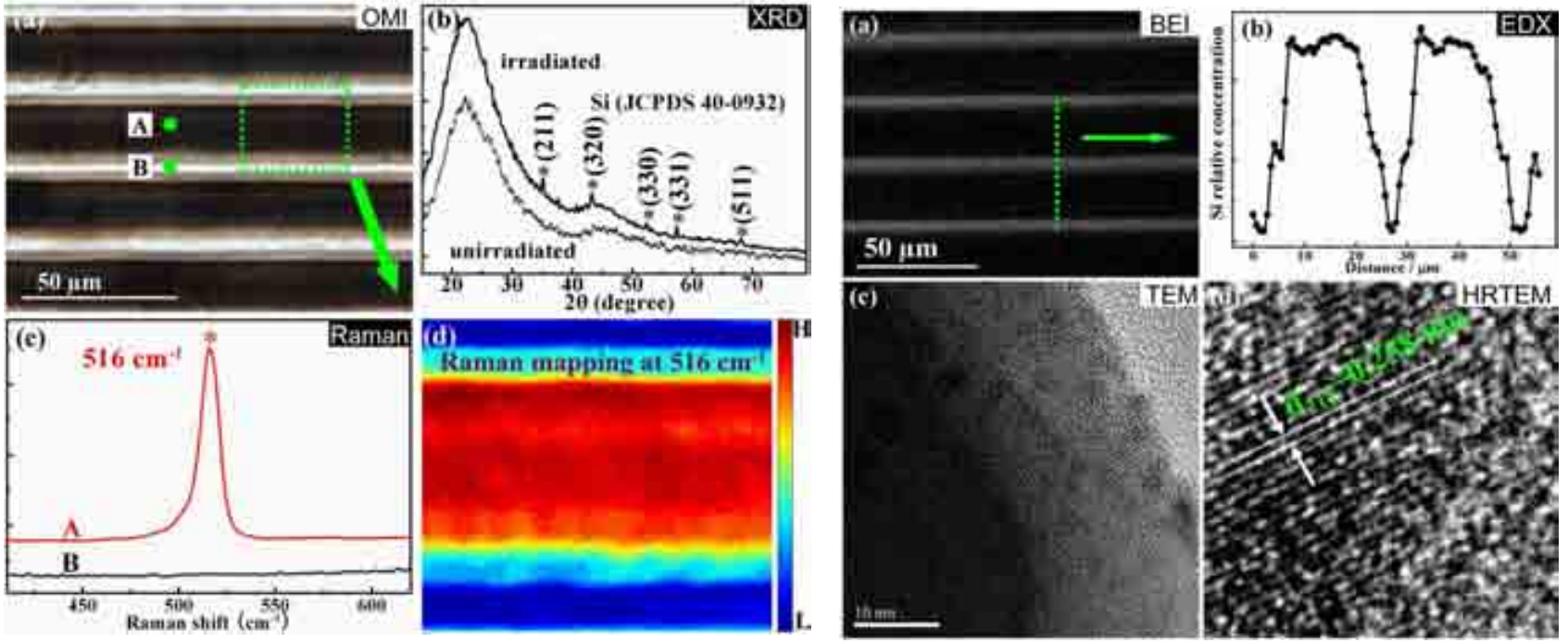

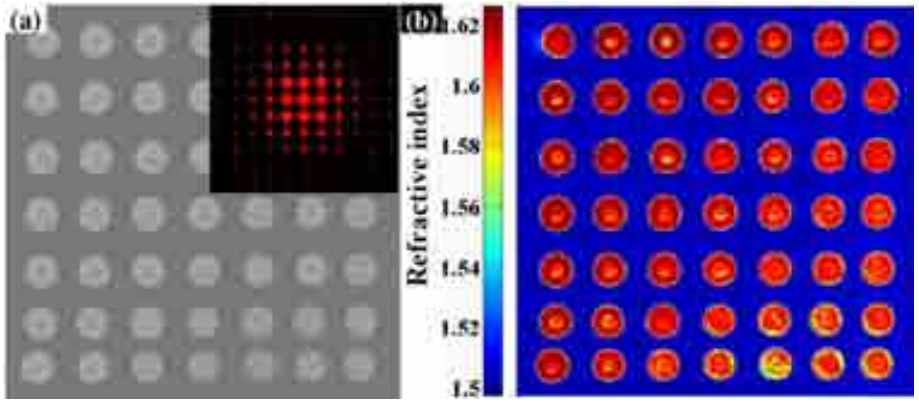

Formation of Ge nanocrystals-glass composites

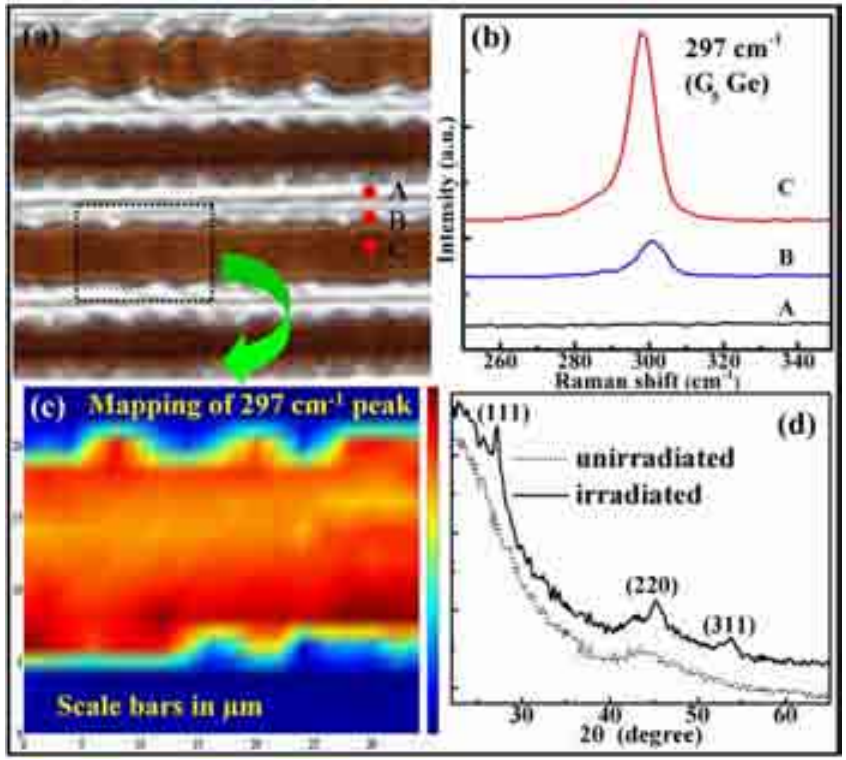

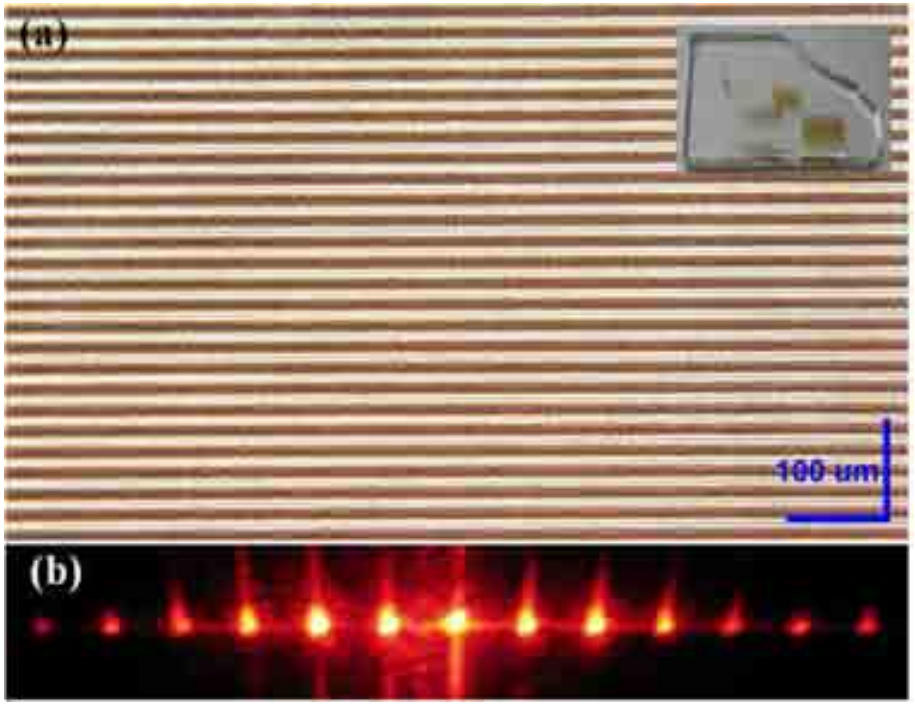

G. Lin *et al.*, Opt. Lett. 36, 262 (2011).

The future of Δn

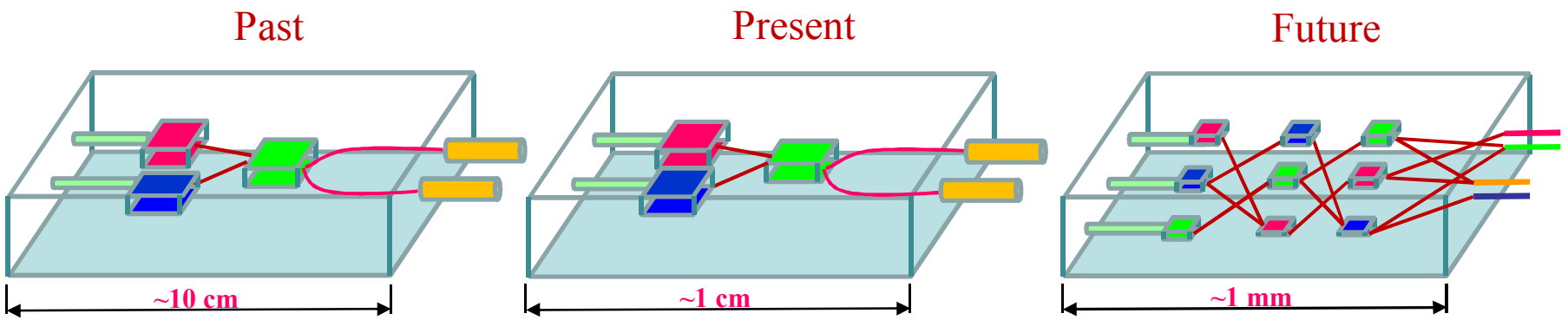

- In the past, refractive indices of core and cladding layers were approximately 1.50 and 1.45, respectively.
- In present case, semiconductors (Si, Ge) and conventional oxide glasses, with indices of about 3.5 and 1.5, respectively.
- In the future, 3D integration of different components in glasses are expected.

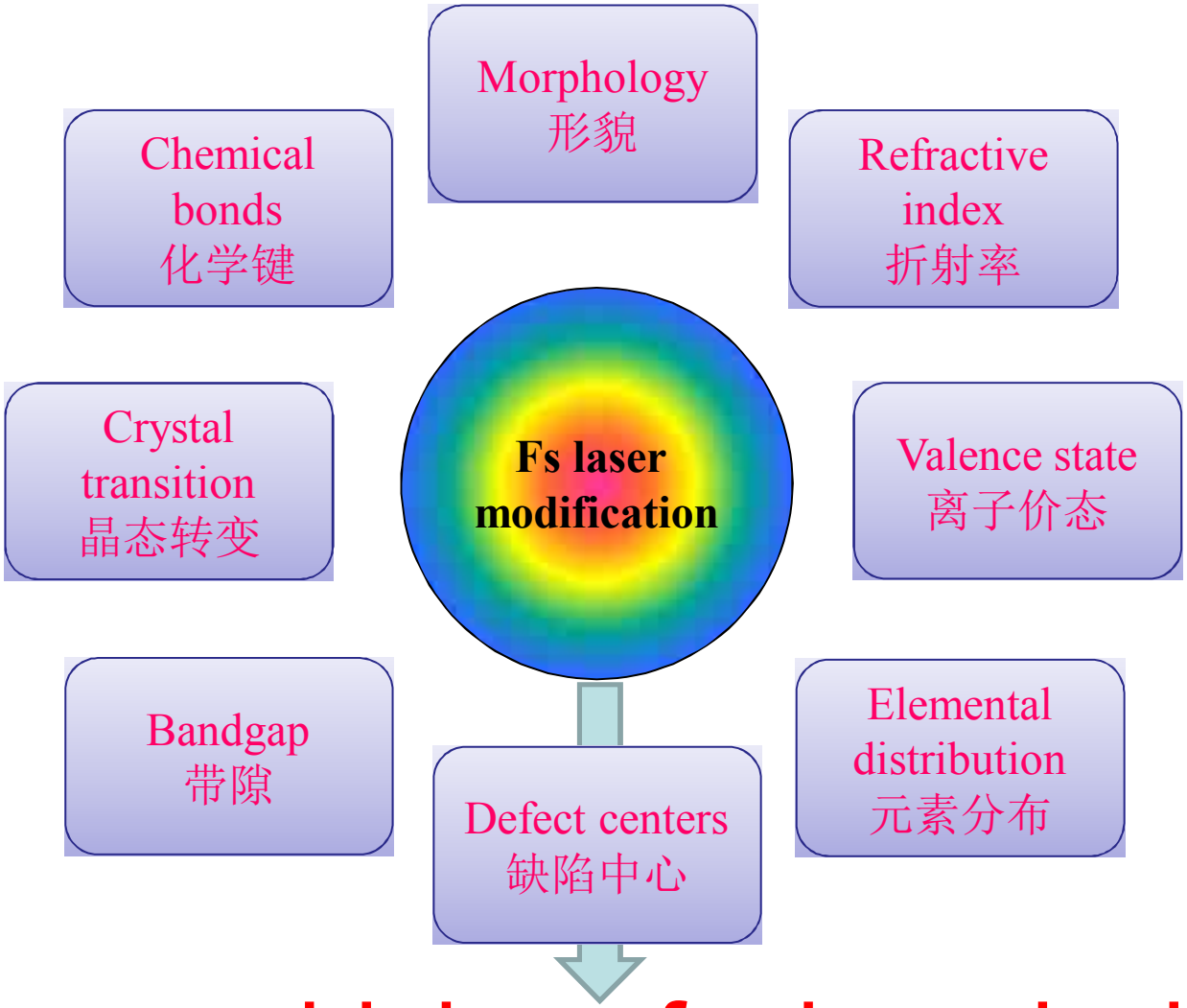

Micromachining of micro-devices

Micromachining by fs laser

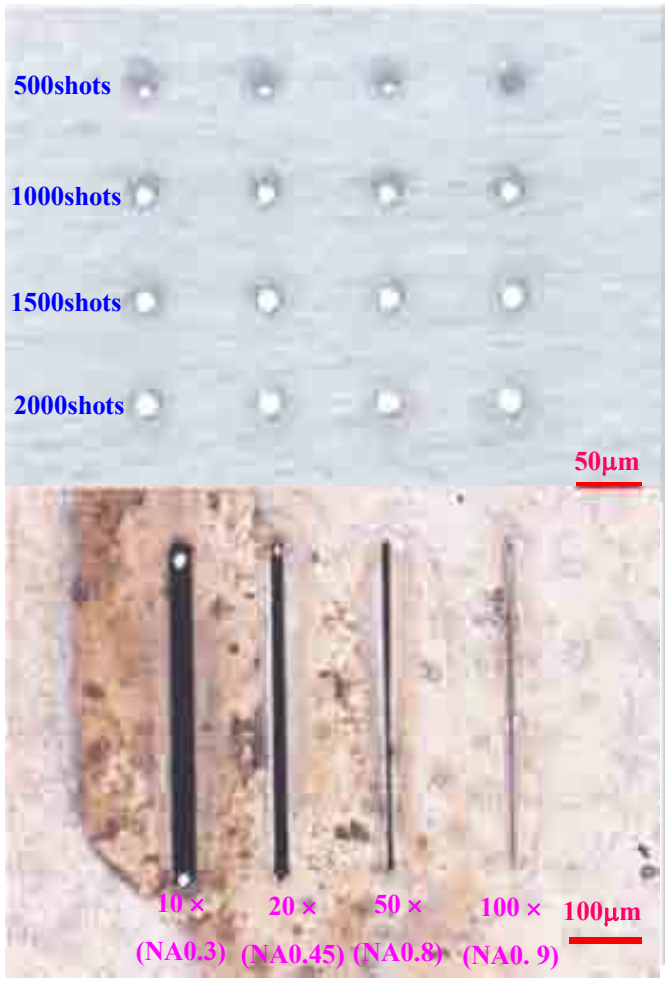

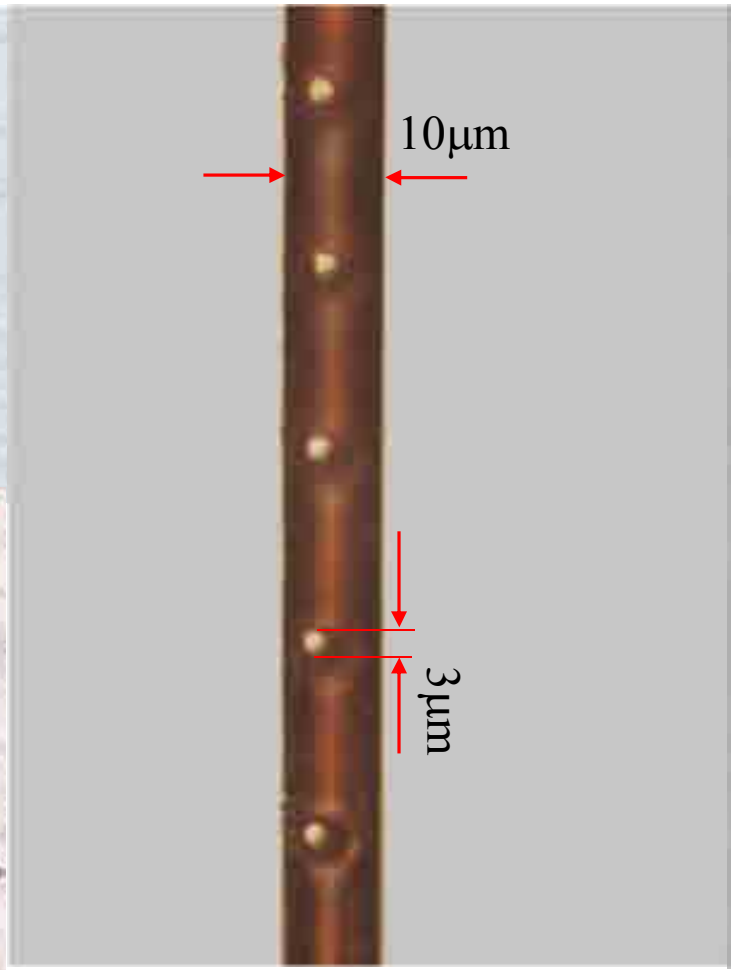

Drilling and cutting of tungsten by fs laser

Laser: 800nm, 1kHz, 10-100mW

Fs laser micromaching micro-mechanical oscillators

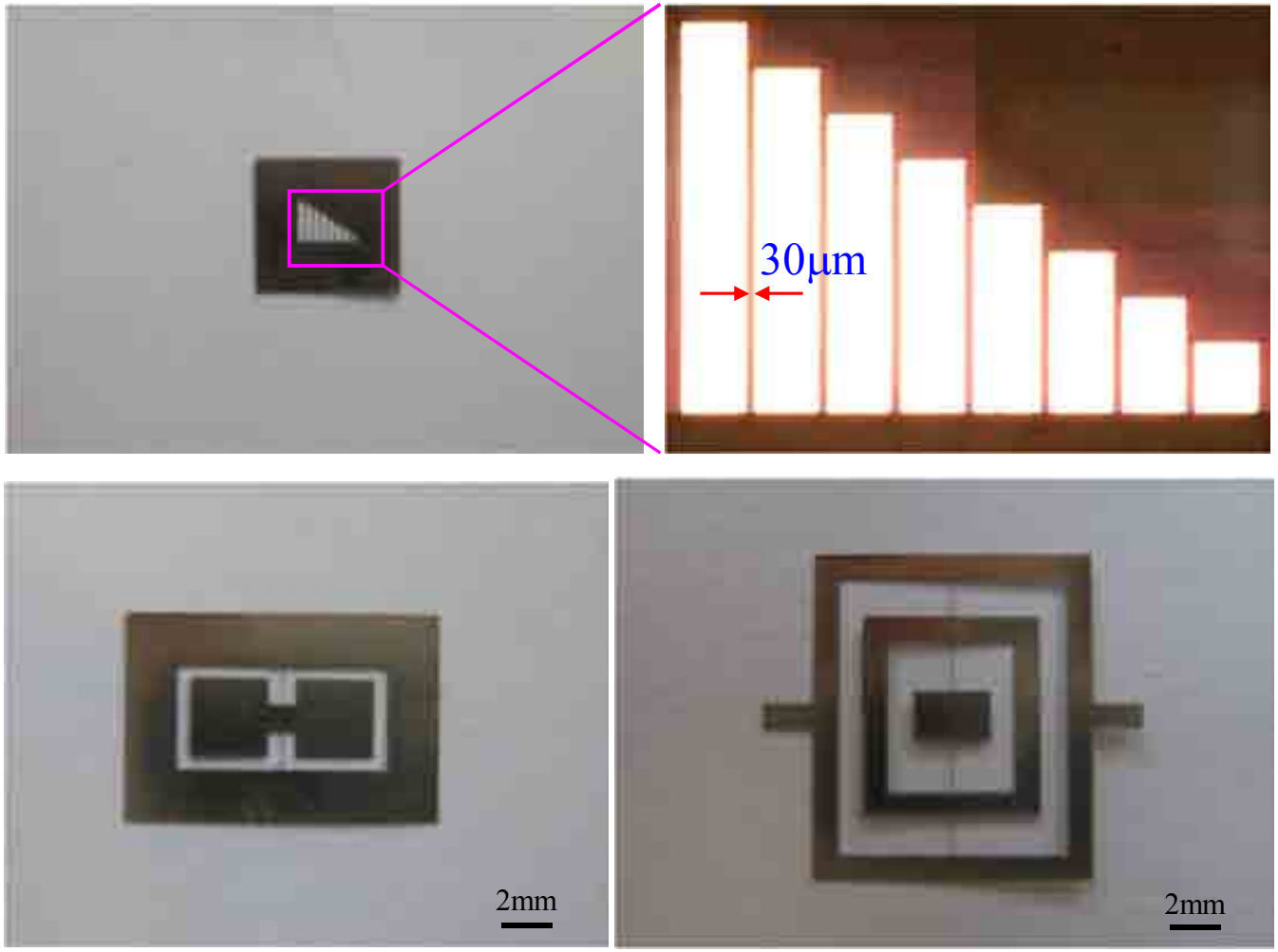

scheme one

scheme two

Laser: 800nm, 1kHz, 20mW

Hole drilling - Steel

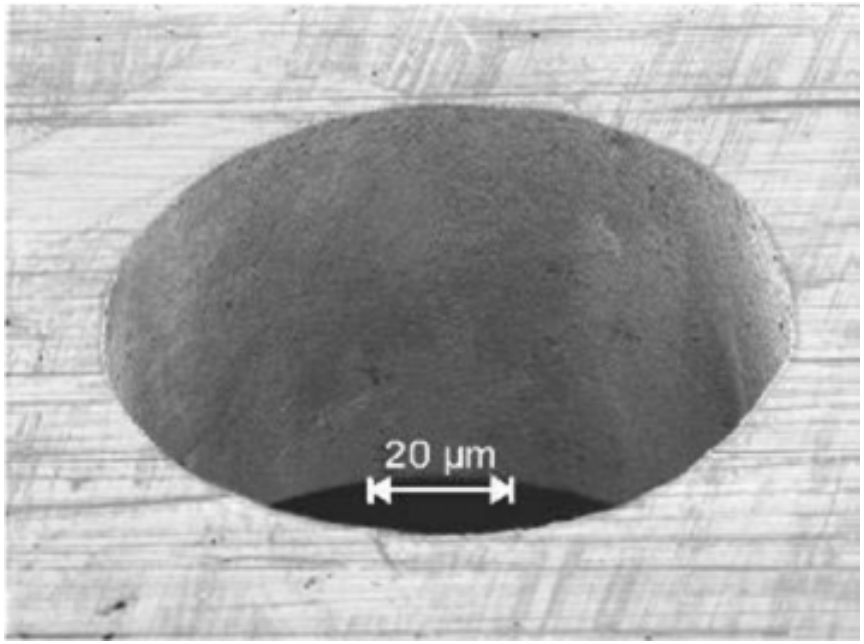

Hole (ϕ100 µm) drilling in 100 µm steel sheet

Laser: 1064nm, 100kHz, 1W

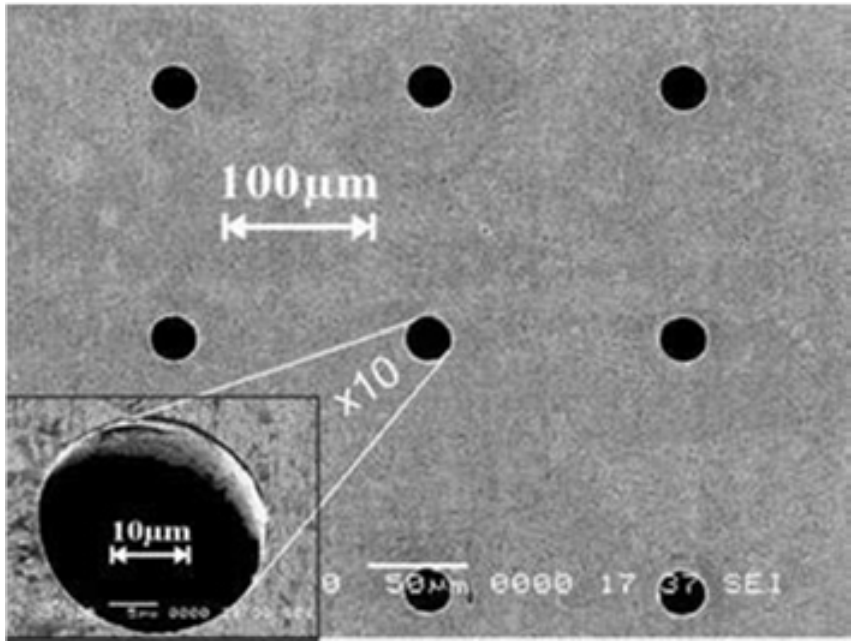

30 µm diameter hole drilled in 25 µm steel foil

Laser: 1064nm, 100kHz, 0.5 W

Throughput ~180 holes/min

Hole drilling -Silicon

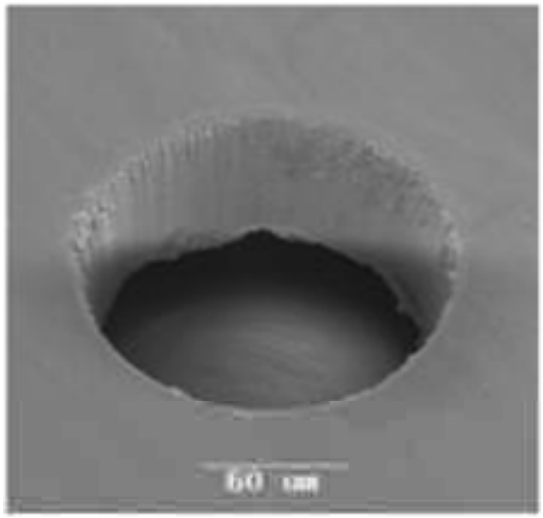

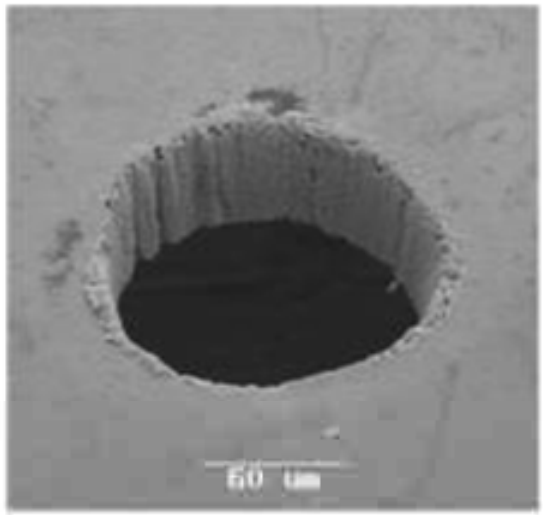

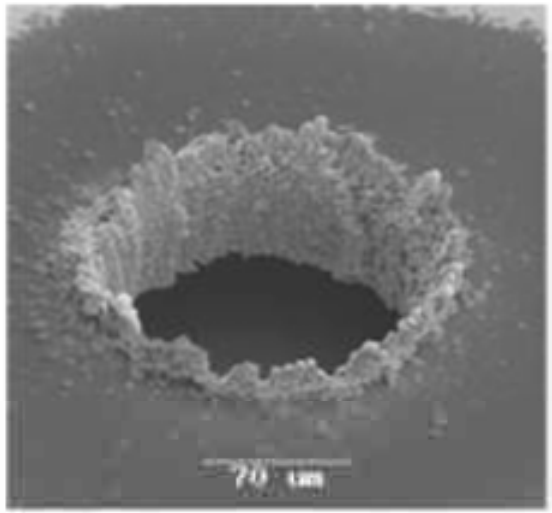

Parameters			
τ_P	150 fs	12 ps	25 ns
λ	780 nm	532 nm	355 nm
E_P	100 µJ	5 µJ	270 µJ
f_P	1 kHz	50 kHz	25 kHz

Hole drilling –Ceramic & Glass

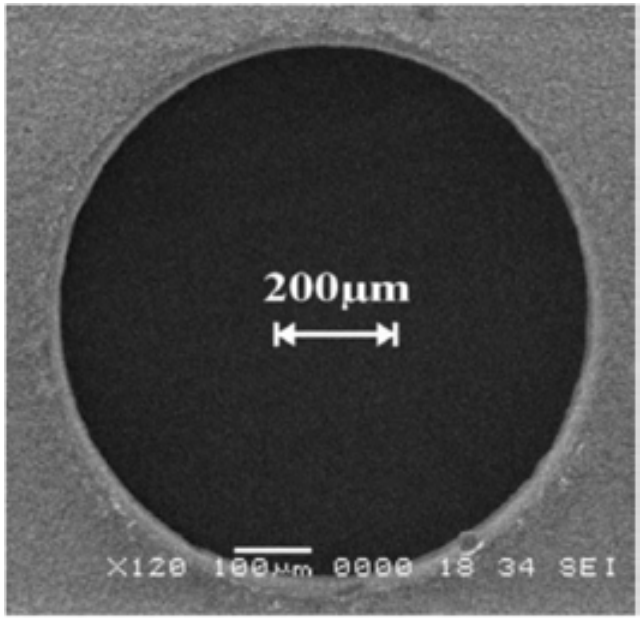

1 mm hole drilled in a 200 µm thick ceramic sheet

Laser: 1064nm, 100kHz, 10W

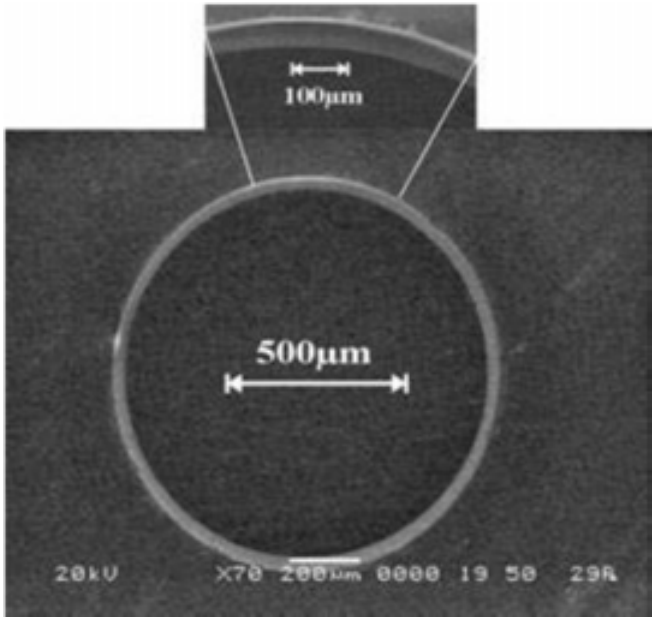

1 mm hole drilled in a 140 µm thick glass coverslip

Laser: 355nm, 100kHz, 2W

Cutting- Steel

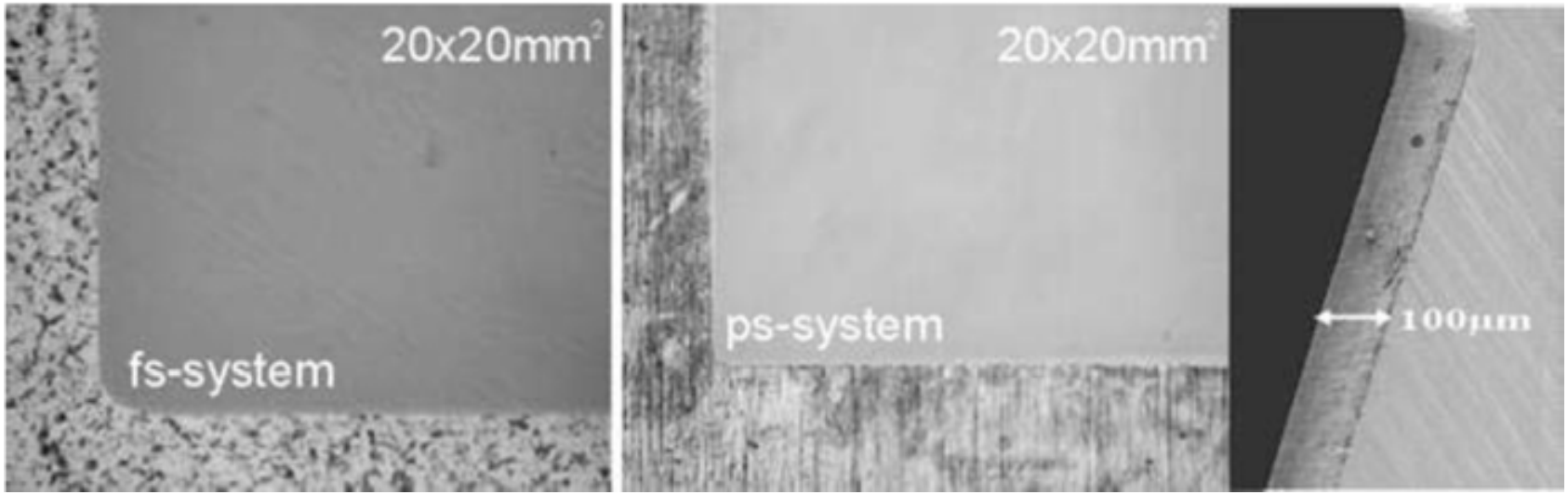

Cutting of 50 µm steel sheet

Cutting- Silicon

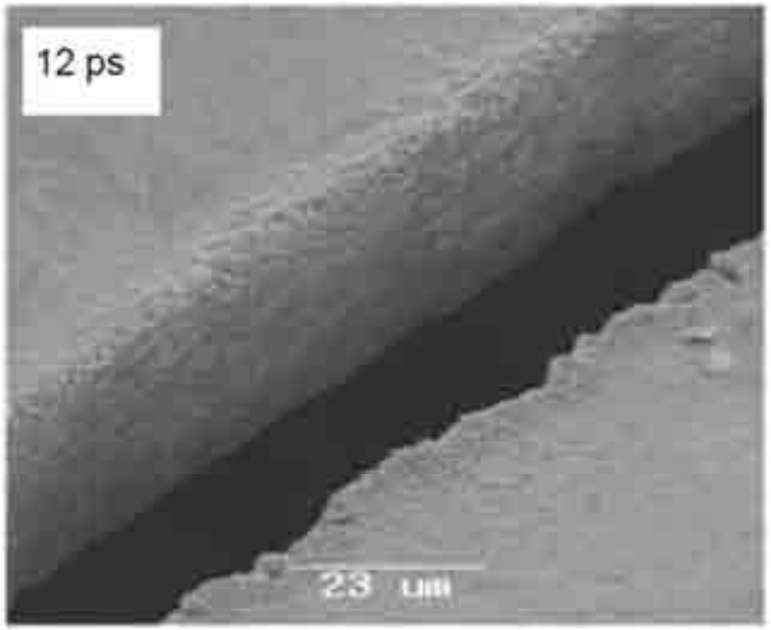

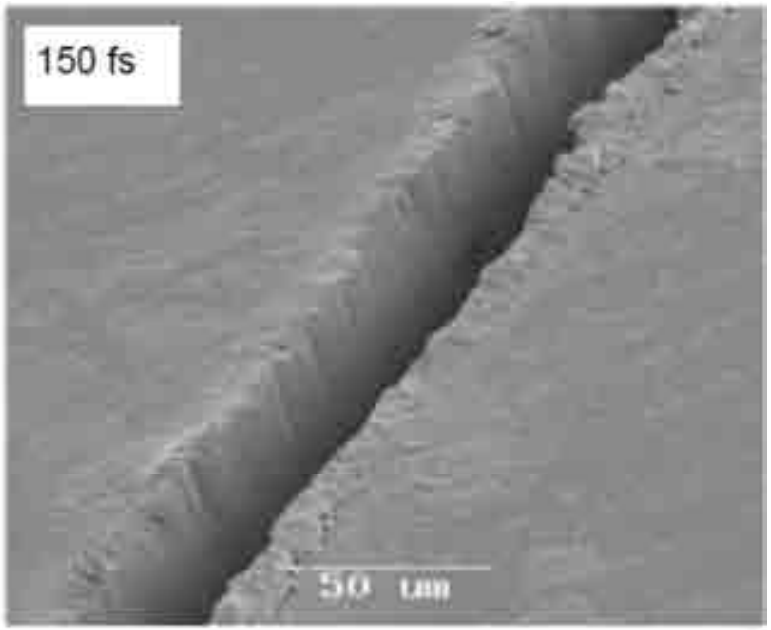

Parameters		
532 nm	λ	780 nm
10 µJ	E_P	800 µJ
50 kHz	f_P	1 kHz
30 µm	d_f	Line-focus

Surface structuring

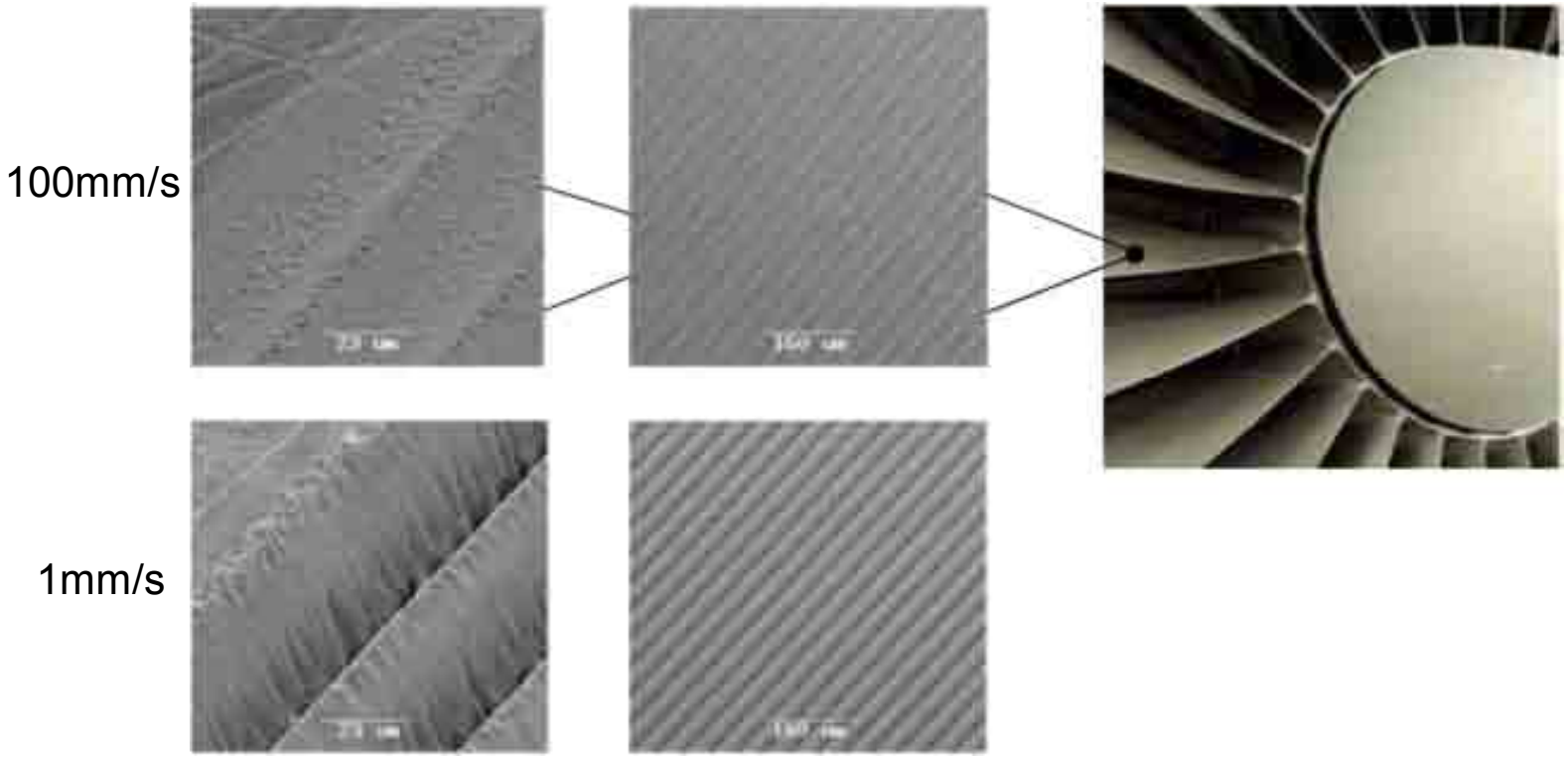

Riplet structures on metallic surfaces with reduced friction

Fs laser fabrication of MEMS device

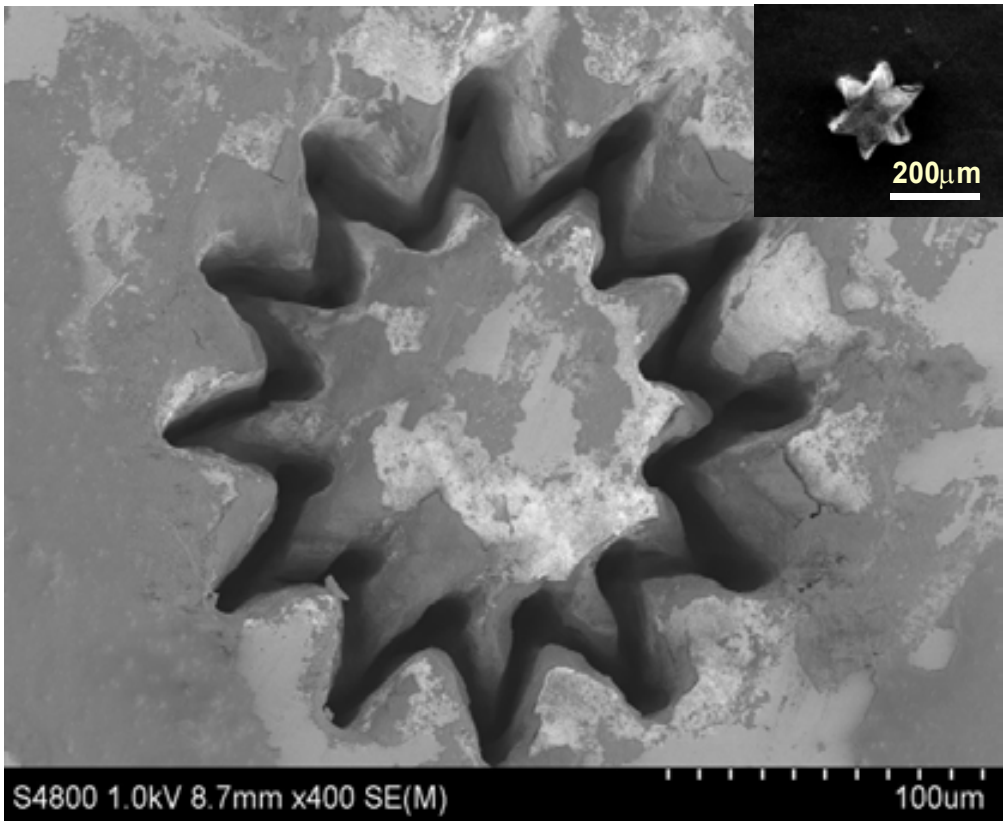

SiC microgears cut by fs laser

Laser: 800nm, 1kHz, 100mW

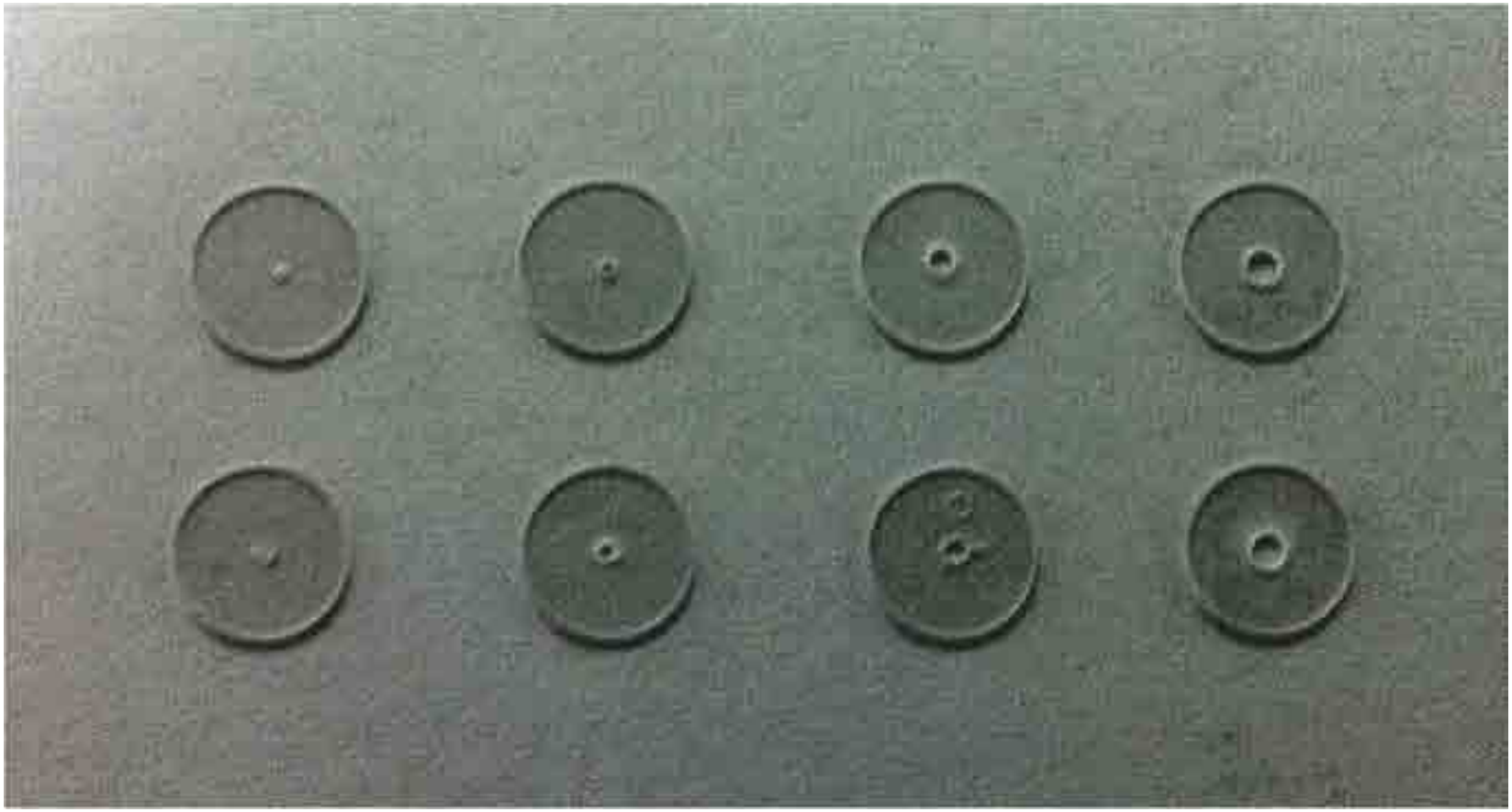

Fs laser cleaning

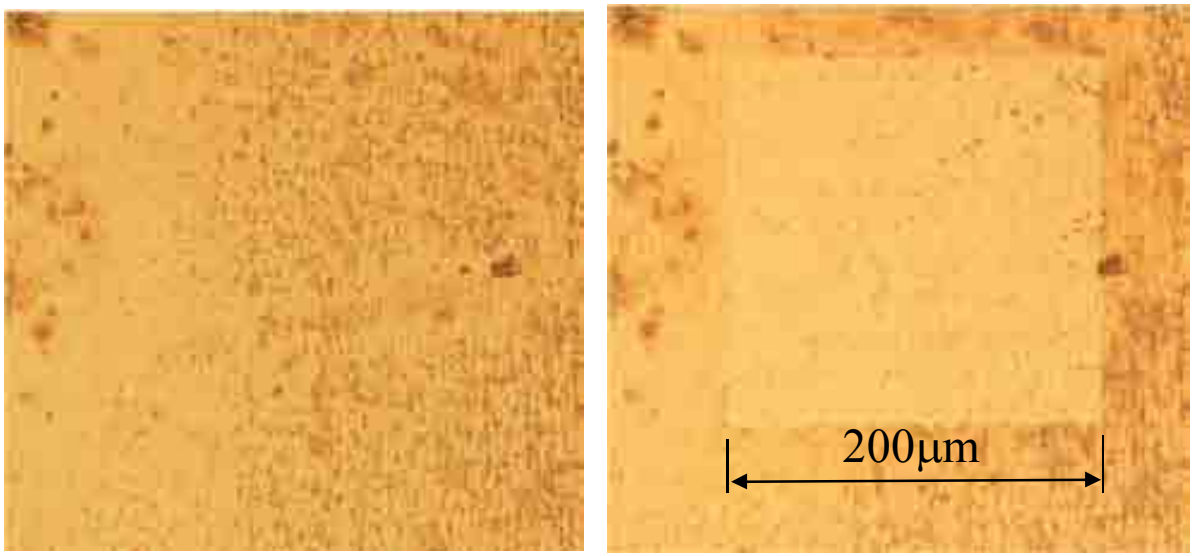

Before cleaning

After cleaning

Tungsten foil

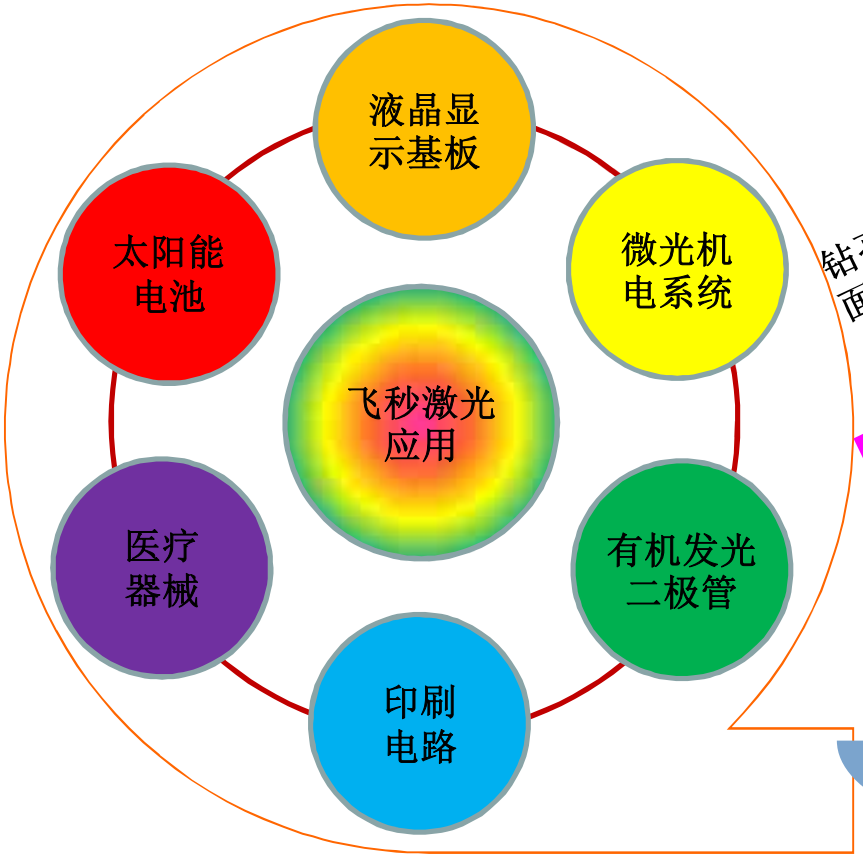

钻孔、刻线、划槽、表面纹理化、表面改性、内部改性、修整、清洗

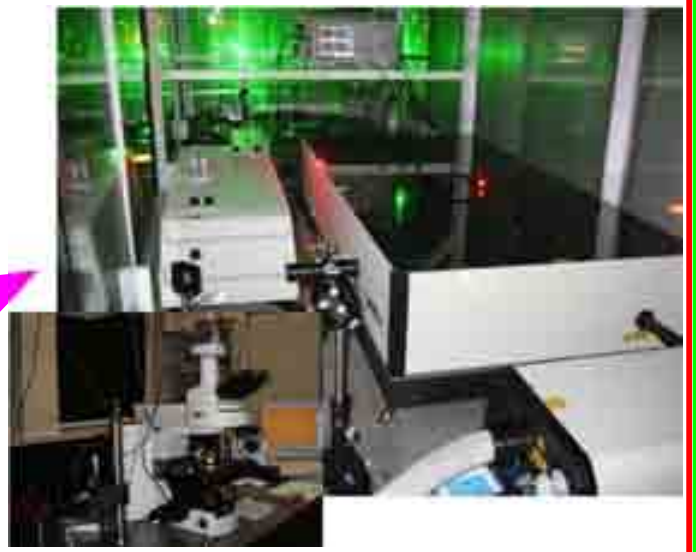

更多应用等待开发


Thanks for your attention!